Department of
Mineral and Petroleum Resources

EXPLANATORY NOTES

GEOLOGY OF THE JACKSON 1:100 000 SHEET

by A. Riganti and S. F. Chen

1:100 000 GEOLOGICAL SERIES

Geological Survey of Western Australia

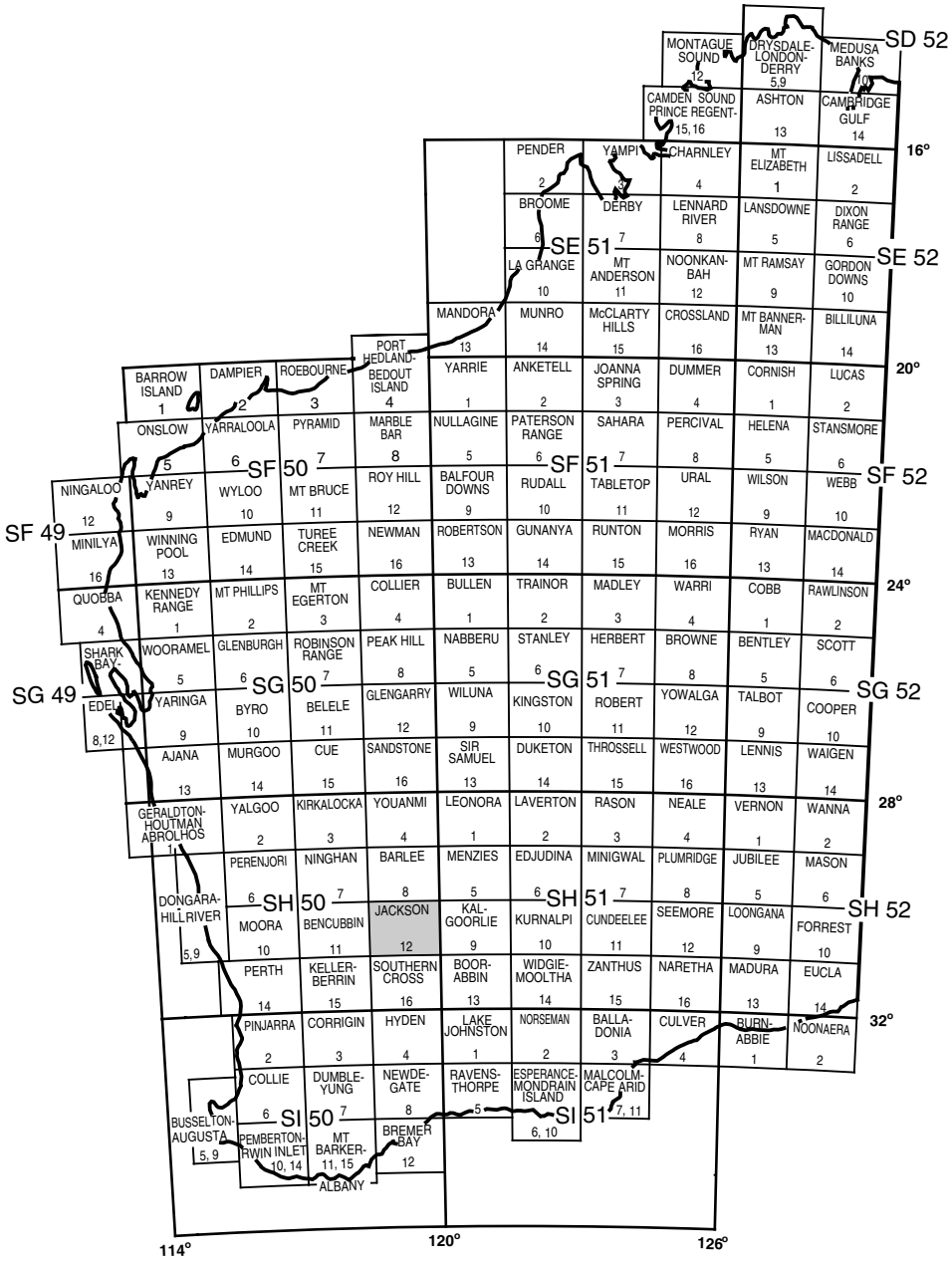

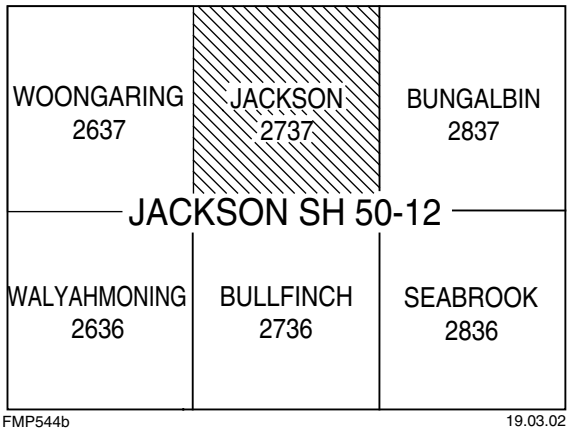

FMP544b 19.03.02

GEOLOGICAL SURVEY OF WESTERN AUSTRALIA

GEOLOGY OF THE JACKSON 1:100 000 SHEET

by
A. Riganti and S. F. Chen

Perth 2002

MINISTER FOR STATE DEVELOPMENT
Hon. Clive Brown MLA

DIRECTOR GENERAL, DEPARTMENT OF MINERAL AND PETROLEUM RESOURCES
Jim Limerick

DIRECTOR, GEOLOGICAL SURVEY OF WESTERN AUSTRALIA
Tim Griffin

REFERENCE
The recommended reference for this publication is:
RIGANTI, A., and CHEN, S. F., 2002, Geology of the Jackson 1:100 000 sheet: Western Australia Geological Survey, 1:100 000 Geological Series Explanatory Notes, 51p.

National Library of Australia Card Number and ISBN 0 7307 5721 8

ISSN 1321–229X

Grid references in this publication refer to the Geocentric Datum of Australia 1994 (GDA94). Locations mentioned in the text are referenced using Map Grid Australia (MGA) coordinates, Zone 50. All locations are quoted to at least the nearest 100 m.

Copy editor: D. P. Reddy
Cartography: G. Williams
Desktop publishing: K. S. Noonan
Printed by Optima Press, Perth, Western Australia

Published 2002 by Geological Survey of Western Australia

Copies available from:
Information Centre
Department of Mineral and Petroleum Resources
100 Plain Street
EAST PERTH, WESTERN AUSTRALIA 6004
Telephone: (08) 9222 3459 Facsimile: (08) 9222 3444
This and other publications of the Geological Survey of Western Australia are available online through the Department's bookshop at www.mpr.wa.gov.au

Cover photograph:
Fragmental ignimbrite outcrop 1 km north-northwest of Butcher Bird No. 1 mine workings (MGA 720200E 6659750N)

Contents

Appendices

Figures

Table

Geology of the Jackson 1:100 000 sheet

by

A. Riganti and S. F. Chen

Abstract

The JACKSON 1:100 000 sheet lies within the Southern Cross Granite–Greenstone Terrane in the central part of the Archaean Yilgarn Craton. On JACKSON the Marda section of the Marda–Diemals greenstone belt comprises a lower (c. 3.0 Ga), mafic-dominated greenstone succession unconformably overlain by felsic volcanic rocks of the Marda Complex (c. 2.73 Ga) and clastic sedimentary rocks of the Diemals Formation. The greenstones are intruded by, or are in tectonic contact with, younger granitoid rocks of mainly monzogranitic composition.

The lower greenstone succession comprises three lithostratigraphic associations. The lower association is characterized by tholeiitic basalt with minor amounts of ultramafic, felsic, and sedimentary rocks. The middle association is dominated by a distinctive banded iron-formation and chert marker unit. The upper association comprises tholeiitic basalt overlain by metasedimentary rocks with prominent units of banded iron-formation. The upper greenstone succession on JACKSON comprises volcanic and volcaniclastic rocks of the calc-alkaline Marda Complex, which has a lower part dominated by clastic sedimentary rocks (mainly conglomerate and sandstone), and an overlying thick package of largely subaerial andesite, rhyolitic ignimbrite, and rhyolite lava flows with subordinate tuffaceous and sedimentary intercalations. The c. 2.73 Ma high-level Butcher Bird Monzogranite intrusion is chemically indistinguishable from the Marda Complex rhyolitic rocks. Fine-grained, clastic sedimentary rocks of the Diemals Formation are also exposed.

At least three major deformation events are recorded by the greenstones and granitoid rocks on JACKSON. An early, north–south D_1 low-angle thrusting produced a layer-parallel foliation and tight to isoclinal folds in the lower greenstone succession. A prolonged period of east–west compression includes two major deformation stages. Large-scale, north-trending upright folds and local development of gneissic banding during D_2 were followed by the development of regional-scale, northeasterly and northwesterly trending ductile shear zones during D_3 (such as the Koolyanobbing and Mount Dimer Shear Zones). Post-D_3 deformation includes the formation of north-northeasterly trending faults and fractures. Mafic and ultramafic dykes of probable Proterozoic age intruded easterly to north-northeasterly trending fractures.

Several stages of granitoid magmatism are recognized on JACKSON. Some granitoid intrusions are coeval with the deposition of the upper greenstone succession (i.e. the c. 2.73 Ga Butcher Bird Monzogranite), whereas some external granitoids were intruded around c. 2.71 Ga, before the D_3 deformation event. Some smaller granitoid intrusions (e.g. the Millars Monzogranite) post-date the D_3 shearing event.

All greenstones have been metamorphosed, with grades ranging from very low (prehnite–pumpellyite facies) to high (amphibolite facies), and the latter is characteristic of areas adjacent to the granite–greenstone contacts. All mineral assemblages are indicative of low-pressure metamorphic conditions.

Gold and iron have been the most sought-after commodities on JACKSON. Small amounts of gold were extracted historically from a number of localities, but no large deposits have been discovered. A number of supergene-enriched iron deposits have been identified.

KEYWORDS: Archaean, granite, greenstone, Southern Cross, Marda Complex, gold, iron.

Introduction

Location and access

The JACKSON* 1:100 000 geological map sheet (SH 50-12, 2737) occupies the central-northern part of the JACKSON 1:250 000 map sheet, from latitudes 30°00'S to 30°30'S and longitudes 119°00'E to 119°30'E (Fig. 1). The sheet is named after Mount Jackson†, a prominent hill in the centre of the area.

Access to the region is provided by the graded Bullfinch–Evanston and Mount Jackson roads (Fig. 2). The former traverses the central part of JACKSON from south to north, linking the town of Bullfinch (about 54 km south of the southern boundary of JACKSON) with the Evanston mine and the Menzies–Evanston Road, about 30 and 35 km north-

* Capitalized names refer to standard 1:100 000 map sheets, unless otherwise indicated.

† MGA coordinates of localities mentioned in the text are listed in Appendix 1.

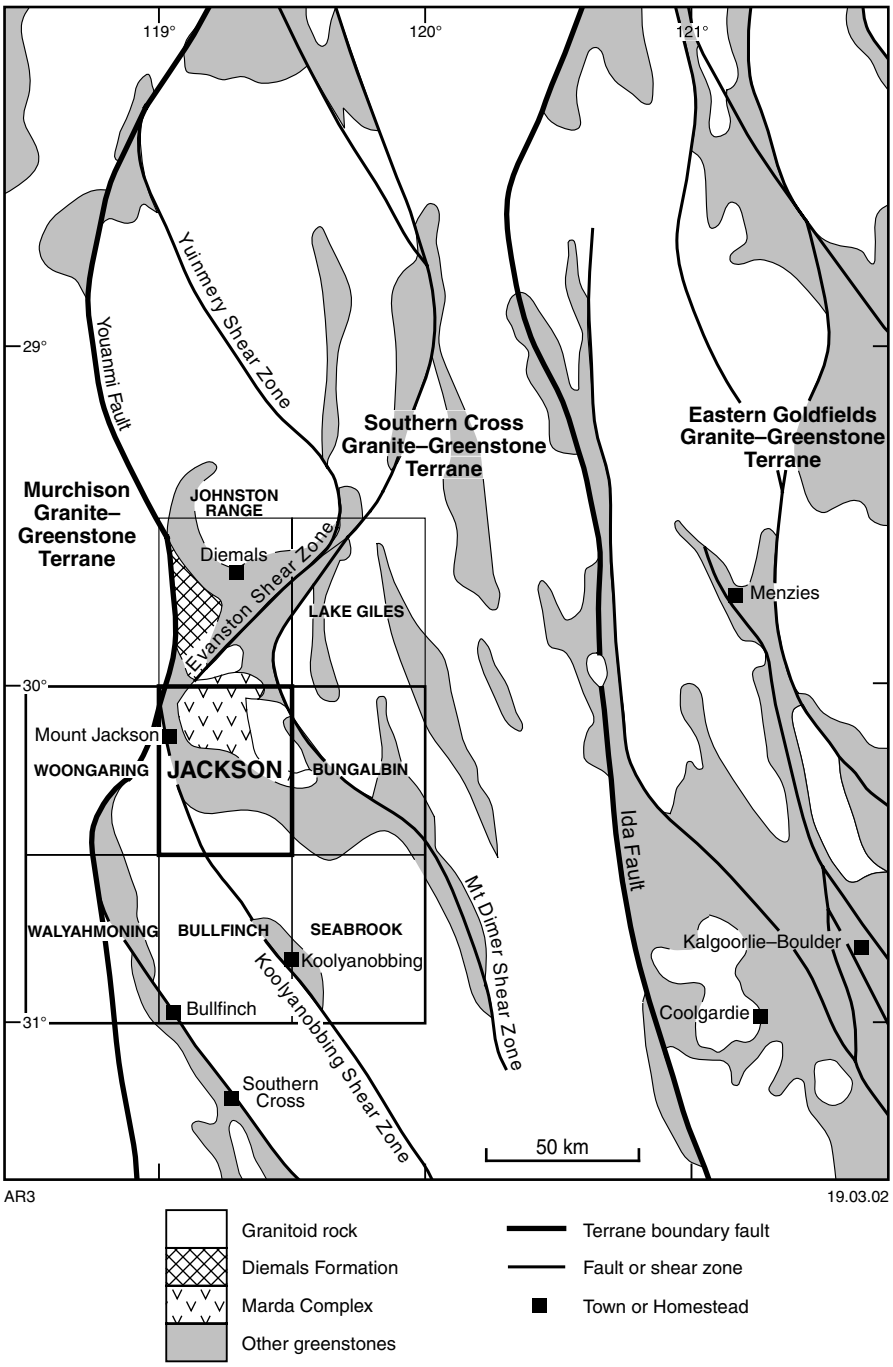

Figure 1. Regional geological setting of JACKSON (adapted from Myers and Hocking, 1998)

northeast of JACKSON respectively. The Mount Jackson Road runs from Bullfinch to the Mount Jackson Homestead and continues east to join the Bullfinch–Evanston Road. A road running north from the Mount Jackson Homestead links the area to the abandoned Clampton mine, 28 km to the north, on JOHNSTON RANGE.

Access to the central-eastern part of the sheet is by a track that links the abandoned Marda Dam to the Bungalbin Hill area on BUNGALBIN. Most of the remaining parts of the map sheet can be reached via station tracks and mineral exploration grids, some of which are not accessible during wet periods.

JACKSON was first explored in 1846 by the Gregory brothers, who named Mount Jackson (Feeken et al., 1970). The area was settled in 1919 when the Mount Jackson Homestead was established in the central-western part. Part of the Diemals pastoral lease lies in the northern portion of the sheet. Cattle grazing for beef is the main commercial activity. Temporary camps are established periodically as a result of mineral exploration and mining activity.

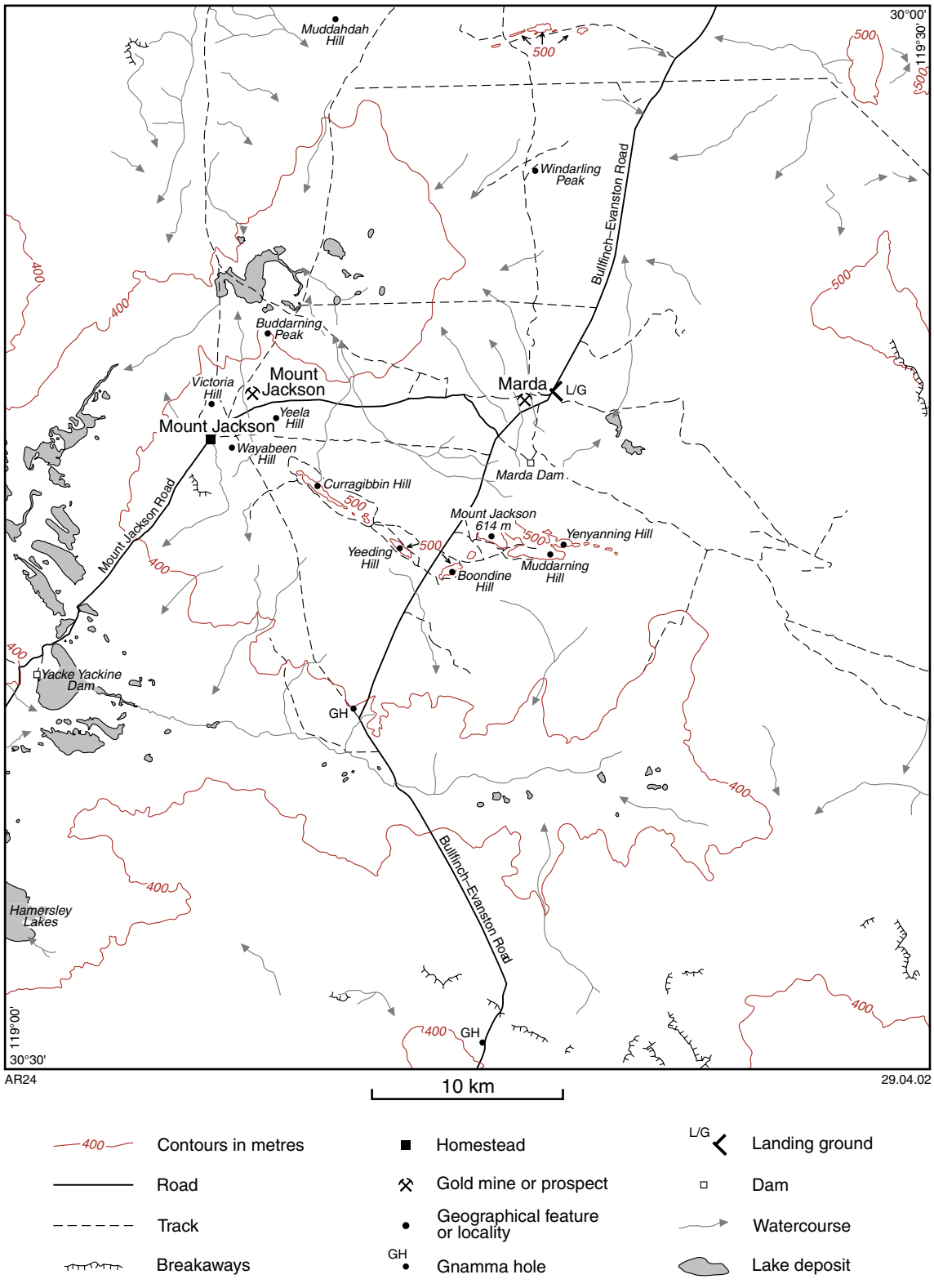

Figure 2. Principal localities, roads, and physiographic features on JACKSON

Climate, physiography, and vegetation

The region that includes JACKSON has a semi-arid climate. Summers are hot, with temperatures regularly in excess of 40°C; winters are cold and frosts are common. Average annual rainfall is similar to that of Diemals (276 mm) and Southern Cross (286 mm)*, with rainfall in the region decreasing in a northerly direction. Rain may fall at any time during the year, but May to July is typically the wettest period. Remnants of south-southeasterly moving tropical cyclones may produce heavier rainfalls during the summer months.

The most conspicuous physiographic element of JACKSON is a series of banded iron-formation (BIF) and chert ridges that rise abruptly from a gently undulating plain lying about 380 to 440 m above sea level (Fig. 2). The most prominent of these is the Jackson–Bungalbin ridge, which runs west-northwesterly through the eastern and central parts of the map sheet to Mount Jackson (614 m Australian Height Datum). From Mount Jackson the ridge swings to the northwest, extending to about 11 km north of Mount Jackson Homestead. There are also prominent BIF ridges in the northern-central part of JACKSON, near Windarling Peak. The undulating plain around the BIF ridges typically consists of low hills and rises underlain by, or with an exposed bedrock of, greenstones. These low relief areas are interspersed with very gently sloping colluvial flats that grade into flat to gently concave broad valleys, which represent the choked remnants of a former drainage system (Biological Surveys Committee, 1985). The western, southern, and northeastern parts of JACKSON are characterized by sand-covered plateaus over siliceous and lateritic duricrust. The duricrust is developed over granitoid rocks and is best exposed in breakaways, a few metres in height, that mark the transition to the erosion-dominated regime of the broad valleys.

The present-day drainage on JACKSON is mainly controlled by the Hamersley Lakes system, the northern extension of which occupies the extreme western part of the sheet (Fig. 2). Here, the Hamersley Lakes consist of a series of small playa lakes, with lake-fringing deposits and dune systems. The two most prominent drainage lines run into the lake from the east and north-northeast. The distribution of most tributaries to these river systems is controlled by the BIF ridges. Drainage in the extreme northeast of the map sheet is to the north, towards Lake Giles, indicating that a major watershed crosscuts the northeastern corner of JACKSON (van de Graaff et al., 1977; Hocking and Cockbain, 1990). All watercourses on JACKSON are intermittent, but in seasons of exceptional rain, water persists in claypans and waterholes until late into the summer months.

JACKSON lies entirely within the Coolgardie Botanical District (or Southwestern Interzone) of Beard (1990). The region is distinguished by eucalypt woodlands and open woodlands (*Eucalyptus salmonophloia*, *E. salubris*, and *E. loxophleba* are the dominant species) with patches of *Acacia* scrub and mallee, and a typical understory of saltbush or broombush with sparse perennial and annual grasses. This vegetation system distinguishes areas of greenstones and the broad valleys. Banded iron-formation ridges are characterized by dense thickets of *Acacia* (*A. quadrimarginea* dominant) and *Casuarina* species up to 2.5 m tall. Felsic rocks support *Acacia*-dominated scrubs and scrub-heaths with patches of gum trees and mallee. Sandplains are dominated by dense *Acacia* thickets interspersed with small low woodland patches, with hummocky spinifex grass developed locally. *Acacia* scrub, with saltbush and a ground layer of more salt-tolerant species (including succulent plants), grows near lakes. Detailed descriptions of the ecosystems on JACKSON are given by Beard (1979, 1990) and the Biological Surveys Committee (1985).

Previous and current investigations

Very few geological investigations were carried out on JACKSON before 1975. The earliest published geological descriptions of the area are those of Woodward (1912a,b) and Blatchford and Honman (1917). A census of the mining centres and their production for the first half of the last century was produced by Matheson and Miles (1947). Details of diamond drilling carried out by the Western Australian Mines Department during 1954–55 near gold workings in the central part of JACKSON are provided by Noldart (1957, 1958), and Sofoulis (1960) reported on a geological reconnaissance trip in the area. The results of an airborne magnetic and radiometric survey in 1957 were detailed by Spence (1958) and the Bureau of Mineral Resources (1965). A reconnaissance gravity survey was conducted in 1969 (Fraser, 1974).

The first systematic regional mapping in the area was carried out by the Geological Survey of Western Australia (GSWA) during mapping of the JACKSON 1:250 000 sheet (Chin and Smith, 1983). Detailed chemical and volcanological investigations of the felsic rocks of the Marda Complex were carried out by Bye (1968), Hallberg et al. (1976), and Taylor and Hallberg (1977). The regional variation in metamorphic grade was researched by Ahmat (1986), and the area is included in the regional metamorphic, structural, and mineralization study of the Southern Cross – Diemals region conducted by Dalstra (1995) and summarized in Dalstra et al. (1999). Libby et al. (1991) detailed aspects of the Koolyanobbing Fault, which is a shear zone that traverses JACKSON and extends farther southeast. An interpretation of the geology for the JACKSON 1:250 000 area based on geophysical data is given by Mackey (1999). High-precision sensitive high-resolution ion microprobe (SHRIMP) geochronological data for the area were presented by Nelson (2001). Several regional studies of the Southern Cross region and geological synopses of the Yilgarn Craton also refer to the JACKSON area. These contributions are referred to where appropriate in these Explanatory Notes.

* Records of rainfall were kept at Mount Jackson Homestead intermittently between 1897 and 1940, during which an average annual rainfall of 232 mm was measured (Beard, 1990). Other climate data quoted in the text are from the Commonwealth Bureau of Meteorology website, 2001.

From the late 1970s, exploration for gold and iron has included detailed mapping, large-scale geochemical soil surveys, and extensive drilling. Unpublished statutory maps and data resulting from these exploration programs are available through the Western Australia mineral exploration (WAMEX) open-file database at the Department of Mineral and Petroleum Resources in Perth and the GSWA Kalgoorlie Regional Office, or via the Department's website (www.mpr.wa.gov.au).

The present work continues the remapping of the central part of the Southern Cross Granite–Greenstone Terrane initiated by GSWA in 1997. Fieldwork on JACKSON was carried out between May 1998 and July 1999, using 1:25 500-scale colour aerial photographs (AP series WA3741C) flown for the Western Australian Department of Land Administration (DOLA) in 1996 and Landsat TM5 (Thematic Mapper) images. Geological interpretation was assisted by 400-m line-spaced aeromagnetic data collected by Kevron Geophysics Pty Ltd in 1997, which are available for purchase from Geoscience Australia (formerly known as Australian Geological Survey Organisation).

Nomenclature

All Archaean rocks described in these notes have undergone low- to medium-grade metamorphism; however, primary textures are commonly preserved and protoliths can be inferred in most instances. For ease of description, the prefix 'meta' is commonly omitted in the following descriptions.

The term 'komatiite' is used in these notes to indicate ultramafic volcanic rocks with relict platy olivine-spinifex textures, which are typical of rocks with more than 18% MgO (Arndt and Nisbet, 1982). The term 'high-Mg basalt' here refers to mafic volcanic rocks with relict pyroxene-spinifex textures, or those that have a proven MgO content between 10 and 18% MgO (cf. Cas and Wright, 1987) and a SiO_2 content less than 52% (Le Bas, 2000).

The nomenclature of other volcanic rocks (e.g. basalt, andesite, dacite, rhyolite) is mainly based on petrography and field relations, and follows the recommendations of the International Union of Geological Sciences Subcommission on the Systematics of Igneous Rocks (Le Maitre, 1989). For the chemically analysed samples from JACKSON, the petrographic classification was commonly found to be in good agreement with the chemical subdivision of Gill (1981), in which basalts have less than 53% SiO_2, basaltic andesites 53 to 57% SiO_2, andesites 57 to 63% SiO_2, dacites 63 to 70% SiO_2, and rhyolites more than 70% SiO_2.

The discrimination diagrams of Winchester and Floyd (1977) were also considered in classifying analysed rocks. The genetic term 'ignimbrite' was reserved for pyroclastic flow deposits consisting predominantly of pumiceous lapilli and blocks, and glass shards, commonly with crystals and lithic clasts (McPhie et al., 1993), in which the welding can be so extreme '…that the original texture shown by the glass shards is lost' (Le Maitre, 1989). The terms 'tuff' and 'tuffaceous' are reserved for primary pyroclastic deposits and reworked and resedimented pyroclast-rich deposits respectively (McPhie et al., 1993). Volcanic textures are described using the terminology of McPhie et al. (1993).

Precambrian geology

Regional geological setting

JACKSON lies in the central-eastern part of the Southern Cross Granite–Greenstone Terrane (Fig. 1), which is one of the major tectono-stratigraphic components of the Yilgarn Craton (Tyler and Hocking, 2001). The Southern Cross Granite–Greenstone Terrane corresponds broadly to the Southern Cross Superterrane of Myers (1997) and the Southern Cross Province of Gee et al. (1981). To the east, the Southern Cross Granite–Greenstone Terrane is juxtaposed against the Eastern Goldfields Granite–Greenstone Terrane, with the distinction between the terranes based on lithological variations, relative volumes of different rock types, and different ages and structural styles of the greenstone sequences. The Ida Fault, a regional-scale structure inferred to represent the boundary between the Southern Cross and Eastern Goldfields Granite–Greenstone Terranes (Myers, 1995, 1997), lies about 100 km east of JACKSON (Fig. 1). To the west, the central and northern parts of the Southern Cross Granite–Greenstone Terrane adjoin the Murchison Granite–Greenstone Terrane (Tyler and Hocking, 2001) along the Youanmi Fault (Myers, 1995, 1997; Myers and Hocking, 1998). The Southern Cross and Murchison terranes may share a broadly similar geological history (e.g. Watkins and Hickman, 1990).

Greenstones occupy or underlie about 50% of JACKSON, with the remainder consisting of granite and subordinate granitoid gneiss (Fig. 3). The greenstones on JACKSON are represented by the Marda section of the Marda–Diemals greenstone belt (Greenfield and Chen, 1999; Chen et al., 2001), which combines the Marda and Diemals belts of Griffin (1990).

The greenstones in the Marda–Diemals region are divided into two supracrustal successions, lower and upper, separated by a major unconformity (Hallberg et al., 1976; Walker and Blight, 1983; Chin and Smith, 1983; Griffin, 1990; see **Stratigraphy**). The lower greenstone succession is dominated by mafic rocks, chert, and BIF, with minor amounts of ultramafic, clastic sedimentary, and felsic volcanic rocks. Within the lower greenstone succession, three associations (lower, middle, and upper) have been distinguished on the basis of different lithological assemblages (Chen and Wyche, 2001a). Limited SHRIMP U–Pb zircon geochronology suggests a depositional age of about 3.0 Ga for the lower greenstone succession (Wang et al., 1996; Nelson, 1999). The upper greenstone succession includes the felsic volcanic and associated volcaniclastic rocks of the Marda Complex (Hallberg et al., 1976) and the clastic sedimentary rocks of the Diemals Formation (Walker and Blight, 1983). Both conventional U–Pb zircon dating (Pidgeon and Wilde, 1990) and SHRIMP data (Nelson, 2001) indicate an age of c. 2730 Ma for the Marda Complex. A maximum

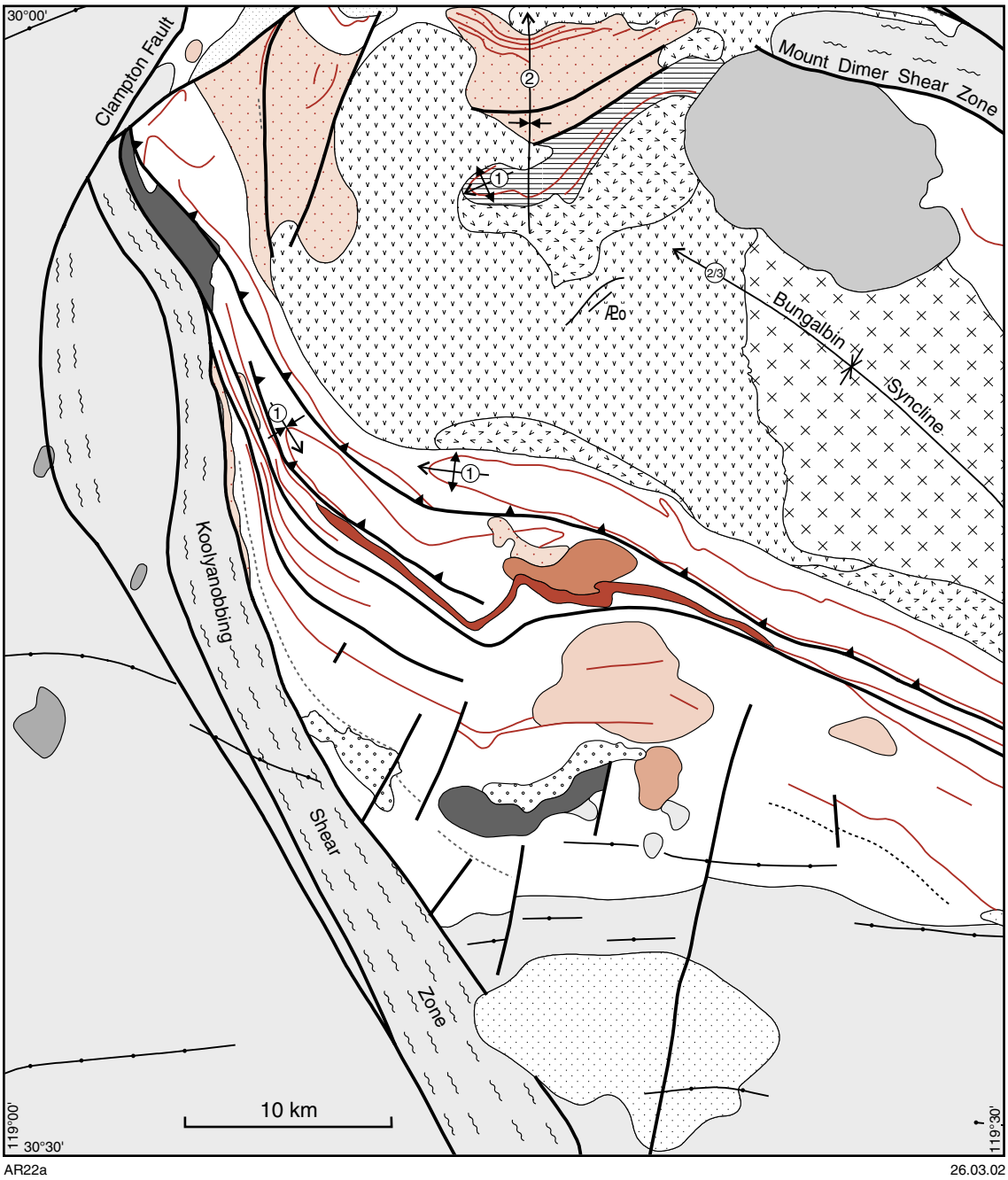

depositional age of 2729 ± 9 Ma (Nelson, 2001) for the Diemals Formation was obtained by SHRIMP dating of detrital zircons. Conspicuous granitoid intrusions in the Marda–Diemals region have ages between c. 2730 and 2650 Ma (Bloem et al., 1997; Dalstra et al., 1998; Wang et al., 1998; Nelson, 1999, 2000, 2001; Qiu et al., 1999).

Several deformation schemes have been proposed for the Marda–Diemals region (Chin and Smith, 1983; Walker and Blight, 1983; Griffin, 1990; Dalstra, 1995; Dalstra et al., 1999; Greenfield and Chen, 1999; Chen et al., 2001), with most schemes recognizing a multi-stage regional deformation history (Table 1). The lower greenstone succession is thought to preserve evidence of an early north–south compressional stage (D_1) that produced low-angle thrusts and tight to isoclinal folds, together with an originally easterly trending, gently dipping foliation and a locally pronounced down-dip mineral lineation (Chen et al., 2001). Large-scale, north-trending upright folds with an axial-planar foliation overprint D_1 structures and are widely attributed to east–west regional compression (D_2). Most granitoid rocks were probably intruded pre- to syn-D_2 because some contain north-trending gneissic banding and foliation. Deposition of the upper greenstone succession was also most likely partly syn-D_2 (Chen et al., in press). East–west shortening during D_3 resulted in the development of regional-scale shear zones and arcuate structures (Chen et al., 2001). Later deformation produced north-northeasterly and east-southeasterly trending faults and fractures, some of which are intruded by mafic to ultramafic dykes of probable Proterozoic age.

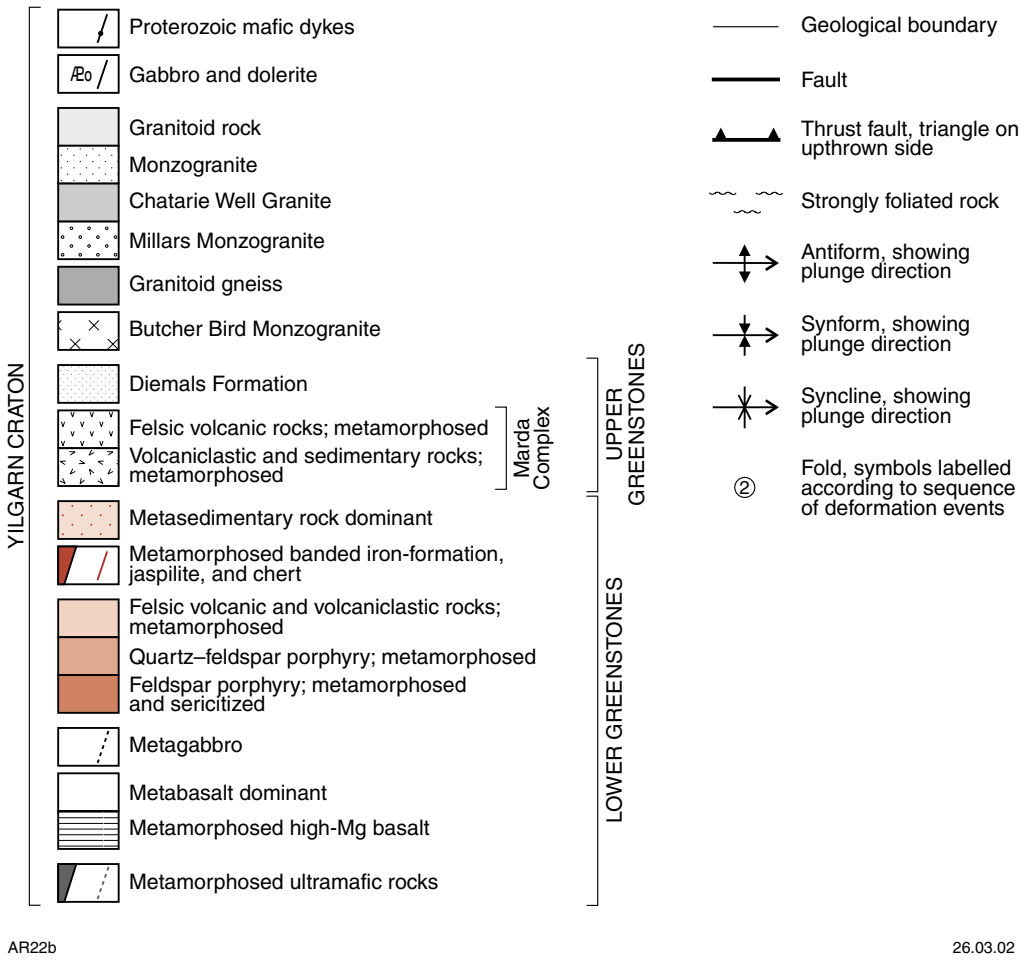

Figure 3. Simplified geological map of Jackson

Table 1. Geological evolution of Jackson

Age	*Deformation event*	*Geology*
c. 3.0 Ga		Deposition of the lower greenstone succession; burial or sea-floor metamorphism
	D_1	North–south compression: layer-parallel foliation and thrusting; tight to isoclinal folding
c. 2.73 Ga		Deposition of upper greenstone succession: Marda Complex (felsic volcanism)
		Granitoid intrusion (e.g. Butcher Bird Monzogranite)
	D_2	Initiation of east–west compressional regime
		Deposition of upper greenstone succession: Diemals Formation (clastic sedimentation)
		Upright to inclined folding (e.g. Bungalbin Syncline)
c. 2.71 – c. 2.65 Ga		Granitoid intrusion (external granitoids); peak metamorphism
		Development of gneissic banding (e.g. Yacke Yackine Dam)
Pre-c. 2656 Ma	D_3	Development of major northeasterly and northwesterly trending shear zones; reorientation of D_2 structures
		Late- to post-kinematic granitoid intrusion (e.g. Millars Monzogranite)
	Post-D_3	North-northeasterly and easterly to east-southeasterly trending brittle faults
		Intrusion of easterly to northeasterly trending mafic and ultramafic dykes along crosscutting fractures

Archaean rock types

Lower greenstone succession

Metamorphosed ultramafic rocks (Au, Auk, Aukf, Aup, Aus, Aux, Aur, Aut)

Ultramafic rocks on JACKSON constitute only a small fraction of the lower greenstone succession (Fig. 3), and are almost exclusively confined to the lowermost exposed part of the sequence. Undivided metamorphosed ultramafic rocks (*Au*) are typically deeply weathered, but can be identified by their tremolite and chlorite content, association with less weathered ultramafic rocks, and development of locally abundant magnesite coatings.

Metakomatiite (*Auk*) outcrops in thin, differentiated units interlayered with minor basalt, 10 km south of Boondine Hill. Despite the rubbly nature of this exposure, the main textural zones of typical komatiitic flows (Pyke et al., 1973; Arndt et al., 1977) can be identified by the repetition of cumulate- and spinifex-textured couplets, separated by intervals of fine-grained amphibolite, which are interpreted as the chilled margins of the flows. Thin, mesocratic to melanocratic gabbroic layers at the transition between cumulate- and spinifex-textured zones are also part of the flow profile. Both platy and random spinifex textures are present, with pseudomorphed olivine plates up to 7 cm long (2–3 cm on average) and a few millimetres thick. Texturally different portions of the flows now consist of serpentine (with abundant magnetite), tremolitic amphibole, and chlorite. Although accurate measurements are precluded by the rubbly nature of the outcrop, individual flow units do not exceed a few metres in thickness. The distribution of various textural zones suggests younging of the sequence to the north. Most komatiites at this locality are weakly deformed, but there are some strongly foliated metakomatiite intercalations (*Aukf*) 10 km to the northwest.

Metamorphosed peridotite (*Aup*) is discontinuously exposed in a northwesterly trending zone, 9 to 14 km north of Mount Jackson Homestead. Peridotite is associated with amphibolite at the southern end of this area, whereas in the north it adjoins a sequence of folded mafic tuffs. Despite extensive alteration, cumulate textures in these rocks are commonly recognizable, with relict mineralogy indicating a considerable compositional variability. Metamorphosed dunites are represented by fine-grained adcumulates, with olivine grains pseudomorphed by serpentine and outlined by fine magnetite. Medium- to fine-grained orthocumulates, most probably corresponding to lherzolite and possibly olivine pyroxenite, typically have idiomorphic, prismatic to pseudo-hexagonal grains replaced by chlorite and serpentine (mainly antigorite), with tremolitic amphibole as the dominant intercumulus phase. Local development of small pods of pyroxene-spinifex textured rocks may indicate differentiation of ultramafic sills or flows. Variably pronounced carbonate alteration is relatively common. Alteration gives peridotite exposures a distinctive pale-green to white appearance on aerial photos, which contrasts with the typical reddish-brown colour, denser vegetation pattern, and more pronounced topography of adjacent amphibolite outcrops. Peridotite is massive to moderately foliated, with a pronounced schistosity near tectonic lineaments (e.g. north of Mount Jackson Homestead, MGA 702790E 6668340N). At these localities, obliteration of primary textures resulted in the formation of serpentinite (*Aus*), which is best observed in mineral exploration drillholes (e.g. MGA 702970E 6667790N). Surface outcrops of these rocks consist of deeply weathered and typically silicified ultramafic schists.

Metamorphosed pyroxenite (*Aux*) forms small lenses within amphibolite immediately south-southeast of the peridotite exposures described above. The pyroxenite has a relict cumulate texture in which metamorphic tremolitic amphibole has partially pseudomorphed and overgrown pyroxene grains up to 3 mm across, which had already been replaced by magnesium-rich chlorite during an earlier alteration or metamorphic event. Chlorite and epidote are locally abundant as interstitial phases. The pyroxenite lenses are only a few metres wide, and gradational relationships with the enclosing metamorphosed basaltic rocks suggest an origin for the pyroxenite as cumulate portions of basalt flows. A chemical analysis of pyroxenite is given in Appendix 2 (GSWA 164808).

Tremolite–chlorite(–talc) and subordinate talc–tremolite(–chlorite) schists (*Aur* and *Aut*) outcrop in numerous, commonly thin, discontinuous units that intercalate with strongly deformed mafic and sedimentary rocks near the granite–greenstone contact in the western part of JACKSON. These ultramafic schists were also intersected in many mineral exploration drillholes 5 km west and southwest of Muddahdah Hill. Small exposures, about 8 km west of Muddahdah Hill, at and near the faulted contact with the granite, represent the southern extension of a discontinuous ultramafic unit that lies west of the Clampton mine on JOHNSTON RANGE (Wyche et al., 2001). Pale- to dark-green, medium- to fine-grained tremolite schists are dominated by tremolite and chlorite, and may also contain talc and opaque oxides (typically magnetite) interstitial to strongly oriented amphibole needles that define a foliation. Ultramafic volcanic rocks are the most likely protoliths for the tremolite schists. Where plagioclase is present as a minor constituent, these schists probably represent a strongly deformed equivalent of spinifex-textured high-Mg basalts. Fine-grained talc schists are dominated by talc, with various amounts of tremolite, chlorite, and sparse serpentine, and are commonly extensively carbonatized. An unusual association of talc with rutile (GSWA 159313) was observed in a thin section of RAB (rotary air blast) drillhole chips from 5 km west of Muddahdah Hill (MGA 705360E 6678030N). Rutile crystallization in this instance may be related to fluid circulation during syndeformational metamorphism along the fault that is interpreted to crosscut this area.

Metamorphosed fine- to medium-grained mafic rocks (Ab, Abar, Abf, Abm, Abmf, Abs, Abt, Abv, Abx)

Metamorphosed fine- to medium-grained mafic rocks are the dominant component of the lower greenstone

succession on JACKSON. They are distributed throughout the succession, but are subordinate to sedimentary rocks at middle stratigraphic levels (see **Stratigraphy, Lower greenstone succession**). Metamorphic grade is typically low, but higher grades are present near granite–greenstone contacts.

Undivided mafic rocks (*Ab*) have no distinctive mineralogical or textural features, and typically consist of deeply weathered, green to dark-grey mafic assemblages of actinolite and altered plagioclase with accessory opaque minerals (pyrite is recognized in places). The absence of primary quartz and presence of chlorite suggest a derivation from either mafic volcanic rocks or sedimentary rocks with a dominantly mafic component.

Mafic rocks metamorphosed to lower amphibolite facies and partly retrogressed to greenschist-facies mineral assemblages (*Abar*) are a significant component of the lower greenstone succession, and are abundant along the granite–greenstone contact in the western part of JACKSON. They are typically dark- to medium-grey, fine- to medium-grained rocks, which in thin section are dominated by an assemblage of plagioclase (commonly concentrically zoned) and deformed amphibole grains frayed at the edges. The latter are commonly actinolite, but hornblende and actinolitic hornblende are locally preserved. Minor amounts of granoblastic quartz and fine amphibole needles are the typical interstitial phases. Epidote minerals and chlorite are rare. Near granite, tourmaline sprays penetrate the amphibolite from joint surfaces (e.g. MGA 699670E 6672580N). A poorly developed, millimetre-scale banding consisting of amphibole-rich and plagioclase-rich layers parallels the regional foliation in the north. In the south the amphibolite is more homogeneous and only weakly foliated. Analyses of amphibolite samples indicate a tholeiitic basalt composition (GSWA 159305 in Appendix 2; cf. GSWA 153299 in appendix 2 of Wyche et al., 2001). However, high-Mg basalt and ultramafic intercalations are common within the amphibolite sequence, and it is likely that these rock types are the protolith for at least part of the amphibolite.

Strongly foliated mafic rocks (*Abf*) are present in shear zones and adjacent to granite–greenstone contacts. Relict igneous textures are completely obscured by deformation, but strongly aligned plagioclase and calcic amphibole, along with chlorite, epidote, and minor quartz, indicate a basaltic composition. This is also supported by transitional contacts between deformed mafic rocks and relatively undeformed basalt, for example about 15 km southeast of Mount Jackson (around MGA 730300E 6640100N).

Metamorphosed high-Mg (or komatiitic) basalt (*Abm*) and its strongly foliated equivalent (*Abmf*) are fine to medium grained (locally coarse grained) and distinguished by the presence of a relict pyroxene-spinifex texture. Pyroxene-spinifex texture typically consists of randomly oriented needles up to 1 cm long, now consisting of tremolite–actinolite or chlorite (relict pyroxene is rarely preserved), with varying amounts of interstitial plagioclase and calcic amphibole. Late epidote is a common accessory mineral. Spinifex-textured high-Mg basalt is commonly associated with variolitic basalt, which characteristically contains discrete, rounded to ellipsoidal varioles ranging from a few millimetres to 15 mm in length. The varioles are pale-green, fine-grained, more plagioclase-rich zones surrounded by a mafic groundmass. Concentric zoning is locally present within varioles, usually in the form of a millimetre-thick darker outer rim. In places, varioles have coalesced into a large amorphous mass, and are commonly stretched in areas of pronounced deformation. On JACKSON high-Mg basalt is most abundant in stratigraphically lower parts of the lower greenstone succession, and high-Mg basalt units are more conspicuous and laterally continuous in the central and eastern parts of the map sheet. A chemical analysis of a spinifex-textured high-Mg basalt is given in Appendix 2 (GSWA 164801).

Chlorite schist (*Abs*) with various amounts of tremolite and talc, interstitial plagioclase, and minor amounts of quartz forms thin intercalations at all stratigraphic levels within the lower greenstone succession. It is particularly abundant in areas of intense deformation, where the schists are commonly crenulated and locally lineated. Finely laminated (from <1 to 5 mm) chlorite-rich schist with bands defined by variable amounts of fine-grained carbonaceous material was intersected in many mineral exploration drillholes 5 km west-southwest of Muddahdah Hill. Here, the chlorite schists appear to be juxtaposed against metamorphosed graphitic shale and phyllite in the west, and grade into more distinctly ultramafic schists at depth in the east.

Metamorphosed mafic tuffs (*Abt*) are rarely exposed on JACKSON. The most conspicuous exposures are about 20 km east-southeast of Mount Jackson and 14 km north-northwest of Mount Jackson Homestead. At the latter locality (MGA 700000E 6670800N), a folded and weakly crenulated tuffaceous sequence is in contact with peridotite and high-Mg basalt. The tuffs are very thinly bedded, with layers varying from less than 1 mm to 3 cm (5–8 mm on average). Bedding contacts are sharp, with parallel laminations and grading in the thickest layers. The tuffs are very fine grained, medium to light greenish-grey in colour, and characteristically contain tremolite and chlorite with interstitial albite and sparse subidiomorphic elongate opaque minerals. Iron-rich chlorite replaces an idiomorphic mineral with square to prismatic cross sections, interpreted to represent primary mafic crystals, therefore suggesting an origin for this lithotype as a pyroclastic rather than epiclastic rock. A higher metamorphic grade was observed in a thin, tuffaceous unit with green-grey to black, millimetre-sized bands and a layer-parallel foliation, exposed just west of the Bullfinch–Evanston Road (MGA 710490E 6643880N). This unit is characterized by a finely granular assemblage of calcic pyroxene (commonly poikiloblastic), untwinned plagioclase, actinolitic amphibole, and minor quartz, with andalusite porphyroblasts up to 1 mm across predominantly oriented parallel to the foliation. The mineralogy and texture of this rock indicate late- to post-kinematic recrystallization, which was most likely induced by the late intrusion of the Millars Monzogranite (see **Granitoid rocks**, *Agmi*) immediately to the southwest.

Very fine to fine-grained, medium- to light-greenish-grey metabasalt (*Abv*) is the dominant mafic lithotype of the lower greenstone succession on JACKSON. Metabasalt

is typically massive to weakly foliated, and locally preserved pillow structures 20 km southeast of Mount Jackson (MGA 733500E 6639150N) indicate younging directions (e.g. way-up) to the north-northeast. The metabasalt contains numerous zones of chlorite schist, high-Mg basalt, and gabbro, which are consistently parallel to chert and BIF units, indicating a stratigraphic control on the distribution of the mafic lithotypes. Many of the sedimentary and mafic intercalations are too small to be mapped separately. The primary mineralogy of the basaltic rocks (pyroxene and calcic plagioclase with or without magnetite) has been almost completely replaced by greenschist-facies assemblages consisting of various proportions of actinolitic amphibole and albite, with chlorite, epidote, clinozoisite, and minor amounts of quartz. Relict pyroxene is present in the core of phenocrysts in places. Opaque oxides are an abundant accessory phase, whereas minute (<1 mm) pyrite grains are less common. Late, patchy carbonate alteration and epidote veinlets are locally superimposed on the metamorphic assemblages, and silicification is common adjacent to quartz vein systems.

Despite the pervasive and extensive mineralogical changes, intergranular igneous textures are abundantly preserved, as well as less common plumose quenching textures characterized by a fine network of plagioclase needles with interstitial fine mafic phases (cf. MacKenzie et al., 1982, p. 57). Other locally preserved volcanic textures include irregularly shaped, quartz-filled amygdales (up to 1.5 cm in length and commonly surrounded by an altered outer rim up to 7 mm wide), as well as incipient formation of varioles, represented by vague rounded areas (up to 1 cm across) that are more felsic than the surrounding matrix. Limited whole-rock geochemistry indicates that the metabasaltic rocks have the composition of tholeiitic basalt (GSWA 164803 and 164822 in Appendix 2). The association of basalt with minor basaltic andesite is suggested by paler intercalations with a microtexture defined by abundant, randomly oriented plagioclase laths.

Metamorphosed, mafic fragmental rocks (*Abx*) form sporadic bouldery outcrops on Jackson, with the largest exposures within retrogressed amphibolite 9 and 13 km north of Mount Jackson Homestead (MGA 702940E 6666330N and MGA 703840E 6670030N respectively) These rocks typically consist of tightly packed, angular to subangular fragments of greenish-grey to black, fine-grained material, averaging 1 to 3 cm in size, but ranging from a few millimetres up to 50 cm, in a dark-green, coarser matrix. The fragments consist of brown, turbid (saussuritized) plagioclase and subordinate amphibole laths, indicating a basalt to basaltic andesite composition. The interstitial spaces are filled by a chlorite–epidote–clinozoisite(–quartz) assemblage. The exact geometry of these fragmental units is unclear, but a conformable relationship is suggested in the southernmost exposure. Here, the breccia unit appears to be a few metres wide, and extends for a few hundred metres in a direction broadly parallel to the bedding of thin BIF units. These features, together with the angularity of the fragments, their poor sorting, and the limited amount of interstitial material, suggest that the breccias are either autoclastic horizons or proximal epiclastic deposits.

Metamorphosed medium- to coarse-grained mafic rocks (Aog, Aogf, Aogx)

Metamorphosed, medium- to coarse-grained mafic rocks are commonly intercalated with metabasalt, particularly in the lower part of the lower greenstone succession. The most abundant of these rocks is metagabbro (*Aog*), which is massive to weakly deformed, with a well-preserved relict igneous texture defined by equigranular assemblages of actinolitic amphibole (pseudomorphing pyroxene) and saussuritized or sericitized plagioclase, with grain size up to 6 mm. Opaque minerals are locally abundant, and include magnetite (partly limonitic) and ilmenite (now commonly altered to leucoxene). The most conspicuous gabbroic units outcrop in the southeastern part of Jackson (around MGA 731000E 6640000N), where lenses of gabbro within metabasalt are aligned parallel to bedding in nearby sedimentary units and are orthogonal to the younging direction indicated by pillow-lava structures. This suggests that the gabbro intercalations represent either conformable sills or the lower portions of thick, differentiated mafic flows. Elsewhere on Jackson, gabbro units are commonly smaller and more scattered. Strongly foliated and partly silicified equivalents (*Aogf*) are adjacent to the Koolyanobbing Shear Zone, about 7 km west-southwest of Yeeding Hill (MGA 705500E 6649700N).

Microgabbroic rocks with sparse pseudomorphed pyroxene megacrysts in a finely crystalline matrix (*Aogx*) are confined to a small area 6 km south of Mount Jackson. These rocks are dark-grey to green, and typically consist of fine-grained (~1 mm), equigranular augite (partially replaced and overgrown by actinolitic amphibole) and plagioclase (pervasively and extensively saussuritized), with little interstitial amphibole, chlorite, and quartz. Subidiomorphic, prismatic, larger grains, up to 4 mm in length, are irregularly distributed within the rock and confer a slightly pitted appearance to weathered surfaces. These phenocrysts now consist of Fe-chlorite and serpentine, and are interpreted to be pseudomorphs after orthopyroxene. Leucoxene and epidote are common secondary phases. Bleaching adjacent to millimetre-thick chlorite–epidote veinlets is locally pronounced. These microgabbroic units typically interfinger with fine-grained porphyritic felsic rocks on a scale ranging from about a metre to a few tens of metres. Although contacts are obscured by the rubbly nature of the exposures, the relatively coarser grain size of the mafic intercalations suggests that they intruded the felsic component, possibly in a subvolcanic environment.

Metamorphosed fine- to medium-grained felsic rocks (Af, Afs, Afp, Afpm, Afv)

Metamorphosed felsic rocks are a minor, but locally significant, component of the lower greenstone succession on Jackson. Most of these rocks are clearly igneous in origin, but in areas of poor outcrop and intense foliation it is difficult to distinguish between felsic igneous (extrusive or subvolcanic) and felsic volcaniclastic (epiclastic or pyroclastic) types.

Undivided, fine-grained felsic rocks (*Af*) are typically deeply weathered and off-white to pale pink, with no

preserved relict igneous or sedimentary textures. Finely granular assemblages dominated by quartz and sericite (locally muscovite) indicate a quartzofeldspathic protolith. Undifferentiated felsic rocks mainly form thin intercalations at various stratigraphic levels within the lower greenstones, with considerable volumes exposed about 4 km southeast of Mount Jackson. Here, juxtaposition with metabasalt and felsic volcanic rocks as well as the intercalation with chert units suggest an extrusive or volcaniclastic origin. Deeply weathered, fine-grained, schistose, quartzofeldspathic rocks (*Afs*) outcrop in the western part of the greenstone belt (e.g. MGA 702000E 6677400N and MGA 704700E 6654500N).

Feldspar–quartz porphyry (*Afp*) on JACKSON is medium to dark grey and fine grained, with abundant phenocrysts that may constitute up to 50% of the rock. Plagioclase, either as discrete grains or glomeroporphyritic aggregates, is the dominant phase; it is commonly zoned and forms idiomorphic to subidiomorphic grains ranging in size from less than 1 mm to 4 cm (3 to 4 mm on average). When present, quartz phenocrysts up to 5 mm are rounded to irregular, with common embayed outlines indicating resorption. Small biotite flakes (1 to 2 mm) may be primary, whereas chloritized grains probably represent altered mafic phenocrysts. Accessory opaque minerals are up to 2 mm across. The finely granular groundmass is quartzofeldspathic. Petrography and geochemistry (GSWA 143380 in Appendix 2) indicate a rhyolitic to dacitic composition. The largest porphyry exposure on JACKSON is about 11 km southeast of Mount Jackson, where it is associated with small rhyolite outcrops and abundant metabasaltic rocks. Locally, the porphyry contains prominent, east-northeasterly, steeply (70°) dipping bands, interpreted as igneous compositional layering. The banding, which is most visible on the dark-brown weathered surfaces, is defined by 1–5 cm-thick layers with diffuse boundaries. No preferential orientation of the plagioclase phenocrysts was observed. Field relationships with the adjacent metabasalts and textural characteristics suggest that the feldspar–quartz porphyry is a subvolcanic or high-level intrusion into the mafic rocks. Zircons separated from a porphyry sample from this area for SHRIMP U–Pb geochronology were metamict and gave discordant results. Metamorphic tremolite–actinolite sprays punctuate a foliated porphyry 12 km northwest of Buddarning Peak (MGA 699500E 6671900N). A feldspar–quartz porphyry dyke in ultramafic rocks of the lower greenstone succession, about 11 km south-southeast of Mount Jackson (MGA 716030E 6639900N), is characterized by smaller phenocrysts (up to 6 mm) and more abundant biotite (commonly in bands several millimetres thick), with sericite and muscovite typically associated with the feldspar phenocrysts. Sprays of fine, acicular amphibole overgrow the groundmass and radiate from grain boundaries and twin planes of plagioclase.

Extensively sericitized felsic porphyritic rocks (*Afpm*) outcrop on thickly vegetated hills immediately north of Mount Jackson and Yenyanning Hill. The rock is typically fine grained and cream to pink, with a locally pronounced, pitted surface due to weathering of phenocrysts up to 4 mm long. In thin section, most phenocrysts are completely pseudomorphed by sericite, but a prismatic shape and relict Carlsbad twinning indicate that they are feldspar. Quartz phenocrysts are rare. The sericitized phenocrysts are surrounded by a very fine, granular groundmass of quartz and sericite, with minor amounts of fine opaque iron oxides. At the poorly exposed contact of the sericitized porphyry with jasperoidal chert and BIF on the northern flanks of Muddarning Hill and Mount Jackson, the porphyry appears to overlie the siliceous units. Small chert bands are intercalated with the porphyry. To the north, the porphyry is juxtaposed against a quartz-rich conglomerate, which is similar to the sedimentary units at the base of the Marda Complex (see **Metamorphosed sedimentary rocks**, *Asc*, and **Marda Complex**, *AfMsc*).

Fine-grained, felsic volcanic rocks (*Afv*) are exposed over a large area southeast of Mount Jackson, where they are intercalated with deeply weathered felsic rocks, metabasalt, pyroxene-phyric microgabbro, and chert. The felsic volcanic rocks are brown-grey, with extensive bleaching common around joints. A rhyolitic to rhyodacitic composition is indicated by variously abundant, idiomorphic plagioclase phenocrysts up to 4 mm long, and subordinate, locally resorbed, quartz phenocrysts (1 to 3 mm in size), in a fine-grained, sericitized quartzofeldspathic groundmass. Minor fine mafic phenocrysts are completely replaced by chlorite. Leucoxene and ?rutile are abundant accessory minerals. Secondary carbonate is common locally. Local differential weathering enhances an easterly trending, centimetre-scale compositional banding, which is broadly conformable with the chert intercalations. In the west, the felsic volcanic rocks typically form small rubbly ridges only a few metres wide, and have been extensively intruded by pyroxene-phyric microgabbro. Locally, contact metamorphism has recrystallized the sericite to muscovite, some of the chlorite to biotite, and the groundmass into a finely granular quartz–feldspar mosaic. These felsic volcanic rocks may be part of the lower greenstone succession. Insufficient zircons were recovered from a rhyolite sample for SHRIMP U–Pb dating.

Metamorphosed sedimentary rocks (As, Asc, Ash, Ashg, Asi, Asq, Ass, Ac, Aci, Acj)

Metamorphosed sedimentary rocks on JACKSON are distributed at all stratigraphic levels within the lower greenstone succession, but are particularly common in the middle part (see **Stratigraphy, Lower greenstone succession**). Metasedimentary rocks are poorly exposed (except for prominent ridges of BIF, chert, and quartzite) and their volumetric proportion to the volcanic rocks is difficult to assess.

Undivided metasedimentary rocks (*As*) are typically deeply weathered. A sedimentary protolith is inferred from the poorly preserved sedimentary structures, and by association with more easily identifiable metasedimentary rocks, including ferruginized, composite units of shale, siltstone, and fine-grained sandstone, intercalated with chert and BIF.

Metamorphosed conglomerate (*Asc*) is exposed in two localities on JACKSON. Near the eastern edge of the map

sheet (MGA 738600E 6666200N), a poorly sorted, clast-supported, polymictic conglomerate contains pebbles of granite, chert, and vein quartz, and is interbedded with quartz-rich sandstone. A larger outcrop of a clast-supported conglomerate with clasts of vein quartz and chert (dark grey, banded grey and white, and jasperoidal) in a quartz–sericite-rich matrix is exposed 1 km north-northeast of Mount Jackson (MGA 718500E 6652250N). Clasts are angular, and range in size from 2 mm to 10 cm. Pressure solution is common along the contacts between clasts. Grading and small scour and fill structures indicate younging towards the north-northwest. A broad upward coarsening is indicated by irregular intercalations of pebbly sandstone, sandstone, and minor siltstone, which become progressively less common and thinner (from several tens of centimetres to a few centimetres only) towards the top. Rare clasts with devitrification textures within the conglomerate indicate some detrital input from felsic volcanic rocks. This conglomerate resembles the coarse sedimentary units at the base of the Marda Complex (e.g. in the abundance of chert and quartz clasts, paucity of felsic volcanic clasts, and clast-supported nature; see **Marda Complex,** *AfMsc*), and is adjacent to outcrops of sericitized felsic porphyritic rocks that may be part of the upper greenstone succession (see **Metamorphosed felsic rocks,** *Afpm*).

Metamorphosed, composite units of shale, siltstone, and fine-grained sandstone (*Ash*) outcrop discontinuously in the northwestern part of JACKSON, where they are typically exposed at the base of breakaways below an extensive lateritic duricrust. These fine-grained metasedimentary rocks are commonly ferruginous and typically weather brown to purple (less commonly white), with black and grey colours preserved only in rockchips from drillholes that extended below the weathering profile. Reprecipitation of iron in spherulitic limonite concretions is common. Local beds of medium-grained sandstone are up to 20 cm thick, and small lenses of conglomerate contain quartz and chert clasts up to 4 cm across in a highly ferruginous matrix (e.g. MGA 705000E 6667000N). Sedimentary structures consist mainly of millimetre-scale parallel laminations and grading, the latter indicating younging of the sequence to the east. Clastic dykes were noted by Chin and Smith (1983) 11 km north-northeast of Mount Jackson Homestead. Siltstone and shale units within the lower greenstone succession are moderately to strongly foliated, have a weak to moderate crenulation, locally preserve evidence of mesoscale folding, and are commonly crosscut by small quartz veins. In thin section, siltstone and shale typically consist of very fine grained, strongly oriented aggregates of sericite (–chlorite) and quartz in a highly ferruginous matrix. Fine-grained sandstones are poorly sorted, with angular to subangular clasts of quartz, minor amounts of BIF, and some ?mafic volcanic clasts in a ferruginous, clay-rich, foliated matrix. Association with chert and BIF was the main criterion used to distinguish units belonging to the lower greenstone succession from lithologically similar fine-grained metasedimentary rocks of the Diemals Formation (*Aesh*) that outcrop immediately to the north. However, poor exposure and discontinuous outcrop made this distinction difficult in places, and where doubtful, the siltstone and shale units are left unassigned.

Metamorphosed graphitic shale (*Ashg*) has only been noted on JACKSON in exploration drillholes about 4 km west of Muddahdah Hill. Here, graphitic shale horizons are intercalated with phyllite and chlorite schist, and appear to overlie mafic and ultramafic rocks. The relationship of the graphitic shale and associated chlorite schists with the adjacent rock types of the lower and upper greenstone successions is unclear. Chlorite schist near the base of the Diemals Formation on JOHNSTON RANGE was interpreted as the product of erosion from a greenstone basement at the onset of sedimentation of the Diemals Formation (Wyche et al., 2001).

Ferruginous, fine-grained metasedimentary rocks (*Asi*) are exposed on the flanks of chert and BIF ridges, mainly in the northwestern quadrant of the map sheet. These shale and siltstone units contain minor amounts of fine-grained sandstone and subordinate small intercalations of BIF and chert. They are poorly exposed and deeply weathered to a purple or red–brown colour.

A well-bedded to massive quartzite unit (*Asq*) outcrops discontinuously for about 10 km north and south of the Mount Jackson Homestead, with the best exposures just north of the homestead and at Victoria Hill. The quartzite forms distinct low ridges flanked by foliated, deeply weathered granitoid rocks to the west, and by poorly exposed, deformed mafic to ultramafic rocks to the east. The quartzite is white to pale grey, with common brown intercalations. Beds are several centimetres thick and either vertical or dip moderately to steeply (55 to 80°) to the northeast. Sedimentary structures are rare in this strongly recrystallized quartzite. Chin and Smith (1983) described cross-bedding defined by flaggy partings showing consistent eastward younging. However, the rocks are strongly deformed and these flaggy partings are not unequivocally representative of bedding. A fine-grained, laminated, strongly silicified unit with chaotic folding outcrops locally along the western side of the ridge in the northernmost exposures. Some quartzite layers contain small concentrations of magnetite, and there are local intercalations of quartz–muscovite and sillimanite-rich schists. The formation of sillimanite is most probably related to contact metamorphism of more aluminous beds during the syntectonic intrusion of the adjacent granite (see **Structural geology**). The quartzite has a well-developed granoblastic texture, with strained quartz grains and sutured boundaries. Layers range in grain size from microgranular to coarse (>2 mm). Scattered chlorite and muscovite flakes are more common in the finer beds where they define a layer-parallel schistosity. A chemical analysis of a quartzite sample is given in Appendix 2 (GSWA 168958).

The quartzite unit on JACKSON is adjacent to the eastern margin of the Koolyanobbing Shear Zone. Although the contact with the foliated granite to the west is mainly covered by scree, the quartzite is strongly sheared and locally interleaved with tectonic slivers of amphibolite and granite. The quartzite has a well-defined bedding–cleavage intersection lineation, and a commonly steep, variably plunging mineral lineation. Crosscutting quartz veins are common. This unit is similar to quartzites exposed farther east in the Illaara greenstone belt (Griffin, 1990; Wyche, 1999) that may be the lowest exposed unit in the regional

lower greenstone succession. On JACKSON the quartzite is in faulted contact with poorly exposed, possibly younger granitoid rocks. Insufficient detrital zircons were recovered from the quartzite at Victoria Hill for a SHRIMP age determination.

Metamorphosed sandstone (*Ass*) is confined to two small outcrops near the northern edge of JACKSON. A weathered sequence of medium-grained, quartzo-feldspathic sandstone, with fine, rounded quartz grains in a clay–sericite-rich matrix west of Muddahdah Hill (MGA 703650E 6679170N), is intercalated with minor siltstone and shale, and flanked by fine-grained amphibolite. The outcrop is disrupted, and there is a strong foliation parallel to poorly defined bedding. Pale-grey, massive to weakly foliated, fine-grained sandstone forms a small outcrop within BIF ridges 7 km north-northeast of Windarling Peak (MGA 703650E 6679170N).

Metamorphosed chert (*Ac*) is present at all stratigraphic levels within the lower greenstone succession on JACKSON. It typically consists of laminated to thinly bedded units of microcrystalline to recrystallized, fine-grained quartz, with minor amounts of iron oxides. Grey and white banded chert is most common, but ferruginous and jasperoidal layers are also present. A lateral transition to BIF is marked by an increase in the proportion of iron oxides and jasper bands. Small-scale, tight to isoclinal (locally chaotic) folds are common.

Metamorphosed BIF with minor ferruginous chert (*Aci*) forms prominent ridges in the central and northern parts of JACKSON. These siliceous metasedimentary rocks are banded on a millimetre to centimetre scale, with steel-grey to black magnetite–hematite-rich layers alternating with red, jasperoidal laminae. Where the latter are dominant (e.g. at Yenyanning Hill) the BIF grades into jaspilite (*Acj*), in which jasper bands form up to 90% of the unit. In both the BIF and jaspilite, white to black, cherty to fine-grained, quartzose intercalations are also present. Despite strong recrystallization, primary fine laminations up to 5 mm thick, defined by varying iron-oxide content, are preserved. Ripple-like structures 7 km north-northwest of Windarling Peak (MGA 719860E 6677880N) consist of small-amplitude undulations of bedding that are typically sinuous and broken up into short, curved crests (Fig. 4). They commonly bifurcate along their length, with a preferred orientation. These structures resemble current ripples (cf. Reineck and Singh, 1980; Nichols, 1999), and although current-generated structures within Archaean BIFs are rare (Trendall, 2002), they have been described from a few localities (Beukes, 1973). More irregular undulations (e.g. MGA 715660E 6678590N) may be related to soft-sediment deformation. Angular slabs, 7 km north-northeast of Windarling Peak (MGA 718350E 6677030N), may have been broken during dewatering. Breccias consisting of beds broken up into tablets, up to 10 cm long and set in a white quartz

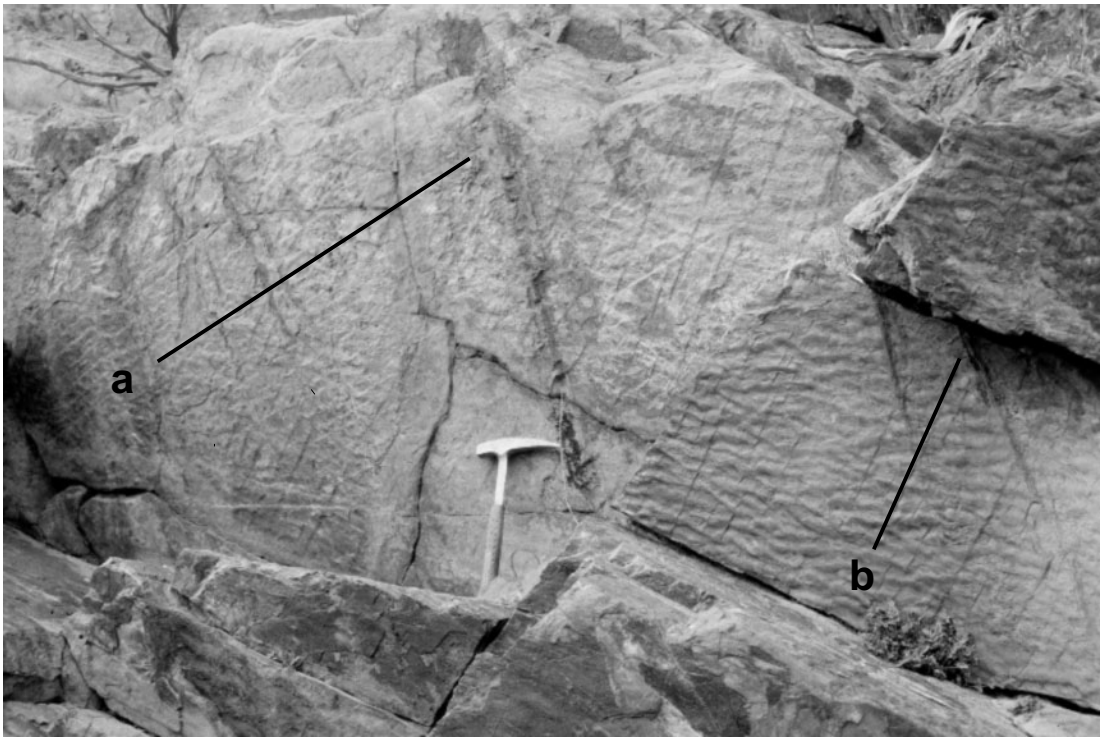

AR4 19.03.02

Figure 4. Sinuous ripple-like structures in banded iron-formation. These structures are on a north-northwesterly facing bedding surface, 7 km north-northwest of Windarling Peak (MGA 719860E 6677880N). These undulations of the bedding surface consistently bifurcate towards the west (right-hand side of photograph). A weak crenulation cleavage (a) dips at a low angle towards the northeast, whereas a set of fractures (b) dips more steeply towards the northeast

Figure 5. First vertical derivative aeromagnetic image of JACKSON (based on 400-m line-spaced data)

cement, are relatively common on the northern flank of Muddarning Hill. They are interpreted as late depositional features. Fractures and small-scale faults are common at some localities. Some tight to isoclinal folds are clearly parasitic to macroscopic structures, but some chaotically folded horizons might be due to soft-sediment deformation. Small-scale brecciation is common along crosscutting quartz veins. Individual ridges may be characterized by a single BIF unit, a few hundred metres thick (e.g. at Muddarning Hill, Mount Jackson, Boondine Hill, Yeeding Hill, Curragibbin Hill, Buddarning Peak, and Muddahdah Hill), or several BIF units (e.g. at Windarling Peak and to the north) that are only up to a few tens of metres thick. In the latter case the material between BIF units is commonly covered by scree or lateritic duricrust, but small outcrops of ferruginous metasedimentary rocks (mudstone, siltstone, and sandstone) and metabasalt are present locally. All BIF units have a strong positive response on magnetic images and form the most prominent aeromagnetic features on JACKSON (Fig. 5). The region has been extensively explored for iron deposits (see **Economic geology, Iron**).

Quartz-bearing talc schist (Altq)

Strongly deformed, quartz-bearing talc schist (*Altq*) is exposed near abandoned mine shafts about 8 km south-southeast of Mount Jackson Homestead (MGA 706600E 6649530N). This rock type is characterized by angular to subrounded quartz grains, up to 2 mm across, set in a white, fine-grained, talcose matrix. The schist is part of a sequence of strongly foliated, commonly silicified, dominantly mafic rocks, immediately east of the Koolyanobbing Shear Zone. Crosscutting quartz veins in the area are also sheared and brecciated, and bright-green stains in mafic schists and quartz veins indicate chromium remobilization. The unusual combination of talc and quartz in the schist at this locality may have resulted from grinding and shearing of quartz veins in mafic and ultramafic rocks during deformation along the Koolyanobbing Shear Zone.

Upper greenstone succession

Marda Complex (AfM, AfMd, AfMf, AfMi, AfMiy, AfMp, AfMr, AfMt, AfMx, AfMs, AfMsc, AfMsh, AfMshd, AfMsq, AfMss)

The Marda Complex comprises metamorphosed, acid to intermediate volcanic rocks and associated meta-sedimentary rocks over an area of about 600 km^2 in the northern part of JACKSON. The complex is surrounded by the lower greenstone succession in the core of the Bungalbin Syncline, and is intruded to the east by the Butcher Bird Monzogranite (Fig. 3; Hallberg et al., 1976; Taylor and Hallberg, 1977; Riganti et al., 2000). Rocks of the Marda Complex are poorly exposed in the southern part of JOHNSTON RANGE (Fig. 1), with outcrops confined to the area southeast of Pigeon Rocks. Marda Complex lithologies are also exposed in the central-western part of BUNGALBIN (Fig. 1), north and northeast of Bungalbin Hill (Chen and Wyche, 2001b). The Marda Complex comprises a lower part dominated by sedimentary rocks, and an overlying thick sequence of lava flows and pyroclastic rocks with only minor sedimentary intercalations (see **Stratigraphy, Upper greenstone succession**).

Where rocks of the Marda Complex are shown as undivided (*AfM*), they are typically deeply weathered and locally capped by silcrete. Their identification is based on fine grain size, poorly preserved volcanic textures, and association with nearby rocks that are more clearly volcanic in origin.

Metamorphosed dacite and rhyodacite of the Marda Complex (*AfMd*) are dark grey to green-grey rocks, commonly weathering to pink-grey and brown. They are invariably porphyritic, although size and abundance of phenocrysts vary considerably. Plagioclase is the dominant phase, as idiomorphic (less commonly broken) phenocrysts and glomeroporphyritic aggregates up to 4 mm across. Quartz and altered hornblende phenocrysts are also present, with quartz abundant in rhyodacite. Phenocrysts are set in a fine-grained quartzofeldspathic groundmass, locally extensively devitrified, with accessory opaque oxides. Iron-rich chlorite, sericite, and carbonate are secondary phases. Subrounded to ellipsoidal amygdales, up to 4 mm long, are locally common and typically filled by granoblastic quartz or chlorite (or both) and, less commonly, by sericite, calcite, and siderite. A weak to moderate foliation is defined locally by the alignment of fine-grained biotite and opaque minerals, as well as by flattening of amygdales. Dacitic and rhyodacitic rocks are a minor component of the Marda Complex, and appear to be largely confined to the lower part of the volcanic pile where they are generally associated with andesite. Geochemically the dacites and rhyodacites are quite evolved, with silica contents around 70 wt% (cf. GSWA 159377 and 159319 in Appendix 3).

Exposures of strongly deformed, deeply weathered felsic rock (*AfMf*), at various stratigraphic levels within the Marda Complex, are commonly quite small, extending for only a few metres in width and up to a few tens of metres in length. The largest exposure (MGA 717700E 6672700N) consists of a fine-grained, white, schistose rock, with no recognizable primary structures, thus preventing identification of a volcanic or sedimentary protolith. Old shafts in the schist are surrounded by quartz vein debris. A few hundred metres west of the Bullfinch–Evanston Road (MGA 723690E 6664630N), a pale- to medium-grey, sparsely porphyritic rhyolite grades into a strongly deformed and weathered felsic schist over a few tens of metres. The foliation in the schist trends northeasterly, the same direction as the fold axes in the banded ignimbrites immediately east of the rhyolite flow.

Metamorphosed andesite and basaltic andesite of the Marda Complex (*AfMi*) form relatively thick sequences of fine-grained grey rocks, commonly with a reddish-brown weathered surface. Andesite is common in the lower part of the volcanic pile, particularly in the east (see **Stratigraphy, Upper greenstone succession**), where it is intercalated with dacitic and rhyolitic lava flows and tuffaceous units. The andesite includes massive to porphyritic and subordinate fragmental types, and ranges in composition from basaltic to quartz-rich varieties. Massive andesite is fine grained, and characteristically consists of interlocking plagioclase and minor amounts of amphibole, with interstitial altered feldspar and subordinate quartz (Fig. 6a). Augite grains are preserved at some localities (e.g. MGA 716280E 663910N), and actinolitic amphibole is locally dominant in basaltic andesite (e.g. just west of the Bullfinch–Evanston Road, at the boundary with JOHNSTON RANGE). Pyrite is an accessory mineral, whereas chlorite and epidote minerals are common secondary phases. Porphyritic andesite is the dominant type, and is distinguished by phenocrysts of plagioclase and subordinate mafic minerals that constitute up to 40% of the rock (Fig. 6b). Plagioclase typically forms idiomorphic phenocrysts or glomeroporphyritic aggregates up to 1 cm (typically less than 2–3 mm). It is generally sericitized or saussuritized to various degrees, but twinning and, less commonly, concentric zoning are clearly distinguishable. Hallberg et al. (1976) noted plagioclase with complex oscillatory zoning, ranging from labradorite (at or near the cores) to calcic andesine in composition. Mafic phenocrysts include augite and hornblende (e.g. MGA 729200E 6657240N), which are commonly extensively replaced by actinolitic amphibole and chlorite. Sparse, euhedral magnetite phenocrysts are

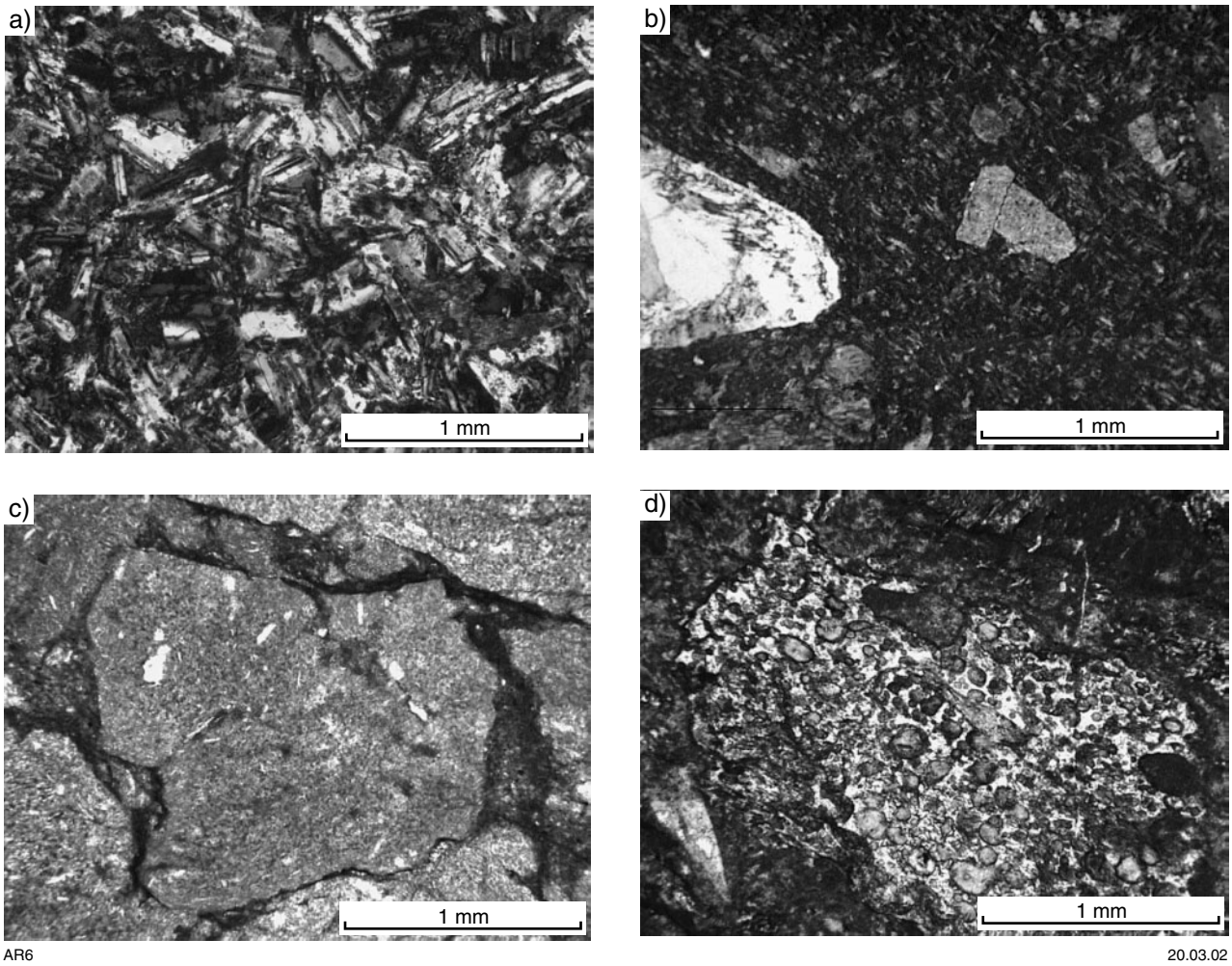

Figure 6. Textural characteristics of metamorphosed andesites from the Marda Complex: a) massive andesite, consisting of interlocking plagioclase laths with subordinate pyroxene and quartz; GSWA 159356, crossed polars; b) porphyritic, amygdaloidal andesite, with plagioclase phenocrysts and quartz-filled amygdales in a pilotaxitic groundmass; GSWA 159380, crossed polars; c) fragmental andesite, showing angular fragments of andesite with a pilotaxitic texture; GSWA 159352, plane-polarized light; d) fragmental andesite, showing a scoria fragment with chlorite-filled rounded vesicles; GSWA 159354, plane-polarized light

variably altered to leucoxene and titanite. Phenocrysts are set in a pilotaxitic groundmass of plagioclase laths up to 0.5 mm long, with interstitial opaque phases and altered augite (Fig. 6b). Relict flow textures are locally indicated by the alignment of plagioclase. Fragmental andesite is subordinate, and typically consists of dark-green, angular to subrounded, andesitic fragments up to 4 cm, cemented by small amounts of darker but compositionally similar material (Fig. 6c). Some fragments are characterized by a pilotaxitic texture, and may contain quartz- or chlorite-filled amygdales. Composite andesitic fragments and sparse broken plagioclase phenocrysts are subordinate, as are scoria grains with rounded vesicles outlined by fine opaque minerals and filled by fibrous chlorite (Fig. 6d). Welding and wrapping of the groundmass around the fragments were also noted.

Amygdales are a distinctive feature of many andesites in the Marda Complex and, where particularly abundant, amygdaloidal outcrops have been distinguished on the map (*Afmiy*). The amygdales are spherical or ellipsoidal to (less commonly) irregular, and range from a few millimetres up to 7 cm in diameter. Their abundance varies markedly from a few scattered amygdales to about 30% of the rock. Quartz is the dominant phase in the amygdales (Fig. 6b), and ranges from microcrystalline and polycrystalline aggregates to individual crystals. Amygdales may also contain chlorite and, less commonly, epidote minerals, pyrite, calcite or amphibole. When two or more mineral phases are present, they tend to be concentrically arranged; radial textures are rare. Siderite with quartz was noted in amygdales in basaltic andesite at the northern edge of Jackson. In some outcrops, (e.g. around MGA 727600E 6658500N) the amygdales show a strong preferred orientation (Fig. 7). The strong undulose extinction of the amygdaloidal quartz and the presence of a parallel fabric in the adjoining groundmass indicate that this is not a flow texture but that the amygdales have been tectonically stretched. Changes in orientation of the stretched amygdales from one exposure to the next suggest

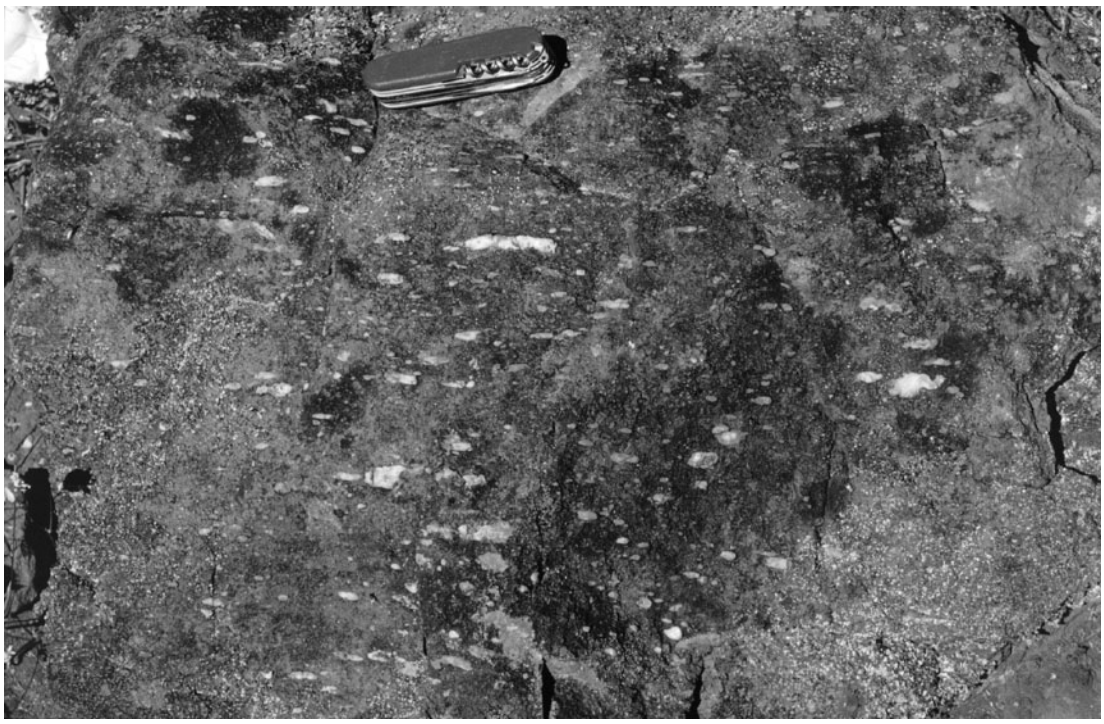

AR7 20.03.02

Figure 7. Strongly oriented quartz amygdales within metamorphosed andesite of the Marda Complex, 7 km east of Atkinsons Find (MGA 727340E 6658640N). Pocket knife for scale is 11 cm long

mesoscale folding. The bulk rock chemistry of the andesite is presented in Appendix 3 (GSWA 159393, 159356, and 159352; see **Geochemistry of the Marda Complex** for a discussion).

Metamorphosed rhyolitic to dacitic feldspar porphyry (*AfMp*) is very poorly exposed in the lower stratigraphic levels of the Marda Complex, and is associated with fine- to coarse-grained metasedimentary rocks. Good outcrops are near the Bullfinch–Evanston Road (around MGA 725500E 6671000N), and a few kilometres to the northwest. Here, porphyritic rocks are characterized by idiomorphic and glomeroporphyritic aggregates of plagioclase up to 5 mm long, with subordinate quartz, actinolitic amphibole, and chloritized mafic and skeletal magnetite phenocrysts. Apatite is a common accessory mineral, and is generally associated with amphibole and magnetite. All these phases are set in a finely granular groundmass of plagioclase laths surrounded by fine granophyric intergrowths, with interstitial biotite and chlorite. The distribution of the porphyry exposures and the attitude of the associated metasedimentary rocks (as inferred from sedimentary textures) indicate a broadly conformable relationship between the two lithotypes. However, the abundance of granophyric intergrowths in the porphyries suggests that they may be high-level intrusions into a sedimentary package, rather than flows. A geochemical analysis from a rhyolitic porphyry 17 km east of Mount Jackson is reported in Appendix 3 (GSWA 143354).

Metamorphosed rhyolite lava flows (*AfMr*) are at all stratigraphic levels within the Marda Complex. The largest exposures are shown on the map, but rhyolite flows up to 1–2 m thick are also present in ignimbrite and andesite units, and within the lowermost sedimentary package. The rhyolite is massive to strongly foliated, dark to light grey, and typically weathers to pale yellow-green, pale green-grey or pink-brown and creamy hues. Texturally the rhyolite varies from fine grained and massive to porphyritic, with or without flow banding. Plagioclase- and quartz-phyric rhyolite varies from sparsely to densely porphyritic. Plagioclase forms idiomorphic grains or glomeroporphyritic aggregates up to 7 mm long (Fig. 8a,b), which are typically sericitized, but partly replaced by epidote in places. Quartz forms rounded to idiomorphic grains with square to pseudohexagonal sections up to 3 mm across, and commonly displays embayed outlines indicating resorption (Fig. 8a,b). Magnetite, K-feldspar, and mafic phenocrysts (now altered to chlorite and titanite) are subordinate, and fine-grained rhyolitic fragments are present locally (Fig. 8a). The phenocrysts are set in a quartzofeldspathic groundmass containing chlorite, white mica, and iron oxides that varies from very fine grained (Fig. 8a), with local perlitic textures, to an extensively recrystallized granular assemblage (Fig. 8b). Sericitization of the feldspar phenocrysts and the groundmass is present in all rhyolites, but is significantly more pervasive and advanced in those adjoining the Butcher Bird Monzogranite (see **Granitoid rocks**, *Agbb*), indicating that potassic metasomatism was associated with this intrusion. In addition to sericite alteration, silicification takes the form of discordant granoblastic quartz veins and local patches of coarse-grained quartz. Carbonate and epidote minerals are locally

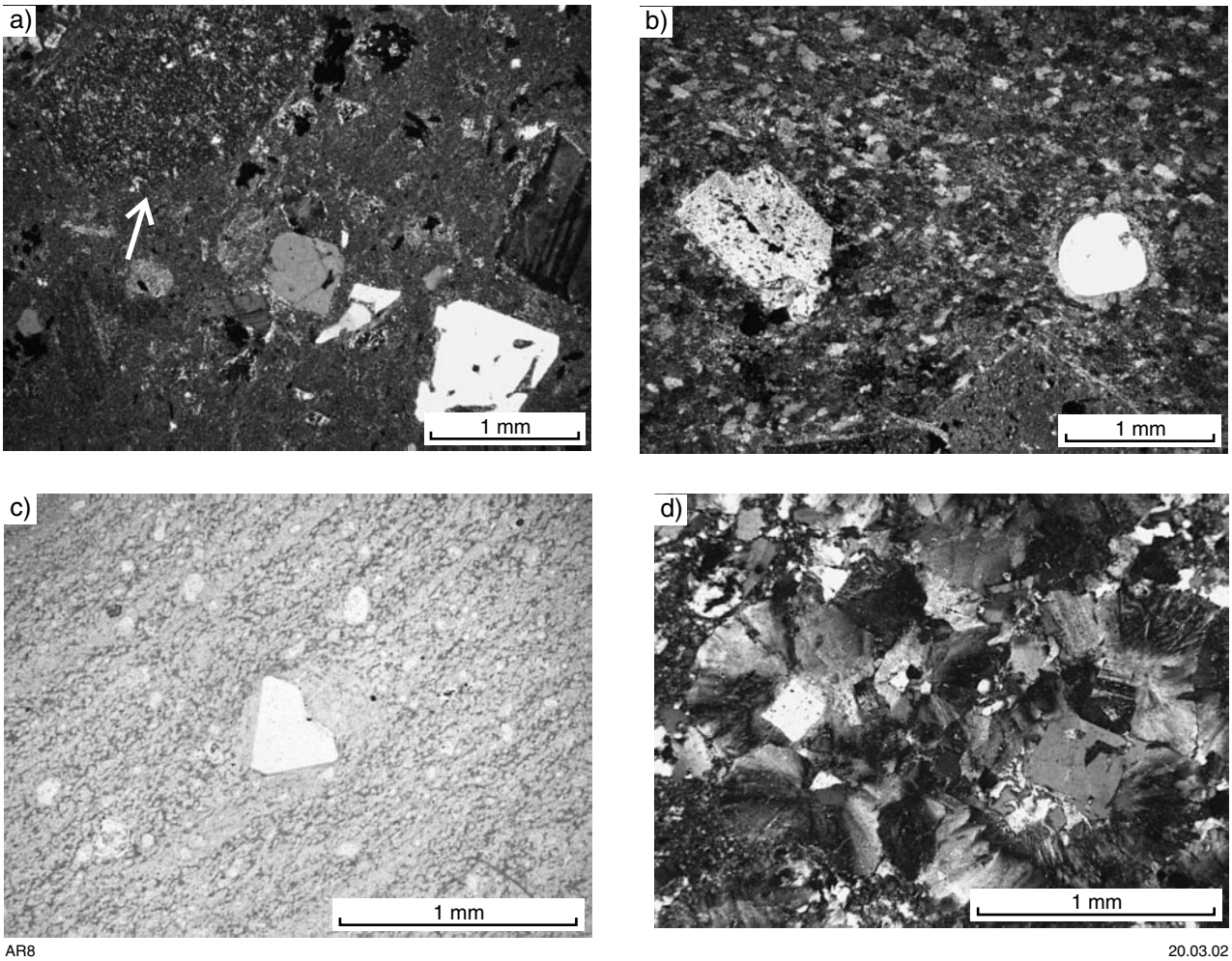

Figure 8. Textural characteristics of metamorphosed rhyolite flows from the Marda Complex: a) porphyritic rhyolite, with idiomorphic, partially sericitized plagioclase and resorbed quartz phenocrysts in a very fine grained groundmass; the arrow indicates a rhyolitic fragment; GSWA 159395, crossed polars; b) plagioclase- and quartz-phyric rhyolite, with recrystallized, sericitized groundmass; GSWA 164834, crossed polars; c) rhyolite flow bands wrapping around a quartz phenocryst; GSWA 159339, plane-polarized light; d) spherulitic textures radiating from quartz and plagioclase phenocrysts; GSWA 159385, crossed polars

abundant. A chemical analysis from one of the least weathered rhyolitic samples (GSWA 159348) is presented in Appendix 3. Flow-banded rhyolites have millimetre-sized bands defined by subtle changes in grain size or the abundance of clay and sericitic material (Fig. 8c), or both, with the bands typically enhanced by weathering. Banding commonly wraps around sparse quartz and feldspar phenocrysts, and quartz-filled amygdales are present in places. Devitrification textures are common in the rhyolites, and vary considerably in scale from isolated, radiating spherulites (0.2 mm in diameter) to coalescent spherulites (up to 1 cm across) nucleating on quartz and feldspar phenocrysts (Fig. 8d). Local autobreccia zones contain tightly packed, angular fragments and blocks of banded rhyolite, ranging from 2 to 30 cm in size (e.g. MGA 729010E 6658000N; Fig. 9).

Metamorphosed felsic tuffs and tuffaceous sedimentary rocks of the Marda Complex (*AfMt*) typically form thin, very fine grained, weathered units of limited lateral extent that are generally associated with rhyolitic rock types, and less commonly, with andesite (e.g. MGA 713920E 6671430N). One of the most conspicuous exposures is immediately north of the Diemals – Mount Jackson boundary fence (about 5 km north of Atkinsons Find, MGA 720500E 6664100N), where a thinly bedded, fine-grained, pale green-grey to black and dark-grey tuffaceous rock contains parallel laminations and possible graded bedding. Accretionary lapilli were observed in some of the layers. These features and the presence of altered feldspar microliths in a very fine grained groundmass, in which no individual mineral phases could be resolved, suggest that this might be an ash-fall deposit.

Metamorphosed ignimbrite (*AfMx*) is the dominant rock type in the Marda Complex (cf. Hallberg et al., 1976). The main outcrops are along the Bullfinch–Evanston Road, in the central-northern part of Jackson. Here, the ignimbrite forms thick sheets and ranges in composition from rhyolite to rhyodacite and, less commonly, dacite.

Figure 9. Autoclastic breccia with angular fragments of banded rhyolite from the Marda Complex, 8.5 km east-southeast of Atkinsons Find (MGA 729010E 6658000N)

Subordinate rhyolitic lava flows and minor tuffaceous and volcaniclastic units are also present. Rheomorphic and fragmental ignimbrite are the two main textural types, both containing textures indicative of subaerial deposition. Two samples of rhyolitic ignimbrite (MGA 720500E 6664440N and MGA 720730E 6659080N) yielded SHRIMP U–Pb zircon igneous crystallization ages of 2734 ± 3 and 2732 ± 3 Ma respectively (Nelson, 2001), confirming the previously determined conventional U–Pb zircon age of 2735 ± 2 Ma for the Marda Complex (Pidgeon and Wilde, 1990).

Rheomorphic ignimbrite is typically a grey to dark-grey rock, characterized by a prominent flow foliation that is commonly enhanced by weathering. The flow foliation is defined by a millimetre-scale eutaxitic texture with alternating black to dark-grey, glassy-looking layers and paler, greyish bands (Fig. 10a). Individual bands are continuous over a few centimetres only, and commonly tail off at the extremities. They most probably represent fiamme that have stretched as a result of secondary mass flow of the rock while still in a plastic state. The foliation wraps around sparse to locally abundant, idiomorphic, and, in places, broken plagioclase phenocrysts up to 3 mm in length, which are generally subparallel to the flow foliation (Fig. 10b). Subordinate, fine-grained lithic fragments are mainly of rhyolitic composition. Silicification is common in the form of quartz-filled cavities that are elongate parallel to the flow foliation, and is likely to have been caused by circulation of aqueous and gaseous solutions. In thin section, the darker bands are characterized by a central portion with granular, commonly sutured quartz, which grades into a fine-grained groundmass with devitrification textures (Fig. 10b). In the paler bands, quartzofeldspathic spherules are surrounded by brown, cloudy, ?clay-rich patches. Idiomorphic to subidiomorphic opaque minerals are ubiquitous accessory phases. Plagioclase phenocrysts have been extensively altered to sericite or saussurite, with local carbonate alteration of the groundmass. The flow foliation is typically steeply dipping to vertical, with considerable variations in strike over short distances. Outcrop discontinuity generally prevents an unambiguous assessment of whether these attitude changes are primary or reflect later tectonic modifications. Both igneous and tectonic fabrics can be clearly distinguished in a rhyolitic ignimbrite just west of the Bullfinch–Evanston Road, about 1.2 km north of the Diemals – Mount Jackson boundary fence. The highly contorted banding in many of the boulders at this locality is interpreted as a flow foliation, whereas the tectonic folding consists of steeply northeasterly plunging upright folds with wavelengths of about 50 cm and a locally preserved axial-planar cleavage (Fig. 11). Rheomorphic ignimbrites are typically rhyolitic in composition (GSWA 159346, 159392, 168961 in Appendix 3).

Devitrification textures are prominent in some ignimbrite exposures. A few hundred metres west of the Bullfinch–Evanston Road (MGA 723690E 6664590N), a rheomorphic ignimbrite grades into a northeasterly trending spherulitic rhyolite with a distinctive knobbly appearance on weathered surfaces. The spherulitic rhyolite unit is about 30 m thick, extends for about 200 m,

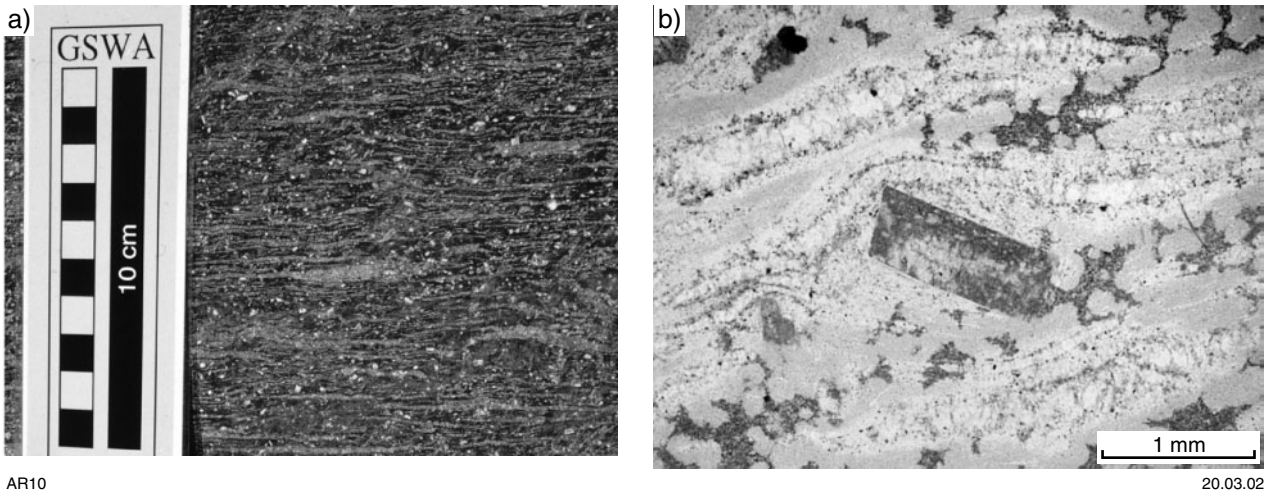

Figure 10. Flow foliation in rhyolitic rheoignimbrite from the Marda Complex: a) millimetre-scale alternating dark and pale-grey bands with scattered white plagioclase phenocrysts up to 3 mm (MGA 721880E 6665550N); b) flow foliation wrapping around an altered plagioclase phenocryst; the paler bands in the photograph consist mainly of granular quartz (devitrified glass; cf. Logfren, 1971); the darker bands are quartzofeldspathic in composition. GSWA 164840, plane-polarized light

and contains tightly packed, light-coloured, rounded spherulites in a medium-grey, fine-grained, locally banded, and welded groundmass (Fig. 12). The spherulites form discrete individuals or coalesce into larger masses, and vary in shape from spherical to ellipsoidal and irregular; the most elongate types have no preferential orientation. Their maximum dimension ranges from a few millimetres to 3 cm, but spherulites up to 10 cm are present in an outcrop about 1.5 km northwest of this locality (MGA 722990E 6665690N). Both the spherulites and the groundmass contain sparse, mostly euhedral plagioclase and minor K-feldspar and quartz phenocrysts, up to 3 mm across. The largest spherulites are lithophysae characterized by dark-green, fine-grained, chlorite-rich cores (Fig. 12) or, less commonly, hollow centres of various sizes and irregular shape. The secondary quartz in these voids confirms that the chlorite-rich portions were vesicles that were later infilled by low-temperature mineral phases. The spherulites represent devitrified glass and have a distinctive radial texture that overprints the flow foliation (Fig. 13). Poorly developed, irregular concentric zoning is locally preserved and consists of alternating grey, pale-green, and cream layers, commonly consisting of granular quartz that is considerably coarser than the material that constitutes the rest of these bodies, and subordinate chlorite patches. Some spherulites have a thin dark-brown to black rind.

Fragmental ignimbrite is typically a dark-grey, brown-weathered rock, which includes crystal and lithic lapilli tuffs as well as minor ash tuff and rare agglomerate. The ignimbrite is characterized by abundant angular to subrounded, mainly fine grained, lithic fragments, from less than 1 cm to a few centimetres in size (Fig. 14), but exceptionally up to 40 cm. These lapilli are typically set in a crystal-rich, fine-grained to aphanitic, largely quartzofeldspathic groundmass, with abundant plagioclase and subordinate quartz phenocrysts up to 4 mm across. Plagioclase grains are variably altered, whereas quartz crystals are commonly resorbed (Fig. 15a,b). Rare mafic grains, now replaced by chlorite or actinolite, are either prismatic or rhombic and may originally have been pyroxene or hornblende phenocrysts (Fig. 15a). Locally, flow foliation wraps around the lithic fragments, and is best observed on weathered surfaces where it is defined by dark-grey layers, a few millimetres thick, which alternate with less resistant, darker, and thinner bands. Microscopically the bands are defined by different proportions of quartz, feldspar, chlorite, and iron oxides. Some lapilli also display internal flow foliation, indicating fragmentation and incorporation of material from previously erupted volcanic units. The lithic fragments are compositionally varied (Fig. 15). Porphyritic, flow-banded or fine-grained (devitrified) rhyolitic to rhyodacitic lapilli are dominant (Fig. 15a,c). Andesite fragments are characterized by a pilotaxitic texture, with weakly oriented plagioclase surrounded by a dark-brown, cloudy matrix (Fig. 15d). Some fragments also have a poorly preserved vesicular texture. There are also cherty fragments (Fig. 15c), as well as locally dominant, dark relict vitric shards (Fig. 15b). Silicified areas with abundant quartz grains within the fragmental ignimbrite may represent fiamme (collapsed pumice). Carbonate, sericite, and chlorite alteration as well as kaolinization vary from minor to locally extensive. Due to the lithological variety of fragments and the higher proportions of andesitic components, the fragmental ignimbrites span a greater compositional range than the rheomorphic types, from rhyolitic to dacitic (GSWA 159335 and 168960 in Appendix 3).

Undivided metasedimentary rocks of the Marda Complex (*AfMs*) include poorly exposed, deeply weathered, locally strongly foliated, metamorphosed shale and siltstone. Primary structures have been largely obliterated, but a sedimentary protolith for these rocks is suggested by the

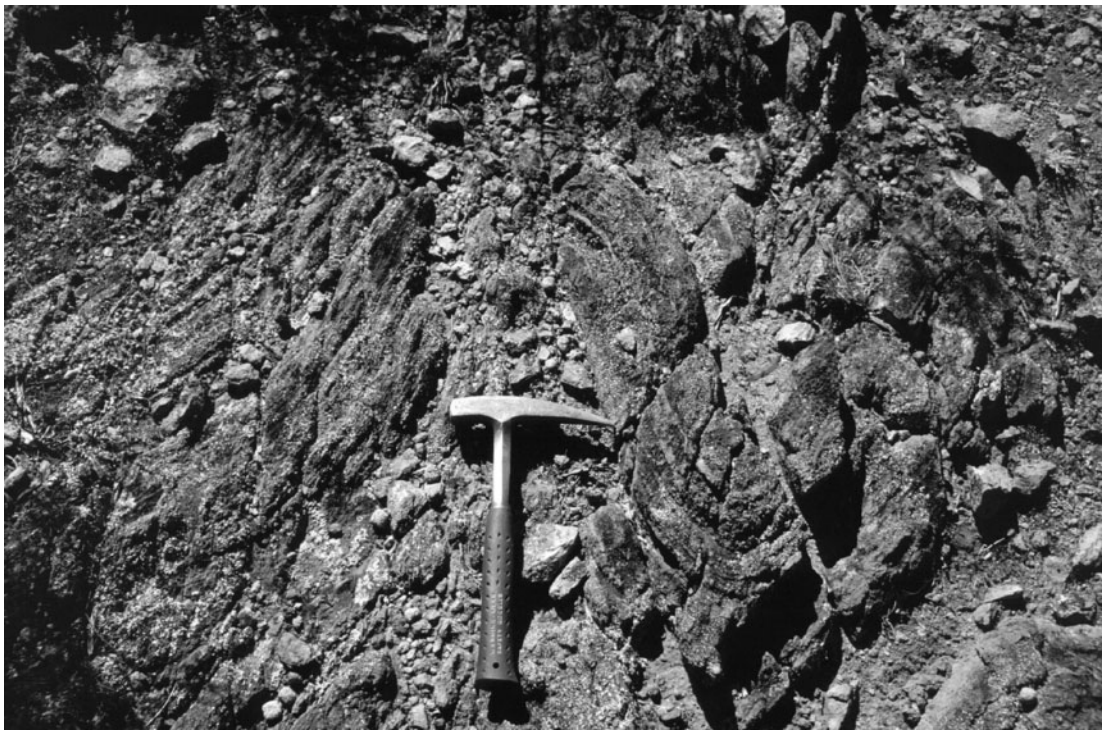

AR11 20.03.02

Figure 11. Folding of flow foliation in a rheomorphic rhyolitic ignimbrite from the Marda Complex (MGA 723790E 6664560N). A cleavage parallel to the axial plane of the folds is visible on the left-hand side of the photo

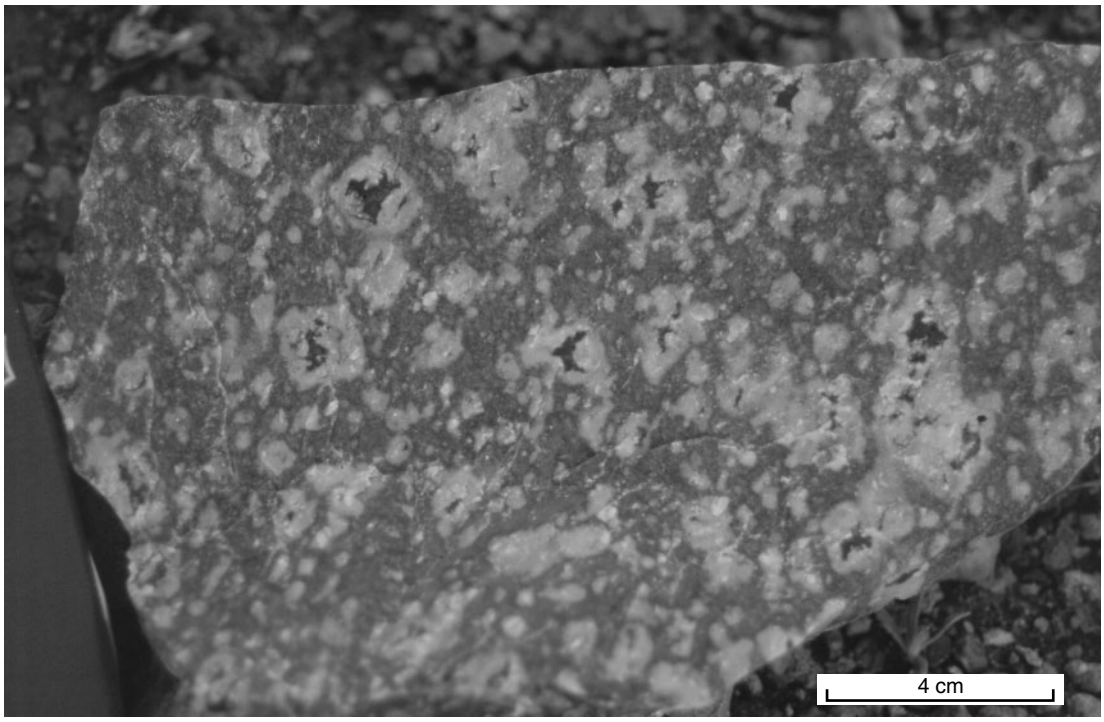

AR12 20.03.02

Figure 12. Individual to coalescent, white to light-grey spherulites, set in a medium-grey, fine-grained groundmass. The largest spherulites are lithophysae with a dark-grey to black, chlorite-filled centre (MGA 723690E 6664590N)

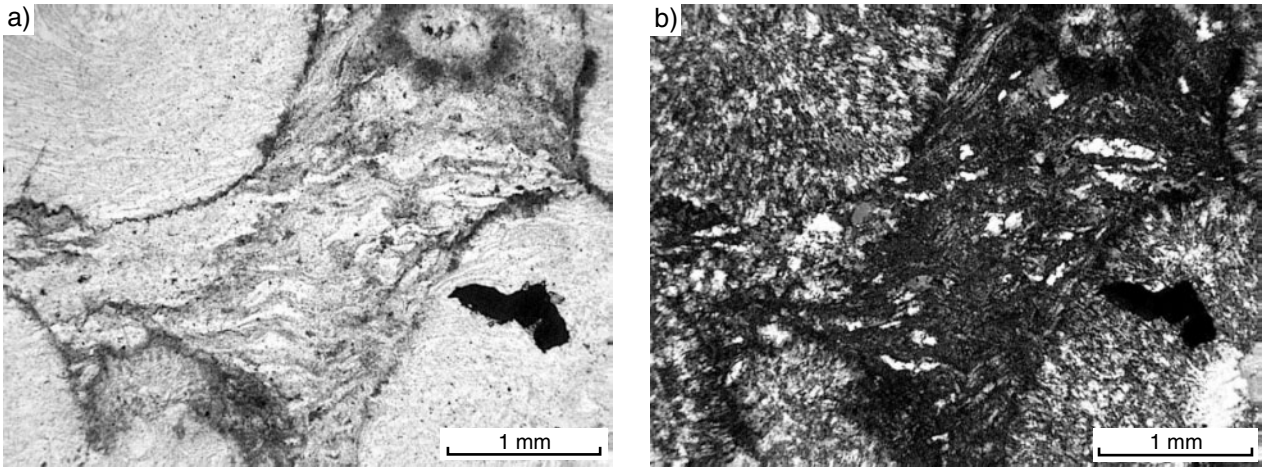

Figure 13. Devitrification textures in spherulitic rhyolite: a) flow foliation overprinted by spherulites; GSWA 159345, plane-polarized light; b) cross-polarized view displaying radial textures within the spherulites

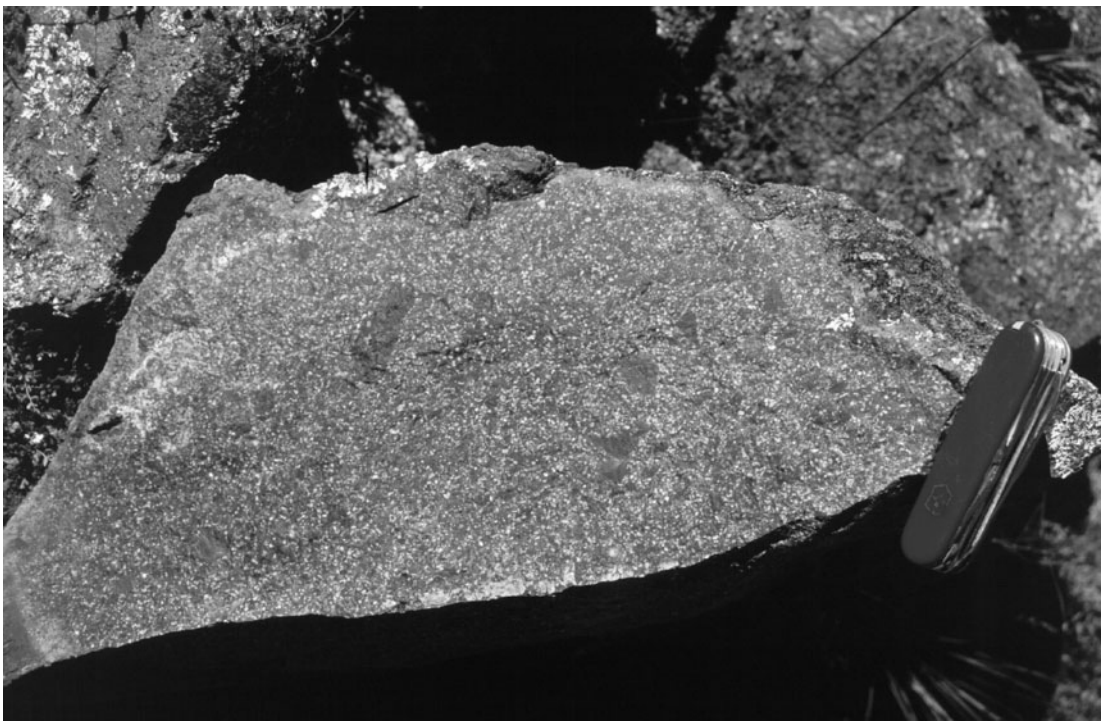

Figure 14. Rhyolitic ignimbrite near Marda, with centimetre-sized fragments and abundant plagioclase phenocrysts (MGA 720730E 6659080N). Pocket knife for scale is 11 cm long

spatial association with distinctively sedimentary lithotypes. However, it is possible that some rocks may have been deposited as tuffs.

Metamorphosed conglomerate of the Marda Complex (*AfMsc*) forms poorly outcropping units around the margin of the complex. The most prominent of these is a thick discontinuous unit that extends southeasterly from Allens Find to the eastern edge of JACKSON and onto BUNGALBIN (Chen and Wyche, 2001b). Subordinate, thinner conglomerate units are exposed along the northern edge of the complex. The conglomerate unit in the south is deeply weathered, with poorly sorted, commonly clast-supported beds characterized by abundant, tightly packed, angular to subrounded clasts of chert, minor jaspilitic BIF, and subordinate vein-quartz fragments. The clasts range in size from a few millimetres up to 15 cm (typically only a few centimetres), but can be up to 40 cm. Some BIF

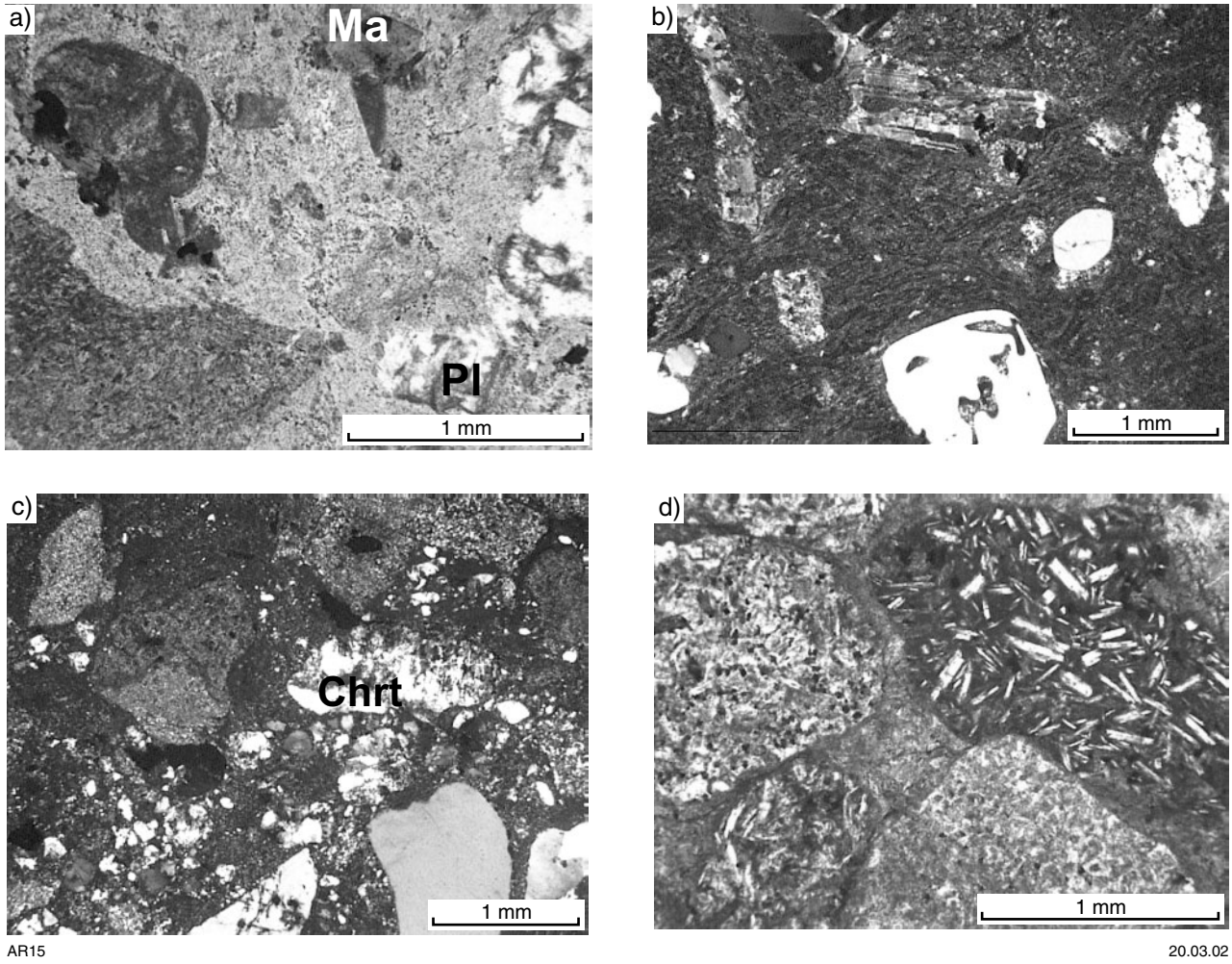

Figure 15. Photomicrographs of fragmental rhyolitic ignimbrite of the Marda Complex showing: a) andesitic and rhyodacitic fragments and altered plagioclase (Pl) and mafic (Ma) phenocrysts in a devitrified quartz–feldspar matrix; GSWA 159335, plane-polarized light; b) plagioclase and resorbed quartz phenocrysts in a matrix of welded glass shards; GSWA 159360, crossed polars; c) rhyolitic, quartz, and possible chert (Chrt) lapilli; GSWA 159337, crossed polars; d) andesitic fragments displaying a pilotaxitic texture (top right and bottom left corners), in association with dacitic lapilli; GSWA 159363, plane-polarized light

clasts contain folds, indicating deformation before erosion and redeposition as part of this unit. A ferruginous cement is typical, and there are some matrix-supported intervals. Intercalations of ferruginized, locally laminated siltstone as well as lenses of pebbly sandstone and weakly laminated sandstone are relatively common; their overall distribution represents a fining of this sedimentary package towards the north. Less ferruginous conglomerate beds are commonly clast supported, and typically contain highly polished, rounded to subangular, dominantly cherty clasts (Fig. 16). Weathering of the cement results in many conglomerate exposures being very poorly preserved and marked by low-lying mounds of loose chert pebbles. South of Allens Find, the conglomerate unit is flanked by jaspilitic BIF of the lower greenstone succession. To the north, it dips steeply under the felsic volcanic rocks of the Marda Complex. Although contacts are not exposed, metamorphosed rhyolitic lavas and deeply weathered, fine-grained, possibly tuffaceous, horizons are intercalated within the metasedimentary unit (cf. Kimber, 1987). The relationships with the adjacent rock types, lithological composition of clasts within the conglomerate, and broad northward-fining of the sequence suggest that these metasedimentary rocks were mainly sourced from, and deposited unconformably on, the lower greenstone succession at the very onset of the Marda Complex volcanic activity.

Conglomerate units at the northern edge of the Marda Complex differ from the thick southern exposures in that they form relatively thin intercalations (locally up to a few metres) within a clastic sequence dominated by sandstone. Conglomerate beds alternate with abundant medium- to coarse-grained sandstone and minor siltstone layers. The coarsest conglomerate beds are poorly sorted and clast supported, with well-rounded quartz pebbles and more angular chert clasts up to 5 cm long (typically around 1 to 2 cm). Chert clasts are aligned parallel to bedding. A few fine-grained clasts contain devitrification textures, possibly indicating some detrital input from felsic volcanic sources.

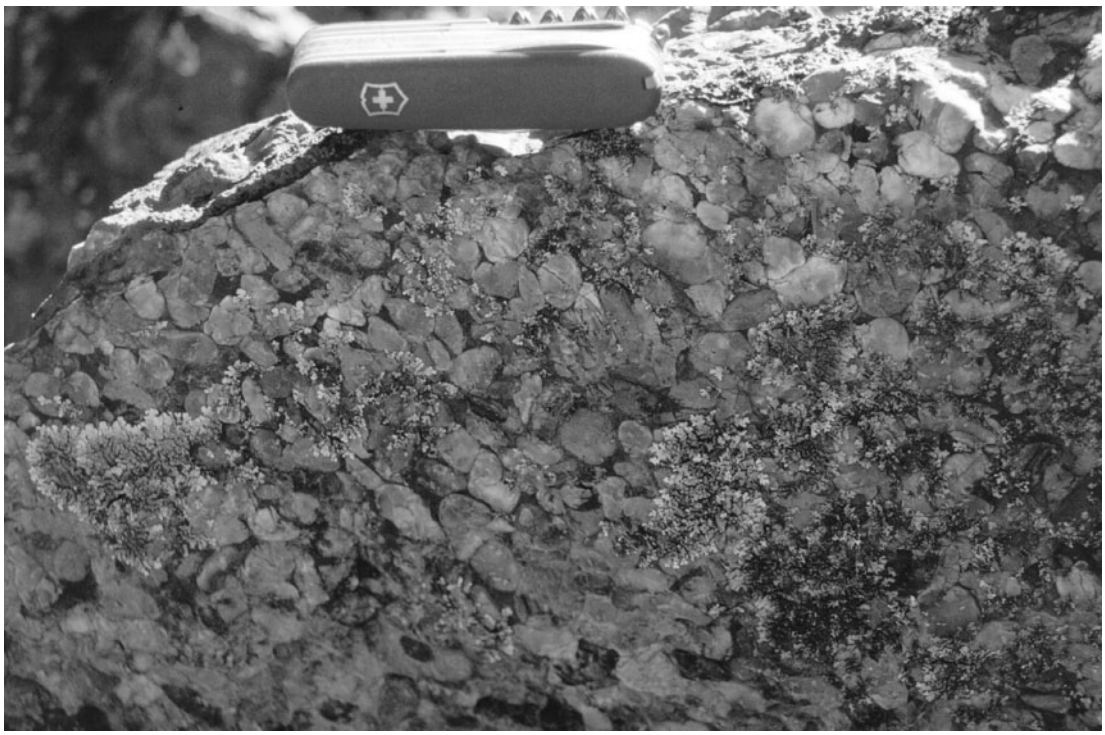

AR16 20.03.02

Figure 16. Clast-supported conglomerate bed near the base of the Marda Complex, 0.5 km west-northwest of Allens Find (MGA 716880E 6658240N). The pebbles are predominantly white and grey chert. Pocket knife for scale is 11 cm long

Finer grained beds are better sorted, with chert clasts up to 1 cm. The matrix is quartz rich and locally ferruginized.

An unusual oligomictic conglomerate unit is present about 7 km west of the Bullfinch–Evanston Road, just north of the Diemals – Mount Jackson boundary fence (MGA 716330E 6664080N). Here, a 10 m-thick, clast-supported conglomerate contains rounded to subrounded clasts of pale-grey rhyolite, from 1 to 15 cm in size, in a quartz-rich matrix (Fig. 17). The unit is crudely bedded, with conglomerate beds up to 1 m thick and subordinate, thinner layers of lithic arenite with parallel laminations. Grading indicates younging to the southwest, where the conglomerate is overlain by a massive andesite flow. Rhyolite clasts in the conglomerate are similar to rhyolites that outcrop poorly to the northeast.

Metamorphosed fine-grained sedimentary rocks of the Marda Complex (*AfMsh*) comprise alternating grey shale, siltstone, and minor fine-grained sandstone, commonly weathered to light grey and white and, in the most ferruginous units, to brown or purple. The metasedimentary rocks are intercalated with minor extrusive felsic rocks and rare, very fine grained, possibly tuffaceous horizons. Individual beds are typically less than 15 cm thick, but locally up to 50 cm thick. Sedimentary structures are poorly preserved due to moderate to strong foliation, but include fine parallel laminations, size grading, and local soft-sediment deformation. Cross-bedding is locally present in loose boulders (e.g. MGA 715290E 6672560N). In thin section, these poorly sorted and clast-supported, fine-grained metasedimentary rocks contain angular to subangular quartz and lithic clasts in a sparse sericitic to ferruginous matrix with locally abundant opaque dust. Quartz clasts are either monocrystalline or polycrystalline aggregates displaying various degrees of recrystallization. Lithic clasts include microcrystalline quartz (most probably chert), as well as micaceous and chlorite-bearing clasts probably derived from extrusive rocks.

Some of the finer and most aluminous, metamorphosed shale and siltstone contain sparse to abundant andalusite and possible staurolite porphyroblasts (*AfMshd*). The most notable exposures are in the northern part of Jackson, immediately west of the Bullfinch–Evanston Road. Here, the proximity of the andalusite-bearing metasedimentary rocks to the poorly exposed, but magnetically well defined, Chatarie Well Granite (Figs 3 and 5; see **Granitoid rocks**, *Agcw*) suggests that andalusite growth is related to the intrusion of this granite body. The andalusite porphyroblasts typically have square to prismatic sections up to 4 mm long and are partially to completely retrogressed to sericite and muscovite. Andalusite grains poikilitically enclose quartz grains and are wrapped around by the foliation, indicating metamorphism that pre-dates the major D_3 regional deformation event (see **Structural geology** and **Metamorphism**).

Metamorphosed quartzite and quartz arenite of the Marda Complex (*AfMsq*) are confined to a single exposure

AR17 20.03.02

Figure 17. Oligomictic conglomerate bed, intercalated within extrusive rocks of the Marda Complex, about 7 km west of the Bullfinch–Evanston Road (MGA 716330E 6664080N). The bed has poorly sorted, rounded to subrounded rhyolite clasts, with small amounts of quartz-rich cement

5 km northeast of Buddarning Peak (around MGA 710170E 6665610N). Here, quartz-dominated metasedimentary rocks form a small but prominent ridge flanked to the west by weathered shale and siltstone. The arenite varies from coarsely bedded in the southern part of the exposure (beds ranging from 10 to 30 cm thick) to more thinly bedded (beds around 5 cm thick) in the northern part of the ridge. The rock is commonly clast supported with subrounded quartz and subordinate chert clasts, ranging from 1 mm up to 2 cm, and little sericitic matrix. Pressure-solution of clasts and precipitation of secondary silica resulted in the formation of quartzite beds. Some of the thicker arenite beds are crudely graded from pebbly sandstone at the base to medium-grained sandstone at the top, with a younging direction to the west. Westward younging is also indicated by localized cross-bedding and centimetre-scale scour channels. Possible ripple marks are recorded from a single locality (MGA 710170E 6665300N).

Metamorphosed sandstone is the dominant lithotype exposed along the northern edge of the Marda Complex (*AfMss*). Commonly moderately to strongly foliated and ferruginized, the sandstone is thin to medium bedded, with individual layers up to 40 cm thick. Grain size grading is common, with medium- to fine-grained sandstone capped by siltstone, which is locally laminated. Younging is predominantly to the north-northwest, but local variations indicate the likelihood of structural complications. Thicker siltstone intercalations and subordinate conglomerate beds are also present, the former locally containing sparse andalusite porphyroblasts up to 3 mm (e.g. MGA 723350E 6672500N and MGA 725300E 6670500N). Most sandstone is poorly sorted, comprising angular to subangular clasts of quartz and chert in a ferruginous, clay- and sericite-rich matrix. An unusually fresh feldspathic wacke forms low bouldery outcrops about 1 km west of the Bullfinch–Evanston Road (MGA 724560E 6671520N). The wacke contains abundant angular clasts of plagioclase (oligoclase to andesine composition) and subordinate quartz, perthite, and lithic fragments (mainly microcrystalline quartz and andesite), indicating an extrusive volcanic source. The matrix contains quartz, biotite, and fine opaque needles. Subordinate muscovite is in the matrix and replaces plagioclase. The abundance of feldspathic clasts, poor sorting, and clast angularity as well as the clast-supported nature of this sandstone indicate a proximal depositional environment.

Diemals Formation (Aesh, Aeshd)

Clastic metasedimentary rocks of the Diemals Formation are confined to the northwestern corner of JACKSON, and best exposed about 6 km west of Muddahdah Hill. The bulk of the Diemals Formation is exposed on JOHNSTON RANGE (Fig. 1), where it comprises basal silty argillites (with lenses of polymictic conglomerate in the eastern exposures) overlain by sandstone and pebbly sandstone (Wyche et al., 2001; Walker and Blight, 1983). Fine-grained metasedimentary rocks of the Diemals Formation are moderately to strongly foliated, and weakly crenulated locally. These rocks are distinguished from similar shaly

units of the lower greenstone succession mainly because they lack BIF and chert intercalations. The contact with the lower greenstone succession is not exposed on JACKSON, but unconformable relationships have been described on JOHNSTON RANGE (Wyche et al., 2001).

Metamorphosed shale, mudstone, and siltstone of the Diemals Formation (*Aesh*) are fawn to yellow-brown and grey to black. Purple weathering and lateritic cappings are common, particularly in the most ferruginous units. Individual beds range in thickness from a few centimetres up to 80 cm, but are typically less than 15 cm. Grading from fine-grained sandstone at the base of single beds to finely laminated siltstone and shale at the top indicates younging of the succession towards the east-northeast. Rounded to subangular, black shaly clasts (from a few millimetres up to 3 cm across) are irregularly distributed near the base of some beds (e.g. MGA 704020E 6678080N). The most elongate clasts are commonly aligned parallel to bedding, and some contain a weak fabric that may be the result of deformation prior to erosion and redeposition. Dark-green chlorite-rich intercalations suggest derivation from a mafic source (cf. Wyche et al., 2001). Microscopically, these fine-grained metasedimentary rocks consist of various amounts of quartz, sericite, and opaque minerals (mainly iron oxides). Metapelite containing locally prominent, tightly packed andalusite porphyroblasts up to 3 mm across (*Aeshd*) outcrops just west of the Mount Jackson Homestead – Clampton mine track (around MGA 703000E 6677000N). Andalusite crystals are now almost completely altered to sericite, and are identified mainly by their subidiomorphic prismatic habit with square cross sections. As noted for similar exposures on JOHNSTON RANGE, proximity to the granite–greenstone contact and the intersection with granitoid rocks in RAB holes near this locality suggest that andalusite growth is probably due to contact metamorphism under locally developed upper greenschist-facies conditions (cf. Wyche et al., 2001; see **Metamorphism**).

Granitoid rocks (*Ag, Agf, Agb, Agm, Agmf, Agcw, Agmi, Agbb, Ang*)

Granitoid rocks, although not well exposed over much of the map sheet, underlie about 50% of JACKSON. Granitoids occupy extensive areas around and within the greenstone succession (Fig. 3), and are predominantly monzogranitic in composition.

Undivided granitoid rocks (*Ag*) are deeply weathered rocks, with a relict granular texture and quartzofeldspathic mineralogy, the original composition of which cannot be ascertained. Many of the exposures are at the base of breakaways, where deep weathering results in a distinct white colour on aerial photographs. The code (*Ag*) is also assigned to inaccessible exposures, for which compositional and textural data are not available. Strongly foliated granitoid rocks (*Agf*) in which deep weathering prevents identification of the original composition are shown separately.

Strongly foliated granite, interleaved with abundant amphibolite and subordinate mafic and ultramafic schists (*Agb*) outcrops extensively along the tectonic granite–greenstone contact at the eastern edge of the Koolyanobbing Shear Zone (Fig. 3). Slivers of fine- to medium-grained amphibolite, up to several metres wide, are elongated parallel to the north-northeasterly, steep to vertical foliation. The amphibolites are intercalated with medium- to coarse-grained monzogranite, which becomes more abundant to the west, away from the sheared granite–greenstone contact. Quartz veins parallel to the tectonic fabric are common in both lithotypes. Structurally controlled interleaving of amphibolite with granite is also present along the southernmost part of the Clampton Fault (Fig. 3; around MGA 699700E 6675400N).

Monzogranite (*Agm*) on JACKSON is typically massive, fine to coarse grained, and equigranular to locally porphyritic, with abundant pegmatite and aplite veins. Plagioclase is commonly zoned, and K-feldspar may form megacrysts up to 1 cm long. Biotite content varies considerably, and defines a weak foliation in some outcrops. Magnetite, apatite, titanite, and zircon are accessory phases. Sericitization of the feldspar is locally pronounced, and biotite is partly replaced by chlorite. About 1 km east of the Bullfinch–Evanston Road (MGA 718300E 6631300N), small outcrops of medium- to coarse-grained, equigranular monzogranite belong to a large pluton, the magnetic signature of which suggests that it might post-date shearing along the Koolyanobbing Shear Zone (Figs 3 and 5). On aerial photographs a distinctive concentric pattern highlighted by the alternation of barren and vegetated sandy patches probably reflects a circular fracturing of the intrusion.

Foliated monzogranite (*Agmf*) on JACKSON is present along the Koolyanobbing and Mount Dimer Shear Zones (Fig. 3). Mineralogically it is similar to the massive monzogranite, but is characterized by a moderate to strong, vertical to steeply dipping foliation defined by strings of strained quartz and feldspar, as well as the alignment of biotite and minor muscovite. Rafts of fine- to medium-grained, strongly foliated mafic rocks are present within the foliated monzogranite in the shear zones (e.g. along the Bullfinch – Mount Jackson Road, MGA 701270E 6654150N). At a number of localities poorly defined compositional banding results from the irregular distribution of biotite. Foliated monzogranite grades into granitoid gneiss in places (e.g. MGA 716930E 6625230N).

The Chatarie Well Granite (*Agcw*) is a very poorly exposed granite body in the northeastern part of JACKSON. Its identification as a separate intrusion is suggested by a distinct magnetic pattern (Figs 3 and 5) that allows the boundaries of the intrusion to be clearly delineated. The Chatarie Well Granite intruded the Butcher Bird Monzogranite (Figs 3 and 5), for which a U–Pb SHRIMP zircon age of 2730 ± 4 Ma has been determined (Nelson, 2001), and its northern boundary is possibly truncated by the Mount Dimer Shear Zone. Aeromagnetic images also highlight a ring pattern in the central-northern part of the intrusion. The circular structure is not exposed and its significance is unknown.

The Millars Monzogranite (*Agmi*) is an undeformed, leucocratic, pale-pink to cream, medium- to coarse-

grained, locally porphyritic monzogranite. It consists of megacrysts of K-feldspar (microcline) up to 2.5 cm long and quartz megacrysts up to 1 cm long in a medium-grained granular host, with accessory biotite, magnetite, apatite, and zircon. The Millars Monzogranite is best exposed near a gnamma hole (rockhole) beside the track leading to the Mount Jackson Homestead, about 0.5 km northwest of the Bullfinch–Evanston Road intersection (MGA 710400E 6642600N). At its northwestern extension the Millars Monzogranite is juxtaposed against strongly foliated granitic rocks in the Koolyanobbing Shear Zone, whereas to the north and east it intruded strongly foliated mafic rocks and crenulated tremolite schists of the lower greenstone succession. These relationships and the lack of deformation of the Millars Monzogranite indicate that this granite intrusion post-dates deformation in the Koolyanobbing Shear Zone. SHRIMP dating of zircons from the Millars Monzogranite produced an uninterpretable scatter of discordant analyses, attributable to variable alteration of zircon crystals. A chemical analysis of the Millars Monzogranite is presented in Appendix 2 (GSWA 168955).

The Butcher Bird Monzogranite (*Agbb*) is a pink-grey to red, massive, medium- to coarse-grained, plagioclase-phyric granophyre that intruded the eastern part of the c. 2733 Ma Marda Complex (Fig. 3). Petrographically the Butcher Bird Monzogranite is distinguished by prominent plagioclase and, less commonly, K-feldspar megacrysts, up to 6 mm long, that are commonly sericitized and cloudy. Subordinate quartz phenocrysts, up to 2 mm long, are typically resorbed, but some preserve a bipyramidal or pseudohexagonal habit. Granophyric intergrowths radiate from the plagioclase and quartz grains, and quartz phenocrysts are in optical continuity with the quartz in the granophyre (Fig. 18). Interstitial spaces are filled by finely granular plagioclase and quartz. Accessory minerals include altered mafic grains, magnetite, opaque oxides, apatite, and zircon. Biotite, actinolitic amphibole, epidote, chlorite, and traces of carbonate are probably late magmatic phases because some partly fill sparse miarolitic cavities a few millimetres across. Chemically the Butcher Bird Monzogranite is indistinguishable from the rhyolitic phases of the Marda Complex (cf. GSWA 168959 in Appendix 2 and Marda Complex samples in Appendix 3; see **Geochemistry of the Marda Complex**).

The outline of the Butcher Bird intrusion is evident on aeromagnetic images (Fig. 5). The intrusion has a sharp western contact that appears to crosscut Marda Complex rocks at different levels. In the field the contact of the Butcher Bird Monzogranite with the Marda Complex is marked by numerous granitic apophyses within flow-

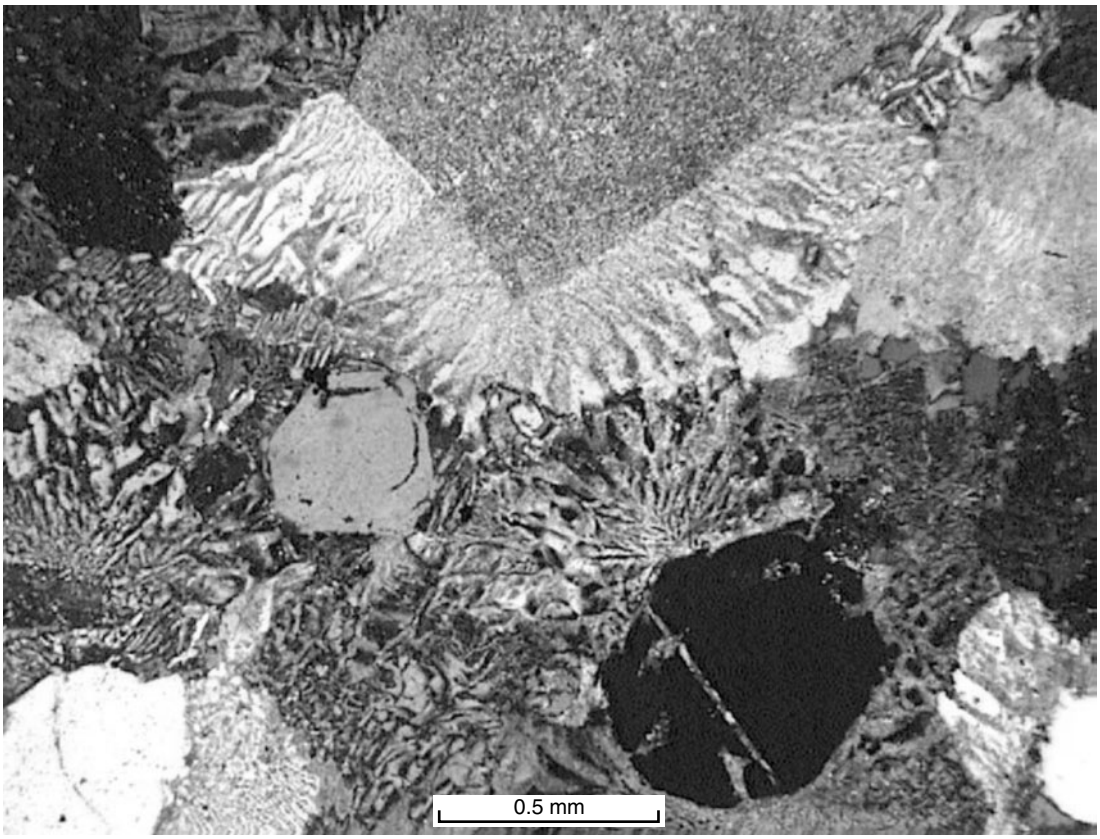

AR18 20.03.02

Figure 18. Textural characteristics of the Butcher Bird Monzogranite: granophyric intergrowths radiate from sericitized plagioclase megacrysts; euhedral quartz crystals show incipient resorption and are in optical continuity with the quartz in the granophyre. GSWA 164833, crossed polars

foliated rhyolites and ignimbrites, extrusive enclaves within the granite (up to a few square metres in surface extent), and the finer grain size of the granophyre adjacent to these extrusive lithotypes. Potassic metasomatism (mainly in the form of sericitization) is pronounced in the country rocks near the intrusive contact. The eastern contact of the Butcher Bird Monzogranite on BUNGALBIN is not exposed, but aeromagnetic images suggest that here the Butcher Bird Monzogranite intruded mafic rocks of the lower greenstone succession. A granite sample from about 12.5 km north-northeast of Mount Jackson (MGA 730250E 6654610N) yielded a SHRIMP U–Pb zircon age of 2730 ± 4 Ma for the Butcher Bird Monzogranite (Nelson, 2001), which is within error (95% confidence level) of the age of extrusive rocks of the Marda Complex (2732 ± 3 and 2734 ± 3 Ma; Nelson 2001). The ubiquitous distribution of granophyric intergrowths and the resorbed, subhedral quartz phenocrysts suggest that the Butcher Bird Monzogranite was emplaced at a high crustal level. The similarities in age and composition to the rhyolitic phase of the Marda Complex support the interpretation that the Butcher Bird Monzogranite represents a high-level intrusion of the magma that was the source of the Marda Complex rhyolitic rocks (Hallberg et al., 1976; Riganti et al., 2000).

Granitoid gneiss (*Ang*) outcrops adjacent to the Koolyanobbing Shear Zone (Fig. 3) and near the Yacke Yackine Dam (Fig. 19). Granitoid gneiss in the Koolyanobbing Shear Zone forms discrete zones in strongly foliated monzogranite. Banding in granitoid gneiss trends north-northwesterly, subparallel to the shear zone, in outcrops about 7 and 8 km southwest and west of the Mount Jackson Homestead (MGA 698850E 6651530N and MGA 694790E 6657580N respectively). The banding is defined by alternating fine- to medium-grained leucogranite, monzogranite, and granodiorite bands, ranging in thickness from 1 to 10 cm, with sharp to diffuse contacts. A 10 cm-thick mylonite zone is parallel to gneissic banding; however, there is considerable evidence to suggest that gneissic banding at many localities pre-date shearing along the Koolyanobbing Shear Zone. One such exposure is a large pavement of banded granitoid gneiss on the western side of the Bullfinch–Evanston Road, near the southern boundary of JACKSON (MGA 716930E 6625230N). Here the granitoid gneiss is mainly monzogranitic in composition, with subordinate pegmatite and biotite-rich microgranitoid bands. Some discordant pegmatite veins are tightly folded, with fold-axial traces parallel to the compositional banding. At this locality, the subvertical gneissic banding trends north to north-northwest, and is associated with a layer-parallel foliation. Both gneissic banding and foliation are overprinted by small-scale sinistral shear zones trending northwest (parallel to the Koolyanobbing Shear Zone; Fig. 3), suggesting that the gneissic banding pre-dates the main D_3 shearing event (see **Structural geology**; Chen and Wyche, 2001a). The granitoid gneiss near Yacke Yackine Dam has no obvious spatial relationship with any major regional shear zone, and contains extensive, undulating pavements of heterogeneous granitoid gneiss with a sharp to diffuse gneissic banding that trends northerly to north-northwesterly. Individual bands range in thickness from 1 cm up to 30 cm (but commonly less than 15 cm), and consist of alternating medium- to coarse-grained leucogranite and biotite-bearing granite as well as granodiorite and minor tonalite (Fig. 19). A weak, steeply dipping to vertical foliation, subparallel to the gneissic banding, is defined by elongate grains of strained quartz and feldspar and alignment of biotite. Asymmetric, Z-shaped folds defined by the gneissic banding are locally common. The outcrop is extensively intruded by granite, pegmatite, and quartz veins. These veins typically cut across the foliation, and crosscutting relationships and a range of deformation intensities for the veins indicate that there are several generations of intrusions. A porphyritic biotite granodiorite phase from this locality yielded a SHRIMP U–Pb zircon igneous crystallization age of 2711 ± 4 Ma (Nelson, 2001). The exposures at Yacke Yackine Dam form an isolated area of granitoid gneiss that is bound to the southwest by undeformed monzogranite and cannot be distinguished from the surrounding granite on aeromagnetic images (Fig. 5). The gneiss at Yacke Yackine Dam may represent an enclave of gneiss, developed during the major regional D_2–D_3 deformation, that has been enveloped by subsequent granitoid intrusion. A chemical analysis for this gneiss is given in Appendix 2 (GSWA 168956).

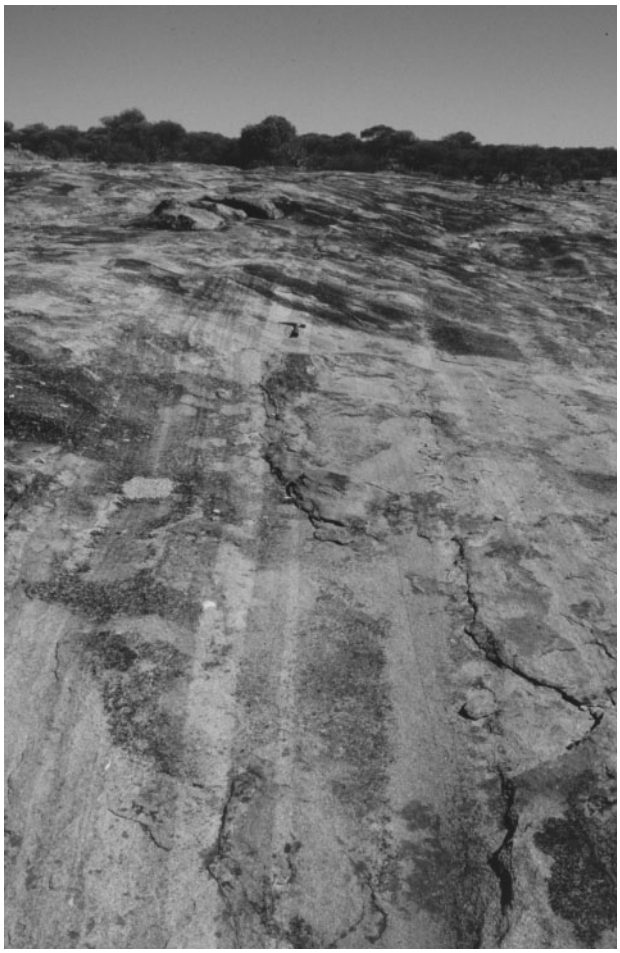

AR19 20.03.02

Figure 19. Pavement of granitoid gneiss with a northerly trending gneissic banding, west of Yacke Yackine Dam (MGA 693590E 6643850N)

Veins and dykes (*q, g*)

Quartz veins (*q*) are common on JACKSON, where they typically form resistant outcrops that can be easily traced on the ground and on aerial photographs. Veins typically consist of massive, milky to clear quartz and rarely contain significant amounts of other minerals. Quartz-vein debris 3 km north of Athlone prospect (MGA 704400E 6669350N) contains abundant iron-oxide stainings and kinked black tourmaline crystals up to 5 cm long and 1 cm across. Most quartz veins are oriented parallel to major structural features and aligned with magnetic lineaments (e.g. the Koolyanobbing and Mount Dimer Shear Zones). Some of these veins are strongly deformed, with a locally developed elongation lineation (e.g. MGA 707750E 6649550N). Gentle folding and jointing are also common, and fuchsite was remobilized in quartz veins adjacent to strongly sheared mafic and ultramafic schists (e.g. 7 km south-southeast of Mount Jackson; MGA 705700E 6650040N). North-northeasterly and subordinate easterly trending quartz veins are generally undeformed and cut across earlier structures (e.g. MGA 694500E 6660750N) and therefore post-date the main deformation events.

Fine- to medium-grained granitoid veins and dykes (*g*) have been mapped in the southeastern part of JACKSON. Mineralogical and textural similarities to the major granitoid bodies suggest that these granitoid dykes may be apophyses from these intrusions.

Gabbro and dolerite (*Æo*)

Undeformed gabbro and subordinate dolerite (*Æo*) are exposed at a few localities in the central and northeastern parts of JACKSON. No absolute ages have been determined, but in all exposures these mafic bodies have intruded rocks of the Marda Complex and associated granitoids, indicating a maximum age of c. 2730 Ma. About 6 km south of Windarling Peak, ignimbrite flows of the Marda Complex were intruded by northeast-trending differentiated mafic sills, which range from dolerite at the margins to medium-grained gabbro and diorite in the centre. The sills characteristically contain relict augite, largely chloritized or replaced by actinolitic amphibole, and generally smaller, extensively saussuritized plagioclase grains, with minor amounts of interstitial quartz and accessory opaque minerals (now largely represented by leucoxene). Prismatic grains of chlorite and serpentine may represent altered orthopyroxene crystals. Hallberg et al. (1976) attributed these dioritic dykes to the andesitic volcanic phase of the Marda Complex. Three kilometres northeast of Windarling Peak (MGA 722300E 6672300N), an equigranular, undeformed gabbro intruded strongly foliated fine-grained sandstone and siltstone assigned to the Marda Complex. Close to the contact with the metasedimentary rocks the medium-grained, mesocratic gabbro becomes progressively finer grained and darker in colour, with sparse plagioclase and pyrite grains in a dark-grey almost aphanitic groundmass, indicating chilling of the mafic intrusion against the metasedimentary country rocks. Primary igneous banding is present locally. About 9 km east-southeast of Windarling Peak (MGA 728900E 6667800N), a dark green-grey, very finely granular dolerite is juxtaposed against the Butcher Bird Monzogranite. The dolerite has a well developed interstitial texture, with twinned plagioclase laths in a tremolite–actinolite groundmass. Smaller exposures of a similar lithotype within the ignimbrite to the west (e.g. MGA 728100E 6667700N) are characterized by quartz(–pyrite) amygdales up to 1 cm long.

Mafic dykes (*Pdy*)

Prominent easterly and northeasterly magnetic lineaments that cut across all other structural trends on JACKSON (Fig. 5) have been interpreted as fractures filled by mafic and ultramafic dykes (*Pdy*). No surface expression of these dykes is known on JACKSON, but the coincidence between similarly oriented magnetic features and outcropping mafic dykes was also noted on EVERETT CREEK (Riganti, 2002). An age between 2.4 and 2.0 Ga was suggested by Hallberg (1987) for mafic and ultramafic dykes in the central part of the Yilgarn Craton, with their emplacement along tensional fractures related to post-cratonization tectonic activity at the northern and southern margins of the craton.

Stratigraphy

The Marda section of the Marda–Diemals greenstone belt comprises two distinct greenstone successions: a lower mafic- and BIF-dominated succession, and an upper succession comprising the felsic volcanic, volcaniclastic, and clastic rocks of the Marda Complex and Diemals Formation (Hallberg et al., 1976; Walker and Blight, 1983; Chin and Smith, 1983; Griffin, 1990). Limited geochronological data and a more complex deformation history (see **Structural geology**) indicate that the lower greenstone succession is considerably older than the upper succession. An age of c. 3.0 Ga is suggested for the lower greenstones by a SHRIMP U–Pb age of 3023 ± 10 Ma (Nelson, 1999) obtained for the Deception Hill Porphyry on JOHNSTON RANGE (which is regarded as a possible intrusion into the lower greenstone succession; Wyche et al., 2001), and by a Sm–Nd model age of 3050 ± 100 Ma for metabasalts near Diemals (Fletcher et al., 1984). Similar age data have been obtained for greenstone successions from the southern part of the Southern Cross and Murchison Granite–Greenstone Terranes (e.g. Wang et al., 1996; Pidgeon and Wilde, 1990). The age of the upper greenstone succession is well constrained at c. 2730 Ma by conventional and SHRIMP U–Pb zircon dating of felsic volcanic rocks of the Marda Complex (Pidgeon and Wilde, 1990; Nelson, 2001), and by a maximum depositional age of 2729 ± 9 Ma (Nelson, 2001) obtained from detrital zircons in the Diemals Formation on JOHNSTON RANGE. The contact between the lower and upper greenstone succession is not exposed on JACKSON, but an unconformable relationship is strongly suggested by relative outcrop distribution and attitudes of BIF units and Marda Complex rocks in the central-northern part of JACKSON. A locally tectonized unconformity between the lower succession and clastic rocks of the Diemals Formation is preserved on JOHNSTON RANGE (Walker and Blight, 1983; Wyche et al., 2001).

Lower greenstone succession

Although no formal stratigraphy has been recognized in the Marda–Diemals greenstone belt, good exposures in places, relatively simple structures, and a low metamorphic grade have allowed a stratigraphic framework to be established for the lower greenstone succession in this region (Wyche et al., 2001; Chen et al., in press). Three informal stratigraphic associations have been documented on the basis of their distinct lithological groupings and positions relative to the major BIF units within the belt: the lower, middle, and upper associations. The lower association comprises tholeiitic basalt with subordinate ultramafic, gabbroic, and mafic tuffaceous rocks, whereas the middle association is dominated by BIF and chert. The lower and middle associations have relatively uniform characteristics across the Marda–Diemals region, and are interpreted to have been deposited in a widespread extensional basin (Chen and Wyche, 2001a). The upper association contains a variety of rock types and varies significantly in different areas, suggesting that it might have been deposited in separate sub-basins (Chen and Wyche, 2001a).

On JACKSON the lower, middle, and upper associations are relatively well exposed, and laterally continuous from the northwestern corner to the southeastern part of the map sheet and extend farther east onto BUNGALBIN (Fig. 20). The upper association is also represented in the northwestern part of the map sheet. The lower and middle associations on JACKSON can be broadly correlated with stratigraphic successions in the Diemals and Die Hardy Range areas on JOHNSTON RANGE (Wyche et al., 2001; Chen et al., in press). The upper association partly resembles the sequence described on BUNGALBIN (Chen et al., in press), but its uppermost part is absent, possibly due to erosion at the onset of deposition of the Marda Complex. Absolute thicknesses are difficult to assess, but gravity modelling across the central part of JACKSON suggests that the lower greenstone succession extends to a maximum depth of 6 km and, although steeply dipping at the surface, has a relatively flat contact with underlying rocks of probable felsic composition (Dalstra, 1995, based on data from the Australian Bureau of Mineral Resources, BMR — now Geoscience Australia).

The lower association on JACKSON is structurally underlain by granitoid rocks, and no basement has been identified. The majority of the association consists of a thick pile of tholeiitic basalt with associated gabbroic sills and intercalations of spinifex-textured high-Mg basalt (Fig. 21). Local pillowed basalts indicate a subaqueous depositional environment. Thin chert and BIF units are present at all levels, but become progressively more abundant and laterally more continuous in the upper part. There are local mafic tuffaceous units and felsic volcanic intercalations. Near the base of the exposed stratigraphy, a discontinuous ultramafic unit includes serpentinized peridotite and tremolite schist.

A characteristic component of the lower association on JACKSON is a distinctive quartzite unit, which is exposed near the Mount Jackson Homestead. Griffin (1990) correlated this unit in the Marda–Diemals belt with similar, but much thicker and more extensive, quartzite units in the Illaara greenstone belt, about 100 km to the northeast (Wyche, 1999). However, the current mapping has not yet established a sufficiently well-constrained regional stratigraphy to support this correlation, because all known contacts between the basal quartzite and the adjacent granites are tectonic or intrusive in nature (Gee et al., 1981). The well-sorted quartzite units in the region are regarded as shallow-marine sediments, derived from a silicic source, that were deposited on a stable platform (Gee et al., 1981). Their position in the lower part of the exposed greenstone stratigraphy is a strong indication of the presence of a sialic basement to the greenstone sequence (Gee et al., 1981; Griffin, 1990). The quartzite unit near Mount Jackson Homestead could not be dated because insufficient zircons were recovered, but SHRIMP ages of c. 3.3 Ga from detrital zircons for quartzites at the base of the exposed greenstone succession of the Illaara greenstone belt to the northeast (Nelson, 2000) provide a maximum depositional age for the lower greenstone succession in the region.

The middle association of the lower greenstone succession on JACKSON is dominated by a major BIF, jaspilite, and chert unit, up to 800 m thick (Fig. 21), that forms prominent ridges up to 150 m above the surrounding areas. Fine-grained clastic metasedimentary rocks are subordinate, and the association lacks the abundant gabbroic intrusions observed on JOHNSTON RANGE (Wyche et al., 2001).

The upper association of the lower greenstone succession is only partly preserved on JACKSON (Fig. 20) and varies lithologically across the sheet area. In the central part of the map sheet the upper association consists of a thick pile of tholeiitic basalt with subordinate BIF intercalations, overlain by a prominent but discontinuous BIF unit. The basalts are best preserved at Yeela Hill and in the core of an F_1 antiform south of the Marda mining centre. High-Mg basalt and fine-grained ferruginous metasedimentary rocks, stratigraphically above the main BIF unit, are exposed locally at Buddarning Peak and a few kilometres southeast and northwest along strike, as well as 15 km east of Mount Jackson. At the latter locality and the Marda mining centre, rocks of the upper association are juxtaposed against sedimentary rocks of the Marda Complex (see **Upper greenstone succession**).

Structural complications and poor exposure due to deep weathering prevent a clear assessment of the lithostratigraphic sequence in the Windarling Peak and Muddahdah Hill areas. In the central-northern part of JACKSON, a prominent BIF and chert unit is underlain by ferruginized fine-grained clastic sedimentary rocks and only minor tholeiitic basalt. This sequence differs from the BIF assigned to the middle or upper associations on JACKSON. It does, however, resemble a part of the upper association exposed on the northeastern limb of the Bungalbin Syncline on BUNGALBIN (Chen et al., in press). In the Windarling Peak area, the BIF unit is commonly juxtaposed against Marda Complex rocks, except for an area 8 km northeast of Windarling Peak, where high-Mg basalt is present. Southwest of Muddahdah Hill, fine-grained clastic metasedimentary rocks are intercalated with BIF and chert layers. This association could represent either a sequence similar to that observed at Windarling

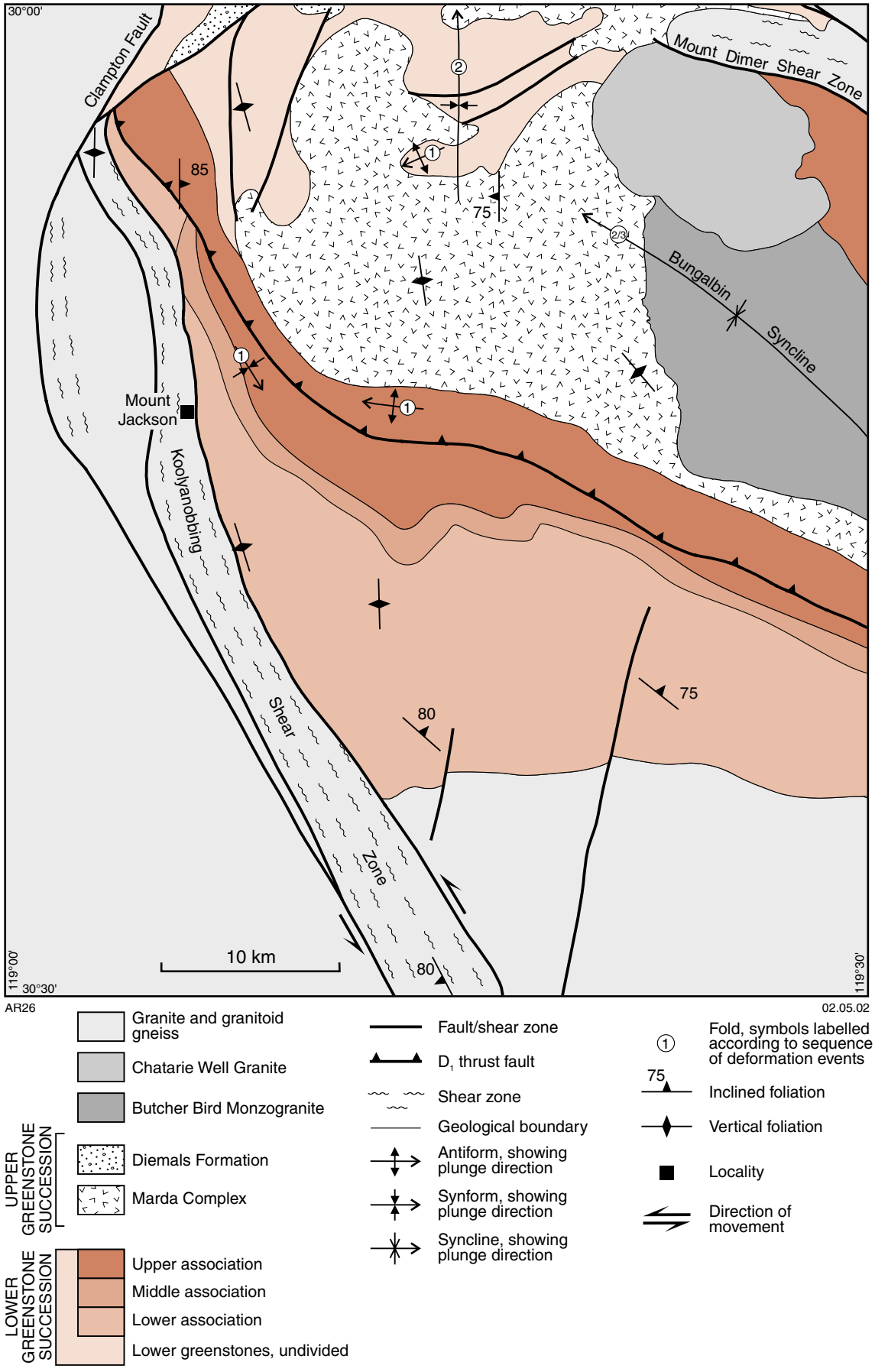

Figure 20. Simplified geological map of Jackson, showing distribution of the lower, middle and upper associations of the lower greenstone succession

Peak and on BUNGALBIN, or the distal equivalent of the quartz-rich, graded and cross-bedded sedimentary unit at the top of the middle association (immediately above the uppermost ridge-forming BIF unit) west of Pigeon Rocks on JOHNSTON RANGE (Wyche et al., 2001).

Although restricted by poor outcrop, mapping on JACKSON supports the observation made by Chen et al. (in press) that the upper association is lithologically varied. However, there is a broad similarity between the stratigraphy of the upper association on JACKSON and the lowermost part of the upper association on BUNGALBIN. This feature, coupled with the observation that the upper association is directly juxtaposed against the Marda Complex at a number of localities, suggests that part of the upper association stratigraphy on JACKSON was removed by erosion before or during the early stages of accumulation of the Marda Complex.

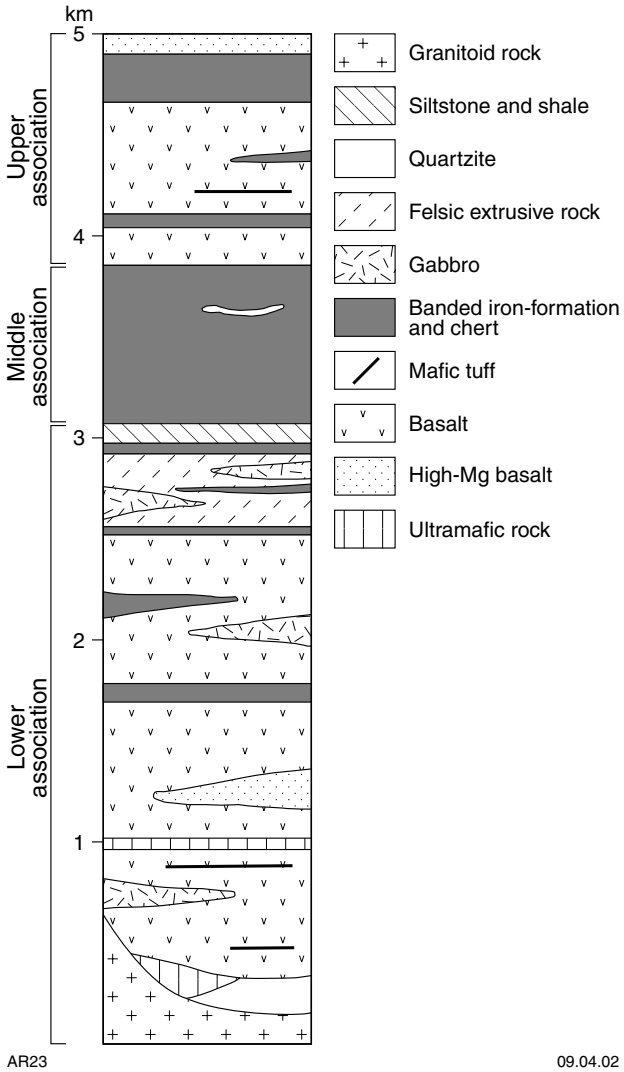

Figure 21. Schematic stratigraphic relationships in the lower greenstone succession on JACKSON

Upper greenstone succession

The upper greenstone succession is represented on JACKSON by the felsic volcanic and volcaniclastic rocks of the Marda Complex and the clastic sedimentary rocks of the Diemals Formation. The Diemals Formation is exposed only in the northwestern corner of JACKSON, with the main exposure farther north on JOHNSTON RANGE (Wyche et al., 2001). Fine-grained clastic rocks of the Diemals Formation are regarded as equivalent to similar rock types of the Marda Complex in the north (Walker and Blight, 1983). SHRIMP dating also suggests that rocks of the Marda Complex and Diemals Formation are broadly contemporaneous (see **Regional geological setting**). Detailed descriptions of the Diemals Formation and its stratigraphy are provided by Wyche et al. (2001).

The Marda Complex (Hallberg et al., 1976; Chin and Smith, 1983) occupies an area of about 600 km^2 in the northern part of JACKSON and in the core of the Bungalbin Syncline (Figs 3 and 22). It is surrounded by BIF units of the lower greenstone succession, which dip moderately to steeply towards the complex, and is intruded to the east by the Butcher Bird Monzogranite. Smaller areas of felsic volcanic rocks straddling the boundary between JACKSON and JOHNSTON RANGE are also attributed to the Marda Complex (Fig. 3); an exposure of altered felsic rocks and conglomerate just north of Mount Jackson may also represent a Marda Complex outlier.

Reconstruction of an accurate stratigraphy for the Marda Complex is hindered by discontinuous exposure, lateral facies variations, primary irregular flow morphologies, and superimposed structural complications. However, the Marda Complex can be broadly subdivided into a lower part dominated by clastic and volcaniclastic sedimentary rocks and an upper part comprising interfingering andesitic and rhyolitic lava flows with voluminous ignimbrite (Fig. 23; Chin and Smith, 1983; Riganti et al., 2000). Absolute thicknesses are difficult to determine, but gravity modelling of BMR data led Dalstra (1995) to infer a maximum thickness of about 6 km for the complex. The same data suggest that the Marda Complex is underlain by high density rocks of the lower greenstone succession (Dalstra, 1995). Metamorphism is typically of lower greenschist facies, but Hallberg et al. (1976) reported biotite hornfels and andalusite porphyroblasts in metamorphosed sedimentary rocks in contact with Marda Complex volcanic rocks.

The basal contact of the Marda Complex with the underlying BIF and basaltic units of the lower greenstone succession is not exposed on JACKSON. However, an unconformable relationship is suggested in the northern part of JACKSON, where the Marda Complex overlies BIF and sedimentary units of the lower greenstone succession that were folded and faulted before the emplacement of the complex (Fig. 3). On the southern side of the complex, the broadly conformable relationship between the Marda Complex and the underlying rocks suggests a disconformable contact.

The lowermost exposed part of the Marda Complex is composed of polymictic conglomerate, sandstone, and siltstone that locally interfinger with thin units of rhyolitic

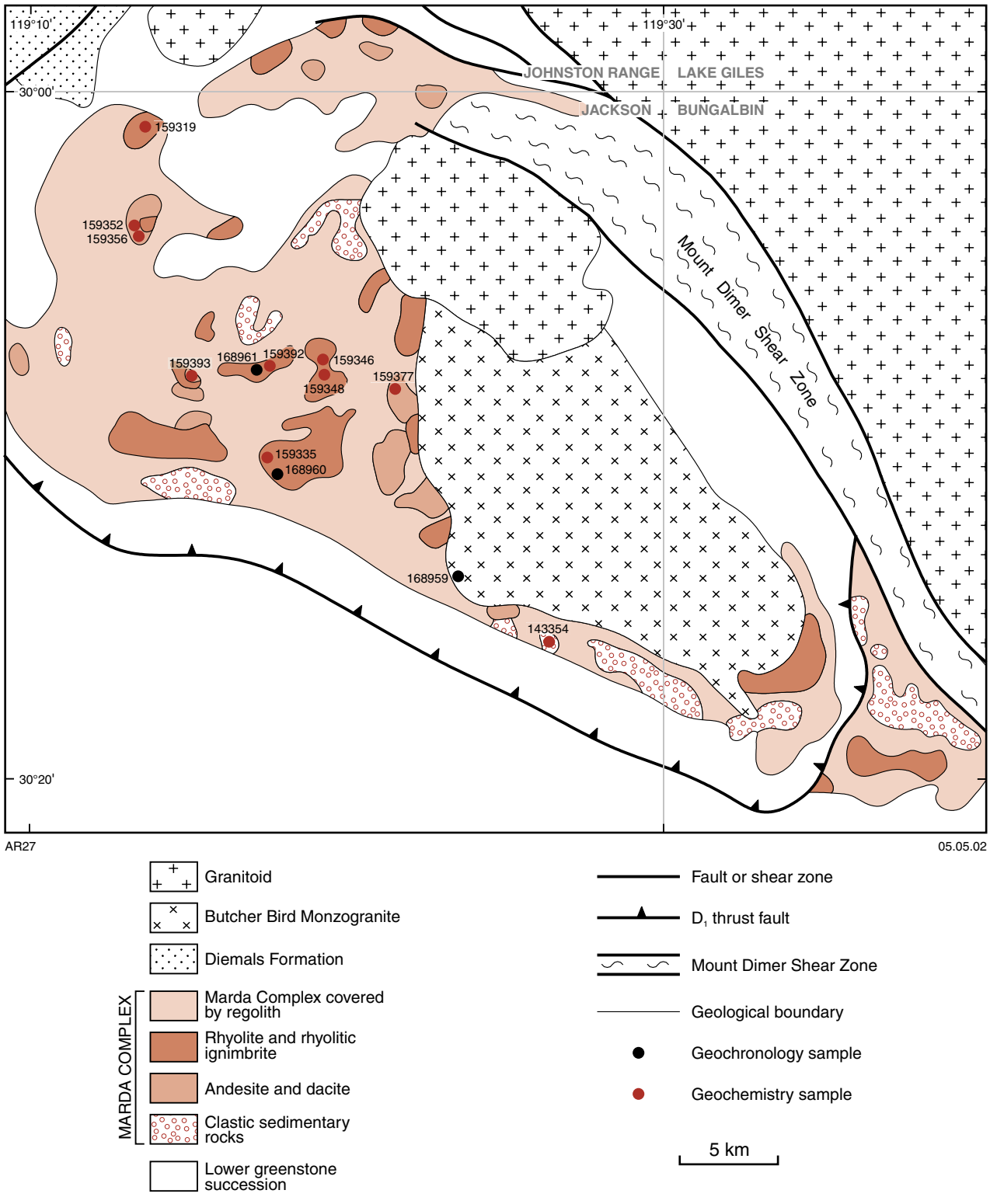

Figure 22. Simplified geological map of the Marda Complex on Jackson, Bungalbin, and Johnston Range, showing the distribution of major rock types and interpreted relationship with adjacent lower greenstone succession. Locations of geochemical and geochronological samples are also shown

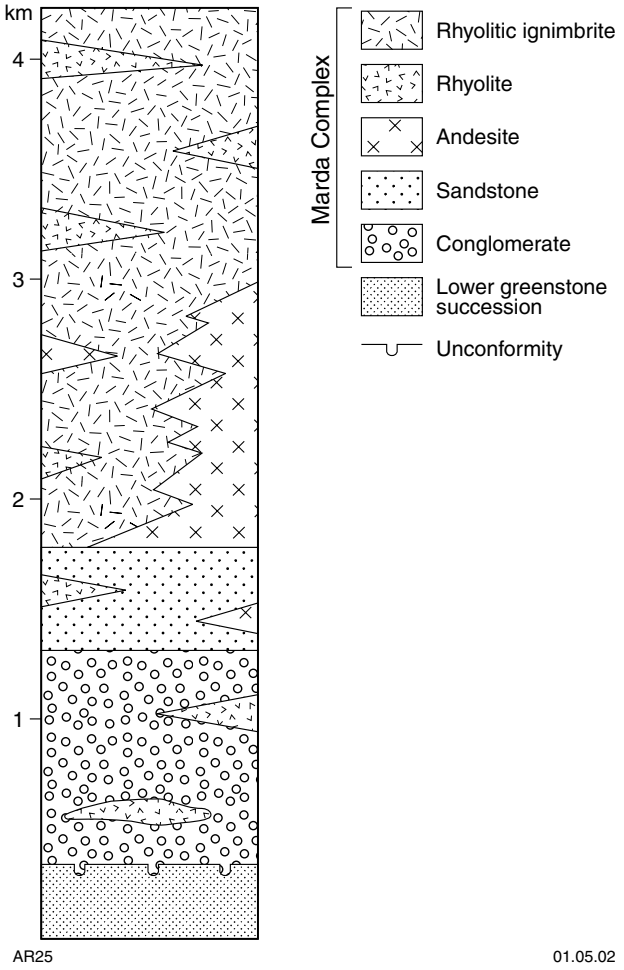

Figure 23. Schematic lithostratigraphic column of the Marda Complex

and andesitic volcanic rocks (Fig. 23). There are some differences in the successions from the south and the north. In the south the sequence is dominated by coarse sedimentary rocks with minor sandstone and siltstone. The composition of clasts in the conglomerate is strongly dependent on the adjacent rock types, with chert and BIF clasts the most abundant. Locally prominent felsic volcanic clasts are interpreted to be derived from contemporaneous felsic volcanism within the Marda Complex (Chin and Smith, 1983). The conglomerate is typically clast supported, with rounded to, less commonly, angular clasts up to 50 cm in size in a poorly sorted, commonly ferruginous, sandy and silty matrix. This sedimentary package broadly fines upward, with conglomerate mainly concentrated in the lower part and grading into lithic sandstone and siltstone. Sandstone beds are crudely graded and locally cross bedded; Chin and Smith (1983) also noted ripple marks.

In the northern part of the complex, the sequence is dominated by poorly sorted, well-bedded lithic sandstone and siltstone with only minor conglomerate. Scours and low-angle cross-bedding are common. A thickness of about 1500 m is indicated in the south, but thickness estimates are difficult in the north because of changes in the facing direction of the sedimentary succession, which suggests structural complications and some possible duplication by folding (cf. Chin and Smith, 1983). The immaturity of the sedimentary rocks at the base of the Marda Complex suggests proximal deposition. The clast composition indicates a predominant derivation from the lower greenstone succession with a limited contribution from felsic volcanic rocks that erupted at the same time as the deposition of sediments. Sedimentary structures indicate a moderate to shallow water depth.

Overlying the sedimentary rocks at the base of the Marda Complex is a thick sequence of felsic (acid to intermediate) volcanic rocks (Fig. 23). Andesite and subordinate dacite and rhyodacite are predominant in the eastern part, where they interfinger with rhyolitic ignimbrite and lava flows, and are intruded by the Butcher Bird Monzogranite. Andesite is more sporadic in the north, where it appears to be confined to the lower part of the volcanic pile. Voluminous rhyolitic ignimbrites with intercalations of rhyolitic lava flows dominate the western and upper parts of the Marda Complex (Figs 22 and 23). They interfinger with and overlie the andesites in the east, but lie directly over sedimentary rocks in the west. The rhyolitic rocks preserve evidence of welding and rheomorphic flow indicating a largely subaerial deposition, an inference supported by the paucity of associated sedimentary rocks (Hallberg et al., 1976; Riganti et al., 2000).

Flow foliation in the ignimbrite is the best indicator of original flow attitudes. However, outcrop discontinuity prevents a clear assessment of whether attitude variations of the igneous foliation over short to medium distances are related to primary flow morphology and topographic irregularities or to subsequent structural modifications. Both highly contorted flow foliation and tectonic folding at a local scale suggest superposition of primary and secondary structures, therefore, a thickness estimate of the volcanic portion of the Marda Complex has not been attempted.

The Diemals Formation is a sequence of clastic metasedimentary rocks comprising metamorphosed shale and siltstone with lenses of polymictic conglomerate at the base, overlain by sandstones and pebbly sandstones, exposed mainly on JOHNSTON RANGE (Wyche et al., 2001). The formation was formally defined by Walker and Blight (1983), but it has now been extended farther south to include fine-grained metasedimentary rocks exposed in the northwestern part of JACKSON. Here the Diemals Formation consists of a succession of metamorphosed siltstone and fine-grained sandstone, and is juxtaposed against metabasaltic rocks of the lower greenstone succession. Chlorite schist, phyllite, and metamorphosed graphitic shale horizons in the lower part suggest derivation of the basal sediments from a mafic to ultramafic source, and locally developed anoxic conditions. A fluviatile to lacustrine environment of deposition has been proposed for the Diemals Formation (Walker and Blight, 1983; Riganti et al., 2000; Wyche et al., 2001).

Geochemistry of the Marda Complex

Twelve samples of Marda Complex rocks were analysed for major and trace elements, including three samples of massive andesite (amygdaloidal samples were not considered), four of rhyodacite and dacite, and five of rhyolite. The analytical techniques and results are presented in Appendix 3. With the exception of the alkali elements and rubidium, most major and trace elements show fairly coherent trends with only limited scatter on most variation diagrams, indicating that synvolcanic alteration and metamorphism did not significantly modify the chemical composition of these rocks. In the following discussion, the geochemical data obtained by GSWA are integrated with those presented by Hallberg et al. (1976) and Taylor and Hallberg (1977).

Whole-rock geochemistry of the Marda Complex volcanic rocks documents a broadly continuous geochemical series with a small gap at about 64 to 68 wt% SiO_2, which effectively separates the andesitic and rhyolitic lithotypes (Fig. 24a; cf. Hallberg et al., 1976). The andesites form a continuous series from basaltic andesite (55 wt% SiO_2) to a silica-rich end member (up to 64 wt% SiO_2). Dacitic to rhyodacitic and rhyolitic rocks also form a continuum from 68 to 77 wt% SiO_2. Compositional gaps between the andesite and the rhyolite–dacite groups are evident on other variation diagrams (particularly MgO, CaO, FeO, Th, U, V, and Sc vs SiO_2). Andesitic and rhyolitic rocks define a distinctive calc-alkaline trend on the AFM diagram, which contrasts with the pronounced tholeiitic affinity of the lower greenstone succession (Fig. 24b).

The chemical distinction between andesites and rhyolite–dacite rocks is even more evident on C1 chondrite-normalized rare earth element (REE) plots (Fig. 24c). Andesites have smooth fractionated profiles, whereas rhyolitic rocks are characterized by variably pronounced negative Eu anomalies. These characteristics preclude a simple crystal fractionation of the more acid rocks from the andesites, but would require a two-stage model with extraction of plagioclase. Rhyodacite sample GSWA 159319 has an unusually low Σ_{REE} (133.08 ppm, as opposed to an average of 159.57 ppm for the andesites and 243.37 ppm for the rhyolite–dacite group) and has the

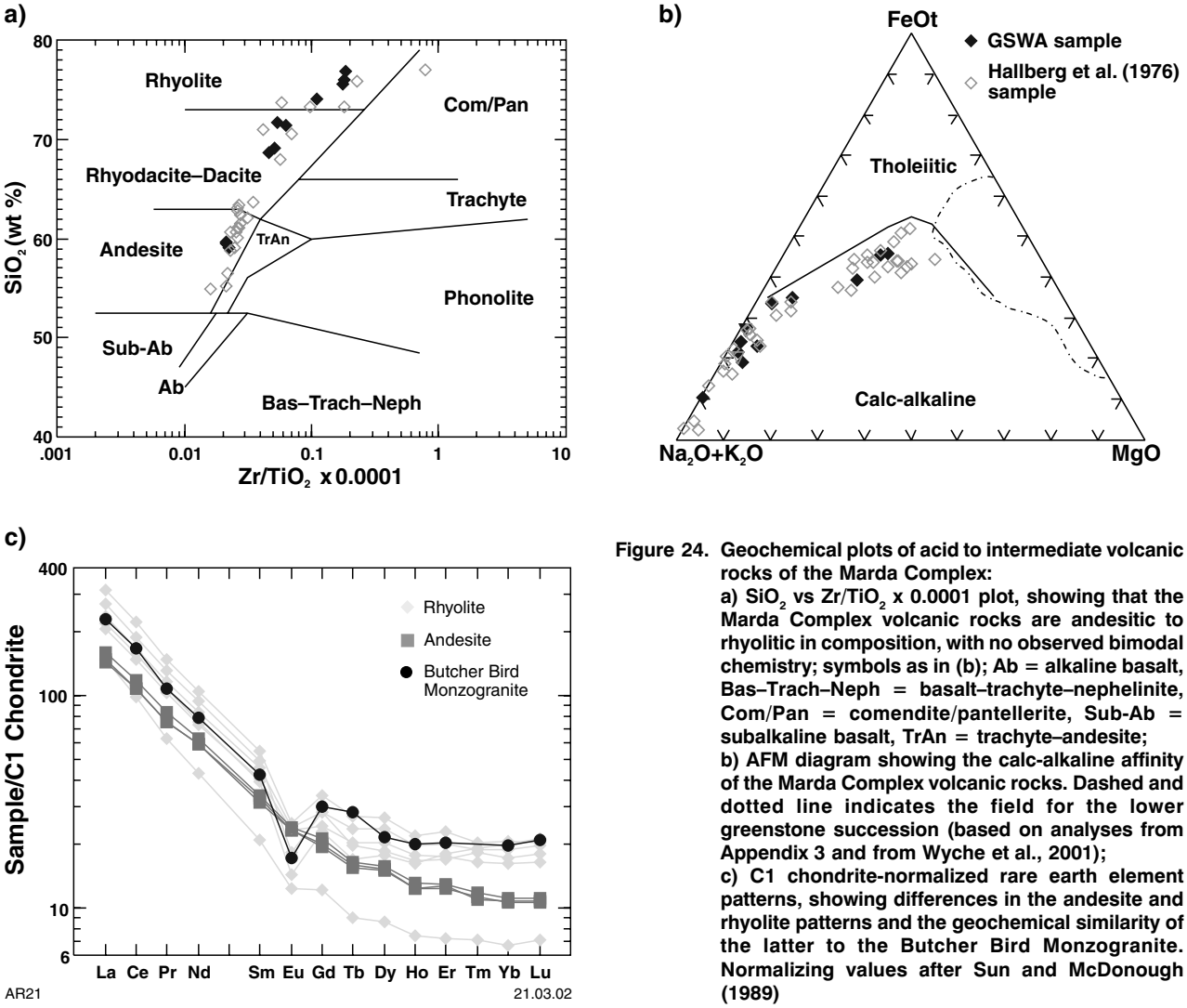

Figure 24. Geochemical plots of acid to intermediate volcanic rocks of the Marda Complex:
a) SiO_2 vs Zr/TiO_2 x 0.0001 plot, showing that the Marda Complex volcanic rocks are andesitic to rhyolitic in composition, with no observed bimodal chemistry; symbols as in (b); Ab = alkaline basalt, Bas–Trach–Neph = basalt–trachyte–nephelinite, Com/Pan = comendite/pantellerite, Sub-Ab = subalkaline basalt, TrAn = trachyte–andesite;
b) AFM diagram showing the calc-alkaline affinity of the Marda Complex volcanic rocks. Dashed and dotted line indicates the field for the lower greenstone succession (based on analyses from Appendix 3 and from Wyche et al., 2001);
c) C1 chondrite-normalized rare earth element patterns, showing differences in the andesite and rhyolite patterns and the geochemical similarity of the latter to the Butcher Bird Monzogranite. Normalizing values after Sun and McDonough (1989)

most fractionated pattern ($(La/Yb)_{CN}$ = 22.02)*, with a lower total heavy REE (HREE) content than the andesite samples. This sample was collected near the base of the volcanic pile, and could represent one of the more primitive rhyolitic magmas (cf. lower incompatible element contents relative to all other Marda Complex samples in Appendix 3).

Several factors point to a crustal source for both andesite and rhyolite rocks. These include the lack of significant HREE depletion; the high Th (7.5 – 8.4 ppm and 16–28 ppm for andesitic and rhyolitic rocks respectively) and U contents (1.0 – 1.7 ppm and 3.1 –4.4 ppm for andesites and rhyolites respectively), and a relatively high Sr^{87}/Sr^{86} initial ratio (0.703) for the andesites as opposed to 0.701 expected from Archaean mantle-derived melts (Taylor and Hallberg, 1977). The slight positive Eu anomaly in the mafic rocks sampled on JACKSON as well as similar HREE contents argue against simple derivation of the Marda Complex (and the rhyolites in particular) from partial melting of basaltic rocks of the lower greenstone succession.

The Butcher Bird Monzogranite (GSWA 168959 in Appendix 2) has a chemical composition (including REE pattern) indistinguishable from the rhyolitic ignimbrites of the Marda Complex (Fig. 24c), and its age is also within error of the rhyolite ages (see **Granitoid rocks**, *Agbb*). These similarities, coupled with the textural characteristics of the Butcher Bird Monzogranite (e.g. granophyric nature) and its intrusive relationship with the Marda Complex rhyolites, strongly support the interpretation that the monzogranite represents a high-level intrusion of the coeval felsic volcanism (Hallberg et al., 1976; Riganti et al., 2000).

The geochemistry of the Marda Complex rocks resembles that of modern Andean calc-alkaline volcanic suites, as already pointed out by Hallberg et al. (1976) and Taylor and Hallberg (1977). However, these authors cautioned against a straightforward analogy because many features characterizing modern subduction zones have not been identified in the Marda–Diemals region. Hallberg et al. (1976) suggested that a mantle hot spot could have led to the formation of an andesitic liquid, from which the rhyolitic ignimbrites were derived by fractionation, with eruption in a stable environment. Taylor and Hallberg (1977) echoed these conclusions, proposing a model of decreasing degrees of partial melting with decreasing depth to account for the lithological and chemical variations of the Marda Complex. Chen et al. (in prep.) suggested that the Marda Complex was deposited before the initiation of the D_2 orogenic compression (see **Structural geology**).

Structural geology

Rocks on JACKSON have been subjected to three major deformation events, which were followed by at least one further deformation stage (Table 1). Although there is evidence for each event on JACKSON, a comprehensive interpretation of the structural history draws heavily on observations on the adjacent JOHNSTON RANGE and BUNGALBIN map sheets, where some overprinting relationships are better exposed (Wyche et al., 2001; Chen and Wyche, 2001b). The regional structural evolution of the Marda–Diemals greenstone belt is further discussed by Dalstra (1995), Dalstra et al. (1999), Greenfield and Chen (1999), and Chen et al. (2001).

Early deformation (D_1)

Evidence for an early deformation event (D_1) is limited on JACKSON. The earliest recognized structures are tight to isoclinal folds, which are mainly preserved in BIF units of the lower greenstone succession (Fig. 3). About 5 km west of Windarling Peak, a D_1 anticline with a wavelength of about 1 km is overprinted by an F_2 open synform. Folds south-southwest of the Marda mining centre and about 1 km north-northwest of Yeela Hill have also been assigned to D_1, although overprinting relationships are not as clear. Bedding and S_1 foliation are folded around a mesoscale F_2 synformal structure, 14 km north-northwest of Mount Jackson Homestead (MGA 700000E 6670800N).

Several D_1 thrust faults in the lower greenstone succession are mainly interpreted from aeromagnetic images to account for structural repetition (cf. Figs 3 and 5). The most pronounced of these faults extends across the map sheet onto BUNGALBIN. Its northwestern part is deflected against the D_3 Koolyanobbing Shear Zone, whereas on BUNGALBIN it wraps around the Bungalbin Syncline, which is a regional-scale F_2 fold reoriented during D_3 (Chen et al., 2001; see below). In the area north of Windarling Peak, two D_1 thrust faults are gently folded by a D_2 structure, but do not transect rocks of the Marda Complex (Fig. 3). Although poorly exposed, these D_1 thrust faults correspond to narrow zones of strongly deformed shale and siltstone.

D_1 structures are restricted to the lower greenstone succession, whereas D_2 structures have also affected rocks of the Marda Complex. This constrains the age of D_1 between c. 3.0 Ga (the approximate depositional age of the lower greenstone succession, see **Stratigraphy, Lower greenstone succession**) and 2.73 Ga (the age of extrusion of the Marda Complex). This conclusion is supported by clasts of folded BIF in the conglomerate at the base of the Marda Complex and is consistent with similar observations made on JOHNSTON RANGE (Wyche et al., 2001).

East–west compression (D_2–D_3)

Following the early deformation, a prolonged period of east–west compression has been recognized by many workers as the main deformation event in the central Yilgarn Craton (Libby et al., 1991; Dalstra, 1995; Dalstra et al., 1999; Greenfield and Chen, 1999; Chen et al., 2001; Wyche et al., 2001). This compressional deformation is largely responsible for the present-day configuration of the greenstones and granitoids in the Marda–Diemals region. Broadly, it comprised an initial phase (D_2) in which

* 'CN' denotes that La and Yb have been normalized against their chondritic values (Sun and McDonough, 1989).

northerly trending open to tight folds were developed, along with a north-trending, regional foliation (Fig. 3). This initial stage roughly coincided with the deposition of part of the upper greenstone succession (Diemals Formation) and the intrusion of voluminous granitoids (Table 1). With ongoing east–west compression, rigid granitoid bodies impinged into the greenstones and reoriented the earlier D_2 structures to produce large-scale arcuate structures bounded by regional-scale northeasterly and northwesterly trending ductile shear zones and faults (D_3; Chen et al., 2001).

Structures attributed to D_2 on JACKSON include a northerly trending open synform west of Windarling Peak (Fig. 3), locally developed northerly trending gneissic banding in granitoid rocks (e.g. at Yacke Yackine Dam), and a northerly trending, vertical to steeply dipping foliation, which is best preserved in the greenstones exposed in the northwestern corner of the map sheet. Elsewhere, D_2 structures were largely overprinted and reoriented during D_3. The most important D_2 structure is the Bungalbin Syncline, which is a regional-scale fold straddling the boundary between JACKSON and BUNGALBIN that is well constrained by younging directions in pillowed high-Mg basalts and cross-bedding in quartzite units (Chen and Wyche, 2001b). The syncline has a wavelength of 35 km, and the hinge plunges moderately to the northwest. It deformed D_1 folds and thrust faults, and its northeastern limb is truncated by the northwesterly trending Mount Dimer Shear Zone. The Bungalbin Syncline is considered to be equivalent to D_2 northerly trending, upright folds on JOHNSTON RANGE (such as the Diemals and Horse Well Anticlines, and the Watch Bore Syncline; Wyche et al., 2001), but is thought to have been reoriented into its present-day northwesterly trend during the D_3 event (Chen et al., 2001).

Northerly to north-northwesterly trending gneissic banding and foliation are present in granitoid rocks at Yacke Yackine Dam and on the western side of the Bullfinch–Evanston Road (MGA 716930E 6625230N). At the latter locality, discrete northwesterly trending shear zones are superimposed on the gneissosity and foliation, suggesting that the shear zones and gneissosity represent different deformation events. The gneissic banding in granitoid rocks was probably developed during D_2 regional shortening, and was subsequently overprinted by D_3 strike-slip shear zones (see below). The timing of D_2 east–west compression is not well constrained: it appears to post-date the emplacement of the Marda Complex (Chen et al., in press) and it affected granitoid gneiss at Yacke Yackine Dam, which yielded a SHRIMP U–Pb zircon age of 2711 ± 4 Ma (Nelson, 2001).

Geochronology data from a range of granitoids and gneissic granitoids in the central Yilgarn Craton indicate a prolonged period of granitoid magmatism from as early as 2.77 Ga (Mueller and McNaughton, 2000), with abundant granite intrusions at about 2.69 Ga (e.g. Bloem et al., 1997; Dalstra et al., 1998; Wang et al., 1998; Nelson, 1999, 2000, 2001; Qiu et al., 1999). A two-stage model was proposed by Dalstra et al. (1999), who suggested that crystallization of granitoids occurred at depth between 2690 and 2660 Ma. A synkinematic rise of the partly solidified granitoids during east–west compression (but before c. 2636 Ma) coincided with deformation of the granitoid margins and the adjacent greenstones. Intrusion of granitoids in the Marda–Diemals area occurred over an extended period from c. 2.71 Ga (the age of granitoid gneiss at Yacke Yackine Dam) to at least 2.65 Ga, as indicated by the 2654 ± 6 Ma SHRIMP U–Pb zircon age of a deformed monzogranite at the Evanston mine on JOHNSTON RANGE (Nelson, 2001).

According to the scheme proposed by Chen et al. (2001), ongoing east–west compression led to impingement of the large rigid granitoid bodies into the greenstones, which induced shearing at a regional scale and reorientation of the earlier D_2 structures. This produced large-scale arcuate structures that are characteristically convex towards the greenstones and bounded by northeasterly and northwesterly ductile shear zones that are linked by north-trending contractional zones in the apex regions (Chen et al., 2001). Typically, northeasterly trending shear zones are dextral, whereas northwesterly trending shear zones have a sinistral shear sense. These shear zones and arcuate structures are assigned to D_3.

The Mount Dimer Shear Zone, exposed in the northeastern corner of JACKSON (Fig. 3) and more extensively on BUNGALBIN, is part of the larger scale Evanston – Mount Dimer arcuate structure (Chen et al., 2001). The sinistral Mount Dimer Shear Zone joins the dextral Evanston Shear Zone through a north-trending zone characterized by folding and thrusting in the Die Hardy Range area on JOHNSTON RANGE (Wyche et al., 2001). The Mount Dimer Shear Zone truncates the northeastern limb of the Bungalbin Syncline and juxtaposes it against foliated to gneissic monzogranite. The asymmetry of feldspar porphyroclasts and well-developed S–C fabrics indicate a sinistral sense of strike-slip movement on the shear zone.

The most conspicuous D_3 structure on JACKSON is the Koolyanobbing Shear Zone. This is a northwest-trending, ductile shear zone between 6 and 15 km wide that may extend for more than 650 km (Libby et al., 1991). Seismic reflection profiling indicates that the Koolyanobbing Shear Zone dips gently eastward to mid-crustal levels (Drummond et al., 1993). On JACKSON the northern section of the Koolyanobbing Shear Zone is defined by a 2 to 6 km-wide zone of foliated to gneissic granitoid rocks. At its northwestern end the Koolyanobbing Shear Zone merges with the Clampton Fault, which is a north-trending regional-scale fault mainly exposed on JOHNSTON RANGE (Wyche et al., 2001). On JACKSON the Koolyanobbing Shear Zone is best exposed near a gnamma hole immediately west of the Bullfinch–Evanston Road in the southernmost part of the map sheet. At this locality a series of small-scale, northwesterly trending discrete shear zones sinistrally deflect or displace an earlier fabric defined by northerly to north-northwesterly trending gneissic banding and foliation (Fig. 25). These discrete shear zones range in width from 3 to 20 cm, but are typically less than 5 cm wide, and are marked by narrow zones of fine-grained, dark-grey ultramylonite. Some discrete, semi-ductile shear zones are intruded by pegmatite or quartz veins. The eastern edge of the Koolyanobbing Shear Zone is characterized by interleaving of moderately to strongly

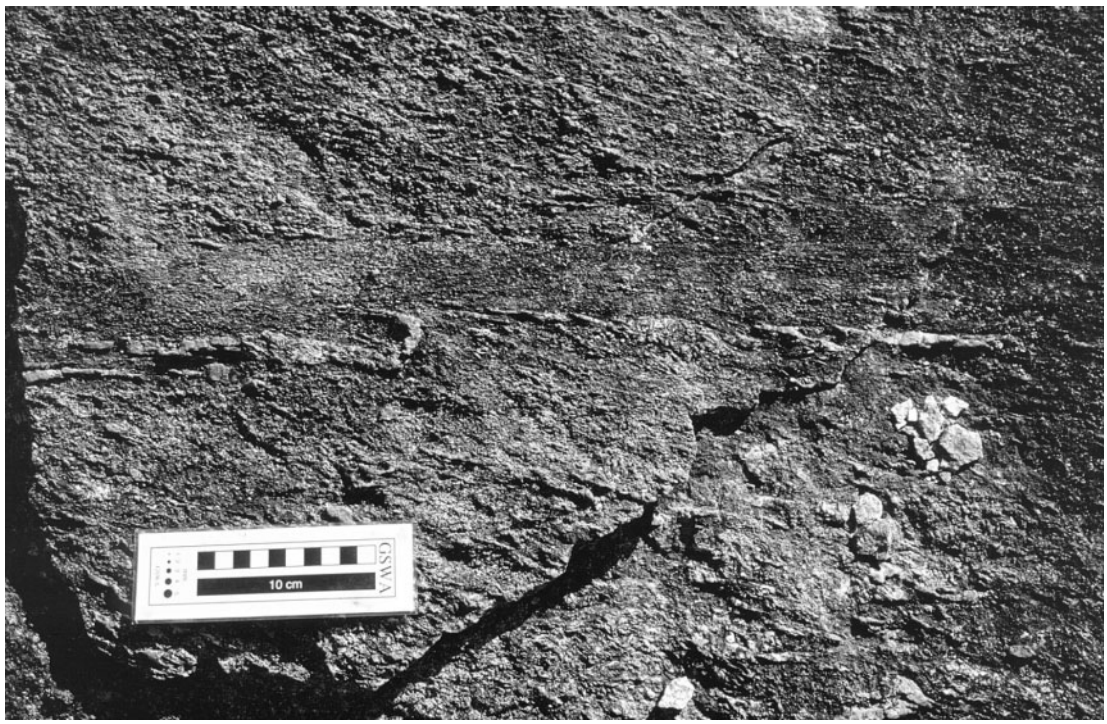

AR20 20.03.02

Figure 25. A small-scale sinistral shear zone in granitoid rocks within the central part of the Koolyanobbing Shear Zone (MGA 716930E 6625230N). The northwesterly trending shear zone is marked by a narrow zone of high strain and superimposed on north-northwesterly trending gneissic banding and foliation

foliated granitoid with amphibolite and subordinate quartzite. The greenstones adjacent to the contact are also strongly foliated and locally crenulated.

Kinematic indicators described by Libby et al. (1991) indicate an essentially sinistral transcurrent movement for the Koolyanobbing Shear Zone. On JACKSON outcrop-scale shear zones in the central portion of the Koolyanobbing Shear Zone sinistrally displace an earlier fabric and, locally, asymmetric porphyroclasts of feldspar and quartz also indicate a sinistral sense of movement. Moderately to steeply plunging mineral lineations preserved along the eastern edge of the shear zone may indicate dominantly compressional stress during granitoid impingement at the northeastern end of the shear zone. An apparent dextral drag pattern on aeromagnetic images (Fig. 5) is probably related to lateral escape of greenstones during impingement of granitoids.

The age of the Koolyanobbing Shear Zone is constrained by a SHRIMP U–Pb zircon age of 2656 ± 3 Ma from an undeformed porphyritic syenogranite that cuts the shear zone near Koolyanobbing, about 50 km south of the southern boundary of JACKSON (Fig. 1; Qiu et al., 1999). This age represents a minimum age for the D_3 event. No ages could be obtained from the undeformed granitoid intrusions that crosscut the Koolyanobbing Shear Zone on JACKSON, but a deformed monzogranite in the D_3 Evanston Shear Zone on LAKE GILES (Fig. 1; Greenfield, 2001) yielded a SHRIMP U–Pb zircon age of 2654 ± 6 Ma (Nelson, 2001). These ages suggest a probable end of the D_3 compression event around 2655 Ma.

Post-D_3 deformation

Evidence for post-D_3 deformation events on JACKSON is best seen on aeromagnetic images, where large-scale, linear, low magnetic anomalies trending north-northeast to northeast cut across greenstones, granitoid rocks, and D_3 structures. The most prominent set is visible in the southern part of the map sheet, where it crosscuts an unnamed post-D_3 monzogranite intrusion (Figs 3 and 5). These anomalies are interpreted as brittle faults and fractures that are locally infilled by quartz veins (e.g. MGA 694500E 6660750N). Dextral offsets up to 200 m were observed on LAKE GILES (Greenfield, 2001) and JOHNSTON RANGE (Wyche et al., 2001). These authors also describe east-southeasterly trending fractures with sinistral offsets (these are not visible on JACKSON), interpreted as conjugate sets formed during a period of east–west to east-northeast – west-southwest compression. Wyche (1999) described similarly oriented structures on RIVERINA, approximately 100 km to the east, that cut across the c. 2632 Ularring Monzogranite.

Easterly trending, linear magnetic anomalies correspond to tension fractures that were infilled by Proterozoic mafic and ultramafic dykes (Hallberg, 1987; see **Mafic dykes**).

Metamorphism

The metamorphic history of the Marda–Diemals region has been investigated by several workers. Binns et al. (1976) examined the regional distribution of metamorphic facies in the central and eastern parts of the Yilgarn Craton, and Ahmat (1986) detailed the metamorphic assemblages of various rock types in the Southern Cross Province. These studies highlighted the broad increase in metamorphic grade from the central parts of greenstone belts (typically greenschist facies) to relatively higher grades (lower to upper amphibolite facies) adjacent to granite–greenstone contacts. Detailed pressure–temperature (P–T) determinations on amphibole–plagioclase pairs in metamorphosed tholeiitic mafic rocks from a number of localities on JOHNSTON RANGE and JACKSON were carried out by Dalstra (1995). Dalstra et al. (1999) proposed a two-stage model to explain the observed metamorphic gradients.

On JACKSON rocks in and around the Marda Complex retain some of their primary magmatic texture and mineralogy, including igneous clinopyroxene (e.g. in fine-grained gabbro around MGA 720100E 6645050N) and andesine–labradorite plagioclase. A matrix assemblage of chlorite, albite, and minor amounts of quartz, epidote, and calcite in the mafic rocks indicate greenschist-facies conditions. Dalstra et al. (1999) calculated P–T conditions of about 300°C and less than 180 MPa in a metamorphosed tholeiitic rock from the lower greenstone succession adjacent to the Marda Complex. These authors attributed the low-grade, low-strain metamorphism and the spilitization of groundmass plagioclase in these rocks to sea-floor alteration occurring over an extended period of time and at a relatively low fluid to rock ratio. Pronounced sericitization in the eastern part of the Marda Complex is ascribed to potassic metasomatism induced by the intrusion of the Butcher Bird Monzogranite. Elsewhere in the complex, sericitization is probably related to fluid circulation within the volcanic pile.

Greenschist-facies metamorphic conditions are dominant in rocks of the lower greenstone succession. Dalstra et al. (1999) distinguished low- and high-strain greenschist-facies rocks. The former preserve igneous features such as vesicles and varioles. In the latter a strong metamorphic foliation overprints and partially to completely obliterates igneous textures. Greenschist-facies mafic rocks typically have mineral assemblages of tremolite–actinolite laths with interstitial albite and accessory ilmenite and magnetite needles. Epidote and chlorite are ubiquitous, but their proportions vary considerably. Biotite, indicative of upper greenschist-facies conditions, is close to the amphibolite-facies domains. Temperatures in the order of 500–540°C and pressures of about 220 MPa were calculated for an actinolite–oligoclase metabasalt along the southwestern margin of the Marda greenstone belt (Dalstra et al., 1999), at the transition between greenschist- and amphibolite-facies domains.

The highest metamorphic grades on JACKSON are adjacent to the granite–greenstone contacts in the western part of the map sheet, and in the metasedimentary rocks in the northernmost part of the Marda Complex. A narrow zone of amphibolite-facies rocks is developed along the margin of the Marda greenstone belt. Mafic rocks contain hornblende, and aluminous intercalations in quartzites are distinguished by sillimanite. Although hornblende cores fringed by actinolitic amphibole are still present in the north, in the south the hornblende has been largely retrogressed to actinolite and chlorite. Dalstra (1995) reported diopside and grossular adjacent to the granite–greenstone contact in the Clampton mine area, a few kilometres north of the northern boundary of JACKSON. For this area Dalstra et al. (1999) calculated P–T conditions of relatively low pressure (<400 MPa), at the boundary between greenschist and amphibolite facies. Retrogressed andalusite and possibly staurolite are common porphyroblastic phases in the northern exposures of fine-grained metasedimentary rocks of the Marda Complex. Their distribution suggests a relationship with the intrusion of the Chatarie Well Granite. Similarly, just north of the boundary with JOHNSTON RANGE, andalusite porphyroblasts in muscovite-bearing quartzite and quartz–mica schist horizons intercalated with Marda Complex rhyolites are attributed to contact metamorphism associated with the Pigeon Rocks Monzogranite (Wyche et al., 2001).

The age of peak metamorphism on JACKSON can only be broadly constrained. The distribution of metamorphic patterns, with the highest grades near granite–greenstone contacts, and the relatively low pressures of formation of the metamorphic minerals indicate that the intrusion of granitoids was the main factor controlling metamorphism in the Marda–Diemals belt. Some of these granitoids are deformed by D_3 shear zones and are interpreted as having been intruded during the main D_2 compressional event (see **Structural geology**). This implies that the peak metamorphism was syn-D_2. Wyche et al. (2001) suggested that the differences in emplacement ages of various granitoids in the region imply that peak metamorphic conditions could have been attained diachronously in different areas.

Cainozoic geology

Cainozoic regolith deposits cover more than 70% of JACKSON, and many of the rocks have been affected by weathering to such an extent that a protolith cannot be inferred. Mapping of the regolith combined field observations with interpretation of aerial photographs and Landsat images. The classification system used is that of Hocking et al. (2001), which is in turn based on the RED scheme (Residual–Erosional–Depositional) of Anand et al. (1993).

Relict units (*Rd, Rf, Rfc, Rgp$_g$, Rk, Rz*)

Undivided duricrust (*Rd*) may be either siliceous or ferruginous, and has been mapped predominantly in areas underlain by granitoid rocks. It is typically covered by a thin layer of yellow sand with minor pisolitic laterite, silt,

and clay (*Sl*). Ferruginous or lateritic duricrust (*Rf*) comprises nodular, pisolitic or massive ferricrete, and is clearly identified on aerial photographs by its distinctive dark red-brown hue. Ferruginous duricrust over granitoid rocks is best exposed along a breakaway system in the southern part of JACKSON. It also forms extensive blankets over greenstones, particularly around BIF ridges. Lateritic duricrust is developed over ferruginized metasedimentary rocks (*Rfc*) at Windarling Peak and north of the Athlone prospect, where relict sedimentary structures (mainly thin bedding) are preserved, and the duricrust grades into BIF and chert units at the top of the ridges.

Residual quartzofeldspathic sand over granitoid rock (Rgp_g) is common in all areas underlain by granitoid intrusions. These areas typically have red-yellow sand with a few scattered, commonly weathered granite outcrops, locally capped by silcrete. Quartz-vein debris and ferruginized silcrete pebbles are locally abundant. There is complete gradation between these residual sand areas, sandy sheetwash, and fresh granite exposures. White massive calcrete (*Rk*) is only preserved in small isolated areas. Siliceous duricrust (or silcrete, *Rz*) is typically developed over granitoid rocks and exposed along the edges of breakaway systems. It consists of millimetre-size, commonly angular quartz clasts set in a cryptocrystalline siliceous, white to creamy and pink cement, locally with a brown tinge due to ferruginous impregnations and coatings.

Depositional units (*C*, Clc_i, *Cf*, Cgp_g, *Cq*, *W*, *Wf*, *A*, A_p, L_l, L_d, L_m, *S*, *Sl*)

Depositional regolith units are the most widely distributed surficial deposits on JACKSON. Following the classification scheme of Hocking et al. (2001), colluvial (*C*), sheetwash (*W*), alluvial (*A*), lake (*L*), and sandplain (*S*) regimes have been identified on this map sheet.

Undivided colluvium (*C*) includes proximal deposits of lithologically mixed gravel, sand, and silt on steeply to gently sloping ground adjacent to greenstone outcrops and below breakaways, as well as coarse talus on ridge flanks. Further subdivisions distinguish colluvium in which gravel is dominated by one lithotype. On the flanks of prominent ridges, coarse angular debris of BIF and chert (Clc_i) grades downslope into finer ferruginous colluvium (*Cf*), and thence into sheetwash areas with abundant ferruginous grit (see *Wf* description below). Adjacent to granitoid outcrops, colluvium of quartzofeldspathic material (Cgp_g) includes granite and subordinate silcrete and quartz vein pebbles with abundant quartzofeldspathic sand. On JACKSON colluvium dominated by granite is typical of areas surrounding the Butcher Bird Monzogranite outcrops, which are morphologically more prominent than other granite exposures. Elsewhere, low-lying granite outcrops grade very rapidly into sandy sheetwash. Colluvium composed predominantly of angular quartz clasts (*Cq*) is typical of areas adjacent to conspicuous quartz veins.

Sheetwash units (*W*) occupy a distal position in the geomorphological profile, gradational between colluvial and alluvial areas. Sheetwash deposits consist of red sand, silt, and clay material. In areas adjacent to ferruginous colluvial units, the sheetwash deposits are characterized by abundant fine, ferruginous grit (*Wf*). Alluvium (*A*) is recognized in areas of channelized drainage (as opposed to sheetflow), and typically consists of broad, slightly depressed alluvial flats with unconsolidated sand, silt, and gravel deposits. These areas are characterized by sinuous lines of gum trees, and the changes in vegetation facilitate distinction from sheetwash deposits on aerial photographs and Landsat images. All drainage is ephemeral on JACKSON, but water can persist for longer periods in claypans (A_p) along the major drainage lines and near lake systems.

The northern extension of the Hamersley playa lake system occupies the western part of JACKSON, controlling the most prominent drainage on the map sheet. Most lakes contain silt, mud, and sand deposits, with a veneer of halite or gypsum, or both (L_l). Active dune systems (L_d) are present on the fringes of and within the lakes. Vegetated sand dunes at the edge of the lakes are composed of red-brown sand and silt, whereas dunes within the lakes are dominated by sand and evaporitic material, and sustain a more sparse, salt-tolerant vegetation. The areas immediately adjacent to the lakes have mixed alluvial, eolian, and lacustrine deposits (L_m).

Sandplain deposits (*S*) on JACKSON form an extensive layer of variable thickness that is developed predominantly over granitoid rocks. This quartz-rich sand may be residual material derived from the disintegration of a quartzofeldspathic bedrock, but it may also contain a significant eolian component. Yellow sand over undivided duricrust (*Sl*) has locally abundant pisolitic and nodular gravel, silt, and clay. On false-colour Landsat images (bands 7, 4 and 2) this type of sand deposit is purple-brown and readily distinguished from dark-green, quartz-rich sandplain areas. It may represent a mixture of residual and eolian deposits.

Economic geology

JACKSON has been extensively explored for gold and iron, with gold being the only mineral commodity that has yielded any significant production in the area to date. Historical mineral production and established mineral resources are presented in Townsend et al. (2000), and are summarized in Appendices 4 and 5 respectively. The following descriptions of mineral deposits and occurrences on JACKSON are based on a summary of both published information and that contained in open-file statutory mineral exploration reports held in the WAMEX database in the Western Australian Department of Mineral and Petroleum Resources library in Perth and Kalgoorlie.

Gold

Gold was historically produced from two areas on JACKSON, the Mount Jackson and Marda mining centres,

each of which comprised several groups of mine workings (e.g. Athlone, Millars, Boondine, Burgoose, Riedels, Butcher Bird, and Allens Find). The first official report of gold production from the Mount Jackson mining centre was in 1894, with a State stamp mill for processing hard ore erected as early as 1895 (Blatchford and Honman, 1917). Gold was discovered at the Marda centre in 1910, and was followed shortly afterwards by the installation of a stamp mill and cyanidation plant (Matheson and Miles, 1947), as well as the construction of a tank to supply water to the mine workings (Blatchford and Honman, 1917). Gold production was intermittent, with 3 main peaks in the periods 1900–02, 1911–13, and 1935–48 (Appendix 4). Very small amounts of gold were produced in the second half of the 20th century, and recent exploration has outlined further limited gold resources (Appendix 5).

Gold mineralization on JACKSON is epigenetic, and largely controlled by the combination of structural and lithological features. Gold is hosted by shear zones and quartz(–sulfide) veins crosscutting a variety of different rock types, with the richest lodes at structural intersections. In the Mount Jackson centre, gold deposits are hosted by sheared mafic and ultramafic rocks with intercalated thin BIF units (Dalstra, 1995). The richest mineralized quartz–calcite–dolomite veins are subparallel to the regional foliation, with a northwesterly trend and an easterly dip (Dalstra, 1995). Historically, some production was obtained from north-trending, west-dipping quartz veins (Blatchford and Honman, 1917). In the Marda centre, BIFs and high-Mg basalts are the most important hosts to gold mineralization (Dalstra, 1995), with the main vein systems trending northwest, northeast, and north (Blatchford and Honman, 1917). The most productive deposits were Mount Jackson and the Great Unknown (Appendix 4) in which the gold mineralization is at the interface of a thin BIF–chert unit and a thick sequence of high-Mg basalts (Dalstra, 1995). The BIF hosting the deposit is strongly brecciated and altered. Gold mineralization at Allens Find is unusual in that north-northwesterly trending, shallowly easterly dipping auriferous quartz veins crosscut felsic metavolcanic rocks (porphyritic rhyolite) of the Marda Complex (Kimber, 1987), indicating that at least some of the gold mineralization post-dates the deposition of the upper greenstone succession.

Several alteration styles are associated with gold mineralization (Dalstra, 1995). Silicification takes the form of pervasive silica replacement, quartz veining, and stockworks. Carbonate alteration is locally very pronounced. Quartz–fuchsite veining and pyritization are widespread, the latter typically forming boxwork textures and pitted surfaces in mineralized chert layers and BIFs. Clay alteration is commonly masked by the deep weathering profile.

Iron

The BIF ridges on JACKSON have been the target of several exploration programs for iron ore, predominantly in the 1960s and 1970s, with renewed interest in the late 1990s. Exploration (which involved reconnaissance mapping, diamond and percussion drilling, and the digging of shafts and drives) delineated several orebodies in the Mount Jackson and Windarling Peak areas (Western Mining Corporation Limited, 1961–69). The ore varies from well bedded to massive, and consists of vuggy goethite–hematite with variable amounts of limonite. The ore is considered to represent the surface enrichment of a magnetite–carbonate facies within the silica-rich iron formation. It is hard and indurated to a depth of about 30 m, below which the oxidized ore becomes friable and cavernous. A siderite–magnetite proto-ore with rare pyrite and chalcopyrite is present below an oxidation surface that extends to a depth of 80 to 115 m. The vuggy nature of the enriched oxidized ore is attributed to leaching of carbonate. Manganiferous zones at Windarling Peak have varying phosphorus values in the different orebodies (0.065 – 0.152 wt%; Townsend et al., 2000). Estimated resources and grades are presented in Appendix 5.

Base metals

Approximately 16 t of carbonate–oxide copper ore was produced in 1942 from a quartz vein crosscutting mafic rocks 12 km southwest of Mount Jackson (Marston, 1979). This deposit is one of the few with cupriferous quartz veins and shear zones in the central Yilgarn Craton (Marston, 1979). The style of mineralization differs from the siliceous copper gossans and ferruginous zones developed in pelitic metasedimentary units west of Diemals on JOHNSTON RANGE (Wyche et al., 2001).

Felsic extrusive rocks of the Marda Complex have been explored for volcanogenic massive sulfide-style deposits (e.g. Kappelle, 1978; Nord Resources Pacific Proprietary Limited, 1981–86; Thompson, 1996). No mineralization of this type has yet been identified.

Acknowledgements

The authors would like to thank geologists of the former Savage Resources Ltd for hospitality at their Marda Camp, and for geological discussions.

References

AHMAT, A. L., 1986, Metamorphic patterns in the greenstone belts of the Southern Cross Province, Western Australia: Western Australia Geological Survey, Report 19, p. 1–21.

ANAND, R. R., CHURCHWARD, H. M., SMITH, R. E., SMITH, K., GOZZARD, J. R., CRAIG, M. A., and MUNDAY, T. J., 1993, Classification and atlas of regolith-landform mapping units: Australia CSIRO/AMIRA Project P240A, Exploration and Mining Restricted Report 440R (unpublished).

ARNDT, N. T., NALDRETT, A. J., and PYKE, D. R., 1977, Komatiitic and iron-rich tholeiitic lavas of Munro Township, northeast Ontario, Journal of Petrology, v. 18, p. 319–369.

ARNDT, N. T., and NISBET, E. G., 1982, What is a komatiite?, *in* Komatiites *edited by* N. T. ARNDT and E. G. NISBET: London, George Allen and Unwin, p. 19–27.

BEARD, J. S., 1979, The vegetation of the Jackson area: Perth, Vegmap Publications, Vegetation Survey of Western Australia, 1:250 000 Series, Map and Explanatory Memoir, 27p.

BEARD, J. S., 1990, Plant life of Western Australia: Kenthurst, N.S.W., Kangaroo Press, 319p.

BEUKES, N. J., 1973, Precambrian iron-formations of Southern Africa: Economic Geology, v. 68, p. 960–1004.

BIOLOGICAL SURVEYS COMMITTEE, 1985, The biological survey of the Eastern Goldfields of Western Australia. Part 3. Jackson–Kalgoorlie study area: Records of the Western Australian Museum, Supplement Number 23, 168p.

BINNS, R. A., GUNTHORPE, R. J., and GROVES, D. I., 1976, Metamorphic patterns and development of greenstone belts in the eastern Yilgarn Block, Western Australia, *in* The early history of the Earth *edited by* B. F. WINDLEY: London, John Wiley and Sons, p. 303–313.

BLATCHFORD, T., and HONMAN, C. S., 1917, The geology and mineral resources of the Yilgarn Goldfield, Part III — The gold belt north of Southern Cross, including Westonia: Western Australia Geological Survey, Bulletin 71, 321p.

BLOEM, E. J. M., DALSTRA, H. J., RIDLEY, J. R., and GROVES, D. I., 1997, Granitoid diapirism during protracted tectonism in an Archaean granitoid–greenstone belt, Yilgarn Block, Western Australia: Precambrian Research, v. 85, p. 147–171.

BUREAU OF MINERAL RESOURCES, 1965, Map showing the results of an airborne magnetic and radiometric survey of the Jackson 1:250 000 area, W.A.: Australia Bureau of Mineral Resources, Record 1965/29 (unpublished).

BYE, S. M., 1968, The acid volcanic rocks of the Marda area, Yilgarn Goldfield, Western Australia: University of Western Australia, BSc (Honours) thesis (unpublished).

CAS, R. A. F., and WRIGHT, J. V., 1987, Volcanic successions, modern and ancient — a geological approach to processes, products and successions: London, Allen and Unwin, 528p.

CHEN, S. F., LIBBY, J. W., GREENFIELD, J. E., WYCHE, S., and RIGANTI, A., 2001, Geometry and kinematics of large arcuate structures formed by impingement of rigid granitoids into greenstone belts during progressive shortening: Geology, v. 29, p. 283–286.

CHEN, S. F., RIGANTI, A., WYCHE, S., GREENFIELD, J. E., and NELSON, D. R., in press, Lithostratigraphy and tectonic evolution of contrasting greenstone successions in the central Yilgarn Craton, Western Australia: Precambrian Research.

CHEN, S. F., and WYCHE, S. (compilers), 2001a, Archaean granite–greenstones of the central Yilgarn Craton, Western Australia — a field guide: Western Australia Geological Survey, Record 2001/14, 76p.

CHEN, S. F., and WYCHE, S., 2001b, Bungalbin, W.A. Sheet 2837: Western Australia Geological Survey, 1:100 000 Geological Series.

CHIN, R. J., and SMITH, R. A., 1983, Jackson, W.A.: Western Australia Geological Survey, 1:250 000 Geological Series Explanatory Notes, 30p.

DALSTRA, H. J., 1995, Metamorphic and structural evolution of the greenstone belts of the Southern Cross – Diemals region of the Yilgarn Block, Western Australia, and its relationship to the gold mineralisation: University of Western Australia, PhD thesis (unpublished).

DALSTRA, H. J., BLOEM, E. J. M., RIDLEY, J. R., and GROVES, D. I., 1998, Diapirism synchronous with regional deformation and gold mineralisation, a new concept for granitoid emplacement in the Southern Cross Province, Western Australia: Geologie en Mijnbouw, v. 76, p. 321–338.

DALSTRA, H. J., RIDLEY, J. R., BLOEM, E. J. M., and GROVES, D. I., 1999, Metamorphic evolution of the central Southern Cross Province, Yilgarn Craton, Western Australia: Australian Journal of Earth Sciences, v. 46, p. 765–784.

DRUMMOND, B. J., GOLEBY, B. R., SWAGER, C., and WILLIAMS, P. R., 1993, Constraints on Archaean crustal composition and structure provided by deep seismic sounding in the Yilgarn Block: Ore Geology Reviews, v. 8, p. 17–124.

FEEKEN, E. H. J., FEEKEN, G. E. E., and SPATE, O. H. K., 1970, The discovery and exploration of Australia (1606–1901): Melbourne, Nelson Press, 318p.

FLETCHER, I. R., ROSMAN, K. J. R., WILLIAMS, I. R., HICKMAN, A. H., and BAXTER, J. L., 1984, Sm–Nd geochronology of greenstone belts in the Yilgarn Block, Western Australia: Precambrian Research, v. 26, p. 333–361.

FRASER, A. F., 1974, Reconnaissance helicopter gravity survey of the southwest of Western Australia, 1969: Australia Bureau of Mineral Resources, Record 1974/26 (unpublished).

GEE, R. D., BAXTER, J. L., WILDE, S. A., and WILLIAMS, I. R., 1981, Crustal development in the Yilgarn Block, *in* Archaean geology *edited by* J. E. GLOVER and D. I. GROVES: 2nd International Archaean Symposium, Perth, W.A., 1980, Proceedings; Western Australia Geological Society of Australia, Special Publication, no. 7, p. 43–56.

GILL, J. B., 1981, Orogenic andesites and plate tectonics: Berlin, Springer-Verlag, 390p.

GREENFIELD, J. E., 2001, Geology of the Lake Giles 1:100 000 sheet: Western Australia Geological Survey, 1:100 000 Geological Series Explanatory Notes, 19p.

GREENFIELD, J. E., and CHEN, S. F., 1999, Structural evolution of the Marda–Diemals area, Southern Cross Province: Western Australia Geological Survey, Annual Review 1998–99, p. 68–73.

GRIFFIN, T. J., 1990, Southern Cross Province, *in* Geology and mineral resources of Western Australia: Western Australia Geological Survey, Memoir 3, p. 60–77.

HALLBERG, J. A., 1987, Postcratonization mafic and ultramafic dykes of the Yilgarn Block: Australian Journal of Earth Sciences, v. 34, p. 135–149.

HALLBERG, J. A., JOHNSTON, C., and BYE, S. M., 1976, The Archaean Marda igneous complex, Western Australia: Precambrian Research, v. 3, p. 111–136.

HOCKING, R. M., and COCKBAIN, A. E., 1990, Regolith, *in* Geology and mineral resources of Western Australia: Western Australia Geological Survey, Memoir 3, p. 591–602.

HOCKING, R. M., LANGFORD, R. L., THORNE, A. M., SANDERS, A. J., MORRIS, P. A., STRONG, C. A., and GOZZARD, J. R., 2001, A classification system for regolith in Western Australia: Western Australia Geological Survey, Record 2001/4, 22p.

KAPPELLE, K., 1978, Final exploration report, Mineral Claim 77/6127, Marda Tank, Yilgarn Goldfield, W.A.; Electrolityc Zinc Company of Australasia Limited: Western Australia Geological Survey, Statutory mineral exploration report, Item 653 A8072 (unpublished).

KIMBER, P. B., 1987, Annual Report 1986, Allens Find gold prospect, MC Mining NL: Western Australia Geological Survey, Statutory mineral exploration report, Item 5231 A19427 (unpublished).

LE BAS, M. J., 2000, IUGS reclassification of the high-Mg and picritic volcanic rocks: Journal of Petrology, v. 41, p. 1467–1470.

LE MAITRE, R. W., 1989, A classification of igneous rocks and glossary of terms. Recommendations of the International Union of Geological Sciences Subcommission on the Systematics of Igneous Rocks: Oxford, Blackwell Scientific Publications, 193p.

LIBBY, J., GROVES, D. I., and VEARNCOMBE, J. R., 1991, The nature and tectonic significance of the crustal-scale Koolyanobbing shear zone, Yilgarn Craton, Western Australia: Australian Journal of Earth Sciences, v. 38, p. 229–245.

LOGFREN, G., 1971, Experimentally produced devitrification textures in natural rhyolitic glass, Geological Society of America, Bulletin, v. 82, p. 111–124.

MacKENZIE, W. S., DONALDSON, C. H., and GUILFORD, C., 1982, Atlas of igneous rocks and their textures: London, Longman, 148p.

MACKEY, T. E., 1999, Jackson, W.A., Interpreted geology, (1:250 000 scale map): Canberra, Australian Geological Survey Organisation.

MARSTON, R. J., 1979, Copper mineralization in Western Australia: Western Australia Geological Survey, Mineral Resources Bulletin 13, 128p.

MATHESON, R. S., and MILES, K. R., 1947, The mining groups of the Yilgarn Goldfield north of the Great Eastern Railway: Western Australia Geological Survey, Bulletin 101, 242p.

McPHIE, J., DOYLE, M., and ALLEN, R., 1993, Volcanic textures: Tasmania, Tasmanian Government Printing Office, 196p.

MUELLER, A. G., and McNAUGHTON, N. J., 2000, U–Pb Ages constraining batholith emplacement, contact metamorphism, and the formation of gold and W–Mo skarns in the Southern Cross area, Yilgarn Craton, Western Australia: Economic Geology, v. 95, p. 1231–1258.

MYERS, J. S., 1995, The generation and assembly of an Archaean supercontinent: evidence from the Yilgarn craton, Western Australia, *in* Early Precambrian processes *edited by* M. P. COWARD and A. C. RIES: Geological Society of London, Special Publication 95, p. 143–154.

MYERS, J. S., 1997, Preface: Archaean geology of the Eastern Goldfields of Western Australia — regional overview: Precambrian Research, v. 83, p. 1–10.

MYERS, J. S., and HOCKING, R. M., 1998, Geological map of Western Australia, 1:2 500 000 (13th edition): Western Australia Geological Survey.

NELSON, D. R., 1999, Compilation of geochronology data, 1998: Western Australia Geological Survey, Record 1999/2, 222p.

NELSON, D. R., 2000, Compilation of geochronology data, 1999: Western Australia Geological Survey, Record 2000/2, 251p.

NELSON, D. R., 2001, Compilation of geochronology data, 2000: Western Australia Geological Survey, Record 2001/2, 205p.

NICHOLS, G., 1999, Sedimentology and stratigraphy: Cambridge, Blackwell Science, 355p.

NOLDART, A. J., 1957, Miscellaneous reports for 1955, Exploratory drilling of abandoned gold shows, Yilgarn Goldfield: Western Australia Geological Survey, Bulletin 112, p. 143–170.

NOLDART, A. J., 1958, Miscellaneous reports for 1954, Progress reports on exploratory drilling of abandoned gold shows, Yilgarn Goldfield: Western Australia Geological Survey, Bulletin 112, p. 143–165.

NORD RESOURCES PACIFIC PROPRIETARY LIMITED, 1981–86, Jackson base metal and gold exploration: Annual Report Prospecting Licence 77/11, Jackson: Western Australia Geological Survey, Statutory mineral exploration report, Item 5177 A16303 (unpublished).

PIDGEON, R. T., and WILDE, S. A., 1990, The distribution of 3.0 Ga and 2.7 Ga volcanic episodes in the Yilgarn Craton of Western Australia: Precambrian Research, v. 48, p. 309–325.

PYKE, D. R., NALDRETT, A. J., and ECKSTRAND, O. R., 1973, Archaean ultramafic flows in Munro Township, Ontario: Geological Society of America, Bulletin, v. 84, p. 955–978.

QIU, Y. M., McNAUGHTON, N. J., GROVES, D. I., and DALSTRA, H. J., 1999, Ages of internal granitoids in the Southern Cross region, Yilgarn Craton, Western Australia, and their crustal evolution and tectonic implications: Australian Journal of Earth Sciences, v. 46, p. 971–981.

REINECK, H.-E., and SINGH, I. B., 1980, Depositional sedimentary environments: Berlin, Springer-Verlag, 549p.

RIGANTI, A., 2002, Everett Creek, W.A. Sheet 2841: Western Australia Geological Survey, 1:100 000 Geological Series.

RIGANTI, A., CHEN, S. F., WYCHE, S., and GREENFIELD, J. E., 2000, Late Archaean volcanism and sedimentation in the central Yilgarn Craton, *in* GSWA 2000 Extended Abstracts: Western Australia Geological Survey, Record 2000/8, p. 4–6.

SOFOULIS, J., 1960, Report on a geological reconnaissance of a greenstone belt extending from Jackson in the Yilgarn Goldfield to Ryans Find in the Coolgardie Goldfield, W.A.: Western Australia Geological Survey, Bulletin 114, p. 27–42.

SPENCE, A. G., 1958, Preliminary report on airborne magnetic and radiometric surveys in Kalgoorlie–Southern Cross region, Western Australia (1956–1957): Australian Bureau of Mineral Resources, Record 1958/45 (unpublished).

SUN, S.-S., and McDONOUGH, W. F., 1989, Chemical and isotopic systematics of oceanic basalts: implications for mantle composition and processes, *in* Magmatism in the ocean basins *edited by* A. D. SAUNDERS and M. J. NORRIS: London, U.K., Geological Society, Special Publication, v. 42, p. 313–345.

TAYLOR, S. R., and HALLBERG, J. A., 1977, Rare-earth elements in the Marda calc-alkaline suite: an Archaean geochemical analogue of Andean-type volcanism: Geochimica et Cosmochimica Acta, v. 41, p. 1125–1129.

TOWNSEND, D. B., GAO MAI, and MORGAN, W. R., 2000, Mines and mineral deposits of Western Australia: digital extract from MINEDEX — an explanatory note: Western Australia Geological Survey, Record 2000/13, 28p.

THOMPSON, R. L., 1996, Partial surrender report for period ending 25 September 1995; Gondwana Resources NL: Western Australia Geological Survey, Statutory mineral exploration report, Item 8717 A48389 (unpublished).

TRENDALL, A. F., 2002, The significance of iron-formation in the Precambrian stratigraphic record, *in* Precambrian sedimentary environments: a modern approach to ancient depositional systems *edited by* W. ALTERMANN and P. L. CORCORAN: International Association of Sedimentologists, Special Publication no. 33, p. 33–66.

TYLER, I. M., and HOCKING, R. M., 2001, Tectonic units of Western Australia (scale 1:2 500 000): Western Australia Geological Survey.

van de GRAAFF, W. J. E., CROWE, R. W. A., BUNTING, J. A., and JACKSON, M. M., 1977, Relict early Cainozoic drainage in arid Western Australia: Zeitschrift fur Geomorphologie, v. 21, p. 379–400.

WALKER, I. W., and BLIGHT, D. F., 1983, Barlee, W.A.: Western Australia Geological Survey, 1:250 000 Geological Series Explanatory Notes, 22p.

WANG, Q., BEESON, J., and CAMPBELL, I. H., 1998, Granite–greenstone zircon U–Pb chronology of the Gum Creek greenstone belt, Southern Cross Province, Yilgarn Craton: tectonic implications, *in* Structure and evolution of the Australian continent *edited by* J. BRAUN, J. C. DOOLEY, B. R. GOLEBY, R. D. VAN DER HILST, and C. T. KLOOTWIJK: American Geophysical Union, Geodynamics Series, v. 26, p. 175–186.

WANG, Q., SCHIOTTE, L., and CAMPBELL, I. H., 1996, Geochronological constraints on the age of komatiites and nickel mineralisation in the Lake Johnston greenstone belt, Yilgarn Craton, Western Australia: Australian Journal of Earth Sciences, v. 43, p. 381–385.

WATKINS, K. P., and HICKMAN, A. H., 1990, Geological evolution and mineralization of the Murchison Province, Western Australia: Western Australia Geological Survey, Bulletin 137, 267p.

WESTERN MINING CORPORATION LIMITED, 1961–69, Yilgarn iron ore exploration: Western Australia Geological Survey, Statutory mineral exploration report, Item 1746 A5085 (unpublished).

WINCHESTER, J. A., and FLOYD, P. A., 1977, Geochemical discrimination of different magma series and their differentiation products using immobile elements: Chemical Geology, v. 20, p. 325–343.

WOODWARD, H. P., 1912a, A general description of the northern portion of the Yilgarn Goldfield and the southern portion of the North Coolgardie Goldfield: Western Australia Geological Survey, Bulletin 46, 23p.

WOODWARD, H. P., 1912b, Miscellaneous reports II, Nos 9–32, The Mount Jackson Centre, Yilgarn Goldfield: Western Australia Geological Survey, Bulletin 48, p. 181–186.

WYCHE, S., 1999, Geology of the Mulline and Riverina 1:100 000 sheets: Western Australia Geological Survey, 1:100 000 Geological Series Explanatory Notes, 28p.

WYCHE, S., CHEN, S. F., GREENFIELD, J. E., and RIGANTI, A., 2001, Geology of the Johnston Range 1:100 000 sheet: Western Australia Geological Survey, 1:100 000 Geological Series Explanatory Notes, 31p.

Appendix 1

Gazetteer of localities

Locality	MGA coordinates Easting	Northing
Allens Find	716820	6658670
Athlone prospect	704100	6665900
Atkinsons Find	720450	6658500
Boondine Hill	715700	6649700
Buddarning Peak	706360	6662250
Bungalbin Hill (on BUNGALBIN)	753100	6634900
Clampton mine (abandoned; on JOHNSTON RANGE)	703700	6685200
Curragibbin Hill	708800	6654100
Deception Hill (on JOHNSTON RANGE)	725600	6696100
Die Hardy Range (on JOHNSTON RANGE)	729000	6687000
Diemals Homestead (on JOHNSTON RANGE)	723000	6715800
Evanston mine (on JOHNSTON RANGE)	740200	6706900
Marda Dam	719900	6655300
Marda mining centre	716000	6658000
Mount Jackson	717800	6651400
Mount Jackson Homestead	703250	6656900
Muddahdah Hill	710150	6678650
Muddarning Hill	720800	6650500
Pigeon Rocks (on JOHNSTON RANGE)	719500	6687500
Victoria Hill	703300	6658650
Windarling Peak	720770	6670500
Yacke Yackine Dam	693630	6644630
Yeeding Hill	713000	6650900
Yeela Hill	706650	6657850
Yenyanning Hill	721500	6651000

Appendix 2

Whole-rock geochemical data for the lower greenstone succession and granitoid rocks on JACKSON

GSWA no.	*143380*[a]	*159305*[a]	*164801*[a]	*164803*[a]	*164808*[a]	*164822*[a]	*168955*[b]	*168956*[b]	*168958*[b]	*168959*[b]
Rock type	*Rhyodacitic porphyry*	*Basaltic amphibolite*	*High-Mg basalt*	*Basalt*	*Pyroxenite*	*Basalt*	*Millars Monzogranite*	*Granitoid gneiss*	*Quartzite*	*Butcher Bird Monzogranite*
Locality	*Mount Jackson southeast*	*Muddahdah Hill west*	*Muddarning Peak*	*Athlone prospect south-southeast*	*Athlone prospect southwest*	*Yeela Hill*	*Millars southeast*	*Yacke Yackine Dam*	*Victoria Hill south*	*Butcher Bird mine southeast*
Easting[c]	*724150*	*701950*	*706800*	*704360*	*703440*	*706200*	*710310*	*693630*	*703370*	*730250*
Northing[c]	*6641500*	*6679330*	*6661540*	*6664970*	*6664890*	*6658260*	*6642800*	*6646630*	*6658450*	*6654610*
					Percentage					
SiO_2	73.14	52.68	52.95	51.60	49.04	52.42	76.70	75.12	99.01	74.79
TiO_2	0.22	0.52	0.62	0.53	0.48	1.28	0.06	0.17	<0.005	0.24
Al_2O_3	14.05	15.98	12.35	13.69	10.92	13.23	12.79	13.54	0.10	12.43
Fe_2O_3	0.48	0.73	2.77	2.48	2.26	2.73	0.34	0.39	0.05	1.50
FeO	1.55	6.25	7.15	7.66	8.22	9.20	0.28	1.13	0.00	0.84
MnO	0.03	0.17	0.15	0.17	0.17	0.16	0.05	0.02	<0.005	0.06
MgO	0.47	6.97	9.58	8.59	13.30	5.92	0.07	0.29	0.02	0.15
CaO	1.70	14.46	9.69	10.69	10.94	8.47	0.48	1.68	0.02	0.83
Na_2O	4.28	1.31	1.92	1.25	0.86	3.59	4.15	3.93	0.04	4.42
K_2O	3.58	0.13	0.11	0.22	0.06	0.17	4.38	3.38	0.01	3.67
P_2O_5	0.06	0.05	0.05	0.04	0.03	0.10	0.01	0.05	0.01	0.03
BaO	0.08	–	0.01	0.01	0.00	0.00	–	–	–	–
S	0.01	0.01	0.02	0.01	0.01	0.00	–	–	–	–
CO_2	0.18	0.06	0.04	0.02	0.08	0.01	–	–	–	–
H_2O-	0.03	0.14	0.12	0.07	0.18	0.19	–	–	–	–
H_2O+	0.35	1.00	3.00	3.11	3.64	2.52	–	–	–	–
Fe_2O_3(Total)	2.21	7.67	10.71	10.99	11.39	12.95	0.65	1.65	0.05	2.43
LOI	–	–	–	–	–	–	0.60	0.00	0.74	0.71
Total	**100.21**	**100.46**	**100.53**	**100.14**	**100.19**	**99.99**	**99.91**	**99.70**	**100.00**	**99.67**
					Parts per million					
Ag	<0.2	0.6	<0.2	<0.2	0.2	<0.2	0.07	<0.05	<0.05	0.05
As	<0.5	8.6	0.5	1.1	<0.5	<0.5	1.4	1.1	0.5	1.4
Ba	708	77	45	49	12	63	57	1 168	16	1 087
Be	–	–	–	–	–	–	3.8	2.2	0.5	3.1
Bi	<0.6	<0.6	<0.6	<0.6	<0.6	<0.6	<0.1	<0.1	<0.1	<0.1
Br	<0.5	0.9	<0.5	<0.5	<0.5	<0.5	–	–	–	–
Cd	<0.2	0.3	0.3	<0.2	<0.2	0.2	<0.1	<0.1	<0.1	<0.1
Ce	50	8.0	8.9	3.4	2.5	11	–	–	–	–
Cr	6.3	517	675	215	1 172	126	<2	<2	<2	<2
Cs	<1	<1	<1	<1	<1	<1	2.2	0.8	0.02	0.9
Cu	4.5	35	91	86	95	84	5	4	3	<1
Ga	18	12	12	14	12	18	18	16	0.2	15

Ge	1.0	1.2	1.2	1.2	1.6	1.4	1.9	1	1.3	1.6
Hf	4.6	3.4	<3	<3	<3	<3	2.6	3.9	<0.1	8.1
I	<0.7	<0.7	<0.7	<0.7	<0.7	<0.7	–	–	–	–
In	<0.2	<0.2	<0.2	<0.2	<0.2	<0.2	–	–	–	–
La	24	3.3	2.9	1.6	1.4	5.1	–	–	–	–
Mo	<0.5	0.5	0.6	<0.5	<0.5	0.5	1.9	2.3	1.1	2.7
Nb	8.6	2.5	2.9	2.3	1.6	4.6	11	3.5	0.2	13
Ni	3.1	168	137	94	324	73	3.2	4	28	10
Pb	29	5.3	2.8	1.5	1.0	1.5	53	30	1	24
Rb	122	4.4	2.1	6.6	2.2	3.6	217	98	4.3	129
Sb	<0.5	2.2	<0.5	<0.5	<0.5	<0.5	0.1	0	0	0.1
Sc	4.2	46	48	49	40	42	4	3	<2	6
Se	<0.5	<0.5	<0.5	<0.5	<0.5	<0.5	–	–	–	–
Sn	1.9	0.5	0.5	0.3	<0.3	0.8	3.6	5.2	0.9	3.9
Sr	199	87	98	75	50	152	28	195	3.9	82
Ta	<8	–	–	–	–	–	1.2	0.4	0.2	1.3
Te	<0.5	<0.5	<0.5	<0.5	<0.5	<0.5	–	–	–	–
Th	21	1.1	1.6	<1	<1	1.1	24	15	0.1	19
Tl	<0.7	<0.7	<0.7	<0.7	<0.7	<0.7	–	–	–	–
U	4.9	<1	<1	<1	<1	<1	5.6	1.7	<0.1	4.4
V	14	193	211	214	187	270	<5	10	<5	<5
W	–	–	–	–	–	–	–	–	–	–
Y	15	13	15	15	13	23	5.3	4.9	0.4	31
Zn	30	64	66	68	62	63	22	26	<1	50
Zr	137	40	43	30	25	79	60	146	1	303
La	–	4.100	3.381	2.233	1.160	5.666	–	31.86	1.47	54.37
Ce	–	8.651	7.528	5.085	2.656	14.404	–	54.45	2.48	102.2
Pr	–	1.114	1.051	0.767	0.449	2.165	–	5.18	0.24	10.24
Nd	–	4.667	4.708	3.516	2.365	10.136	–	17.69	1	36.97
Sm	–	1.314	1.435	1.133	0.956	3.029	–	2.63	0.25	6.53
Eu	–	0.581	0.552	0.476	0.500	1.094	–	0.596	0.026	1.006
Gd	–	1.658	1.863	1.630	1.487	3.679	–	1.91	0.18	6.21
Tb	–	0.287	0.333	0.307	0.282	0.605	–	0.21	0	1.06
Dy	–	1.947	2.307	2.210	2.021	3.859	–	0.97	0.08	5.48
Ho	–	0.429	0.504	0.504	0.452	0.791	–	0.17	0.02	1.13
Er	–	1.276	1.463	1.480	1.325	2.240	–	0.43	0.01	3.36
Tm	–	0.198	0.225	0.230	0.202	0.323	–	–	–	–
Yb	–	1.265	1.437	1.491	1.273	1.965	–	0.4	0	3.36
Lu	–	0.203	0.222	0.229	0.198	0.305	–	0.07	0	0.53
Σ_{REE}	–	27.69	27.01	21.29	15.33	50.26	–	116.57	5.76	232.45
$(La/Yb)_{CN}$	–	2.32	1.69	1.07	0.65	2.07	–	57.13	–	11.61

NOTES: (a) Analysed at the Australian National University, Canberra. All major and trace element analyses were carried out by X-ray fluorescence (XRF); all rare earth element analyses were carried out at the University of Queensland by inductively coupled plasma mass spectometry (ICP-MS)
(b) Analysed by Geoscience Australia, Canberra. For these samples, all major element and As, Ba, Cr, Cu, Rb, Sc, Sr, V, Zn, and Zr analyses were carried out using XRF; the remaining trace and the rare earth elements were analysed by ICP-MS
(c) MGA coordinates
LOI Loss on ignition

REFERENCE: Analytical techniques discussed in Morris (2000):
MORRIS, P. A., 2000, Composition of Geological Survey of Western Australia geochemical reference materials: Western Australia Geological Survey, Record 2000/11, 33p.

Appendix 3

Whole-rock geochemical data for felsic rocks of the Marda Complex on JACKSON

GSWA no.	*159393*[a]	*159356*[a]	*159352*[a]	*159335*[a]	*168960*[b]	*159377*[a]	*159319*[a]	*143354*[a]	*159392*[a]	*159346*[a]	*168961*[b]	*159348*[a]
Rock type	*Andesite*	*Andesite*	*Andesite*	*Dacitic fragmental ignimbrite*	*Rhyodacitic fragmental ignimbrite*	*Rhyodacite*	*Rhyodacite*	*Rhyolitic porphyry*	*Rhyolitic ignimbrite*	*Spherulitic rhyolitic ignimbrite*	*Rhyolitic ignimbrite*	*Rhyolite*
Locality	*Butcher Bird mine north-northwest*	*Windarling Peak west-northwest*	*Windarling Peak west-northwest*	*Butcher Bird mine*	*Butcher Bird mine*	*Butcher Bird mine northeast*	*Muddahdah Hill south-southeast*	*Mount Jackson east*	*Butcher Bird mine north*	*Butcher Bird mine north-northeast*	*Butcher Bird mine north*	*Butcher Bird mine north-northeast*
Easting[c]	*716290*	*713830*	*713900*	*720290*	*720730*	*727470*	*714340*	*734840*	*720960*	*723690*	*720500*	*723680*
Northing[c]	*6663910*	*6671260*	*6671570*	*6659740*	*6659080*	*6662300*	*6677100*	*6650050*	*6665110*	*6664580*	*6664440*	*6664570*
						Percentage						
SiO_2	59.04	59.52	59.62	69.07	69.51	71.41	71.74	73.92	75.61	75.95	76.04	76.86
TiO_2	0.95	0.84	0.84	0.52	0.52	0.49	0.27	0.29	0.20	0.18	0.18	0.20
Al_2O_3	15.28	15.71	15.59	13.95	14.13	13.19	14.48	12.05	12.54	11.81	12.17	13.23
Fe_2O_3	1.79	1.20	1.03	1.41	1.99	1.03	0.53	0.36	0.51	0.32	0.68	0.17
FeO	5.81	5.89	5.88	2.91	2.32	2.82	1.94	2.27	1.72	2.32	1.47	0.89
MnO	0.10	0.10	0.10	0.07	0.06	0.08	0.04	0.05	0.04	0.07	0.01	0.06
MgO	3.43	3.39	3.26	0.87	0.88	0.41	0.59	0.33	0.24	0.20	0.42	0.04
CaO	5.82	6.84	4.64	2.67	2.58	2.27	2.10	4.42	0.67	0.02	0.30	0.04
Na_2O	3.55	3.14	5.58	4.08	4.14	4.21	4.30	2.02	4.25	3.65	4.15	7.01
K_2O	1.93	1.68	1.63	2.87	2.92	2.74	3.12	3.08	3.49	4.34	3.80	1.43
P_2O_5	0.28	0.25	0.25	0.12	0.13	0.09	0.08	0.04	0.01	0.02	0.02	0.02
BaO	0.09	0.07	0.07	–	–	0.10	–	0.12	0.13	–	–	–
S	0.01	0.01	0.01	0.01	–	0.01	0.01	0.01	0.01	0.01	–	0.00
CO_2	0.04	0.01	0.05	0.26	–	0.04	0.06	0.07	0.19	0.29	–	0.46
H_2O-	0.05	0.05	0.10	0.14	–	0.07	0.09	0.10	0.05	0.07	–	0.04
H_2O+	1.99	1.53	1.61	0.96	–	0.82	0.76	1.17	0.53	0.51	–	0.05
Fe_2O_3(Total)	8.24	7.74	7.56	4.64	4.57	4.16	2.68	2.88	2.42	2.89	2.31	1.11
LOI	–	–	–	–	0.35	–	–	–	–	–	0.41	–
Total	**100.16**	**100.23**	**100.26**	**99.91**	**99.53**	**99.78**	**100.11**	**100.30**	**100.19**	**99.76**	**99.66**	**100.50**
						Parts per million						
Ag	<0.2	0.3	<0.2	<0.2	0.05	<0.2	<0.2	<0.2	<0.2	<0.2	0.05	<0.2
As	<0.5	0.8	<0.5	1.2	2.6	<0.5	<0.5	<0.5	<0.5	<0.5	0.9	<0.5
Ba	752	618	585	892	864	860	1 007	1 041	1 101	1 220	958	263
Be	–	–	–	–	2.8	–	–	–	–	–	3.5	–
Bi	<0.6	<0.6	<0.6	<0.6	0.1	<0.6	<0.6	<0.6	<0.6	<0.6	<0.1	<0.6
Br	0.7	<0.5	<0.5	<0.5	–	<0.5	<0.5	<0.5	0.5	<0.5	–	<0.5
Cd	0.2	0.2	0.2	0.4	0.25	0.4	0.2	0.2	<0.2	<0.2	0.13	<0.2
Ce	66	62	59	87	–	94	53	82	125	114	–	95
Cr	22	43	39	13	3	2.1	7.7	2.6	2.1	3.0	<2	2.4
Cs	<1	<1	<1	<1	0.69	<1	3.1	<1	<1	3.2	0.39	<1

Cu	28	31	30	7.0	10	7.0	9.8	7.8	6.9	1.5	4	1.6
Ga	18	18	17	15	17	15	16	12	15	14	16	11
Ge	1.0	1.0	0.9	1.4	1.4	1.0	1.1	1.2	1.0	1.3	1.3	0.8
Hf	3.9	3.8	4.1	10	7.1	7.1	6.3	8.0	8.0	11	9.5	8.9
I	<0.7	<0.7	<0.7	<0.7	–	<0.7	<0.7	<0.7	<0.7	<0.7	–	<0.7
In	<0.2	<0.2	<0.2	<0.2	–	<0.2	<0.2	<0.2	<0.2	<0.2	–	<0.2
La	30	28	27	46	–	47	30	39	66	57	–	46
Mo	0.9	1.2	1.1	1.5	4.3	2.1	0.8	1.7	1.7	1.3	2.8	0.7
Nb	9.0	7.8	6.9	11	11	13	7.3	12	14	14	14	15
Ni	26	43	41	8.5	12	0.8	6.5	<1	0.2	<1	2.7	<1
Pb	9.6	14	9.8	37	27	17	30	24	34	15	7.3	8.1
Rb	52	39	44	89	84	84	103	63	106	78	99	22
Sb	<0.5	<0.5	<0.5	<0.5	0.1	<0.5	<0.5	<0.5	<0.5	<0.5	0	<0.5
Sc	19	18	19	11	10	9.1	3.5	4.9	6.0	6.5	7	4.9
Se	<0.5	<0.5	<0.5	<0.5	–	<0.5	<0.5	<0.5	<0.5	<0.5	–	<0.5
Sn	1.1	1.1	1.0	1.8	4.5	2.2	1.2	2.0	2.3	1.6	3.1	0.9
Sr	338	376	258	184	200	130	215	121	74	29	34	27
Ta	–	–	–	–	1	–	–	<8	<8	–	1.2	–
Te	<0.5	<0.5	<0.5	<0.5	–	<0.5	<0.5	<0.5	<0.5	<0.5	–	<0.5
Th	8.4	7.7	7.5	18	16	21	16	20	23	22	17	28
Tl	<0.7	<0.7	<0.7	0.7	–	<0.7	0.7	<0.7	<0.7	0.8	–	<0.7
U	1.0	1.0	1.7	3.1	3.3	3.9	4.1	2.6	4.0	3.9	4.0	4.4
V	124	121	121	28	28	5.3	22	4.7	1.4	1.7	<5	1.6
W	–	–	–	–	–	–	–	–	–	–	–	–
Y	21	20	20	28	28	33	12	30	38	29	30	27
Zn	70	71	63	82	65	73	41	46	65	53	26	8.4
Zr	213	179	179	271	294	311	145	315	347	326	340	372
La	38	35	34	49	48.21	56	35	–	74	64	60.1	52
Ce	72	66	66	90	89.29	102	60	–	135	116	117.8	96
Pr	8	7.2	7.2	9.8	9.27	11	6	–	14	12.5	11.34	10.2
Nd	29.5	27.5	27.5	34	34.16	39	20	–	49	44	41.11	35
Sm	5.2	5	4.8	6.2	6.05	7	3.2	–	8.4	7.6	7.32	6
Eu	1.4	1.35	1.35	1.35	1.357	1.4	0.72	–	1.45	1.06	1.234	0.84
Gd	4.4	4.1	4	5	5.72	5.8	2.5	–	7	5.8	6.77	4.7
Tb	0.62	0.6	0.58	0.76	0.95	0.88	0.34	–	1.02	0.74	1.16	0.64
Dy	4	3.9	3.8	5.2	4.93	6	2.2	–	6.8	4.7	5.91	4.5
Ho	0.74	0.7	0.7	1	1	1.12	0.42	–	1.25	0.94	1.21	0.92
Er	2.15	2.05	2.1	2.9	2.93	3.3	1.2	–	3.8	2.8	3.59	3
Tm	0.3	0.29	0.28	0.42	–	0.48	0.18	–	0.52	0.47	–	0.49
Yb	1.9	1.8	1.85	2.75	2.87	3.2	1.14	–	3.5	2.95	3.4	3.4
Lu	0.285	0.27	0.275	0.42	0.45	0.5	0.18	–	0.52	0.46	0.5	0.54
Σ_{REE}	168.50	155.76	154.44	208.80	207.19	237.68	133.08	–	306.26	264.02	261.44	218.23
$(La/Yb)_{CN}$	14.35	13.95	13.18	12.78	12.05	12.55	22.02	–	15.17	15.56	12.68	10.97

NOTES: (a) Analysed at the Australian National University, Canberra. All major and trace element analyses were carried out by X-ray fluorescence (XRF); all rare earth element analyses were carried out by Genalysis Laboratory Services Pty Ltd by inductively coupled plasma mass spectometry (ICP-MS); LOI = Loss on ignition

(b) Analysed by Geoscience Australia, Canberra. For these samples, all major element and As, Ba, Cr, Cu, Rb, Sc, Sr, V, Zn, and Zr analyses were carried out using XRF; the remaining trace and the rare earth elements were analysed by ICP-MS

(c) MGA coordinates

REFERENCE: Analytical techniques discussed in Morris (2000):

MORRIS, P. A., 2000, Composition of Geological Survey of Western Australia geochemical reference materials: Western Australia Geological Survey, Record 2000/11, 33p.

Appendix 4

Recorded gold production from JACKSON

Site	*Start date*	*End date*	*Ore treated (kt)*	*Contained metal (kg)*[a]
Allens Find	1912	1940	3.532	56.471
Ass. Mt Jackson Gm (WA) Ltd	1900	1902	0.814	6.989
Athlone Reward Leases	1911	1912	0.107	3.26
Best Known	1912	1912	0.021	1.037
Bullseye	1936	1940	0.785	0.002
Bullseye	1936	1940	0.785	3.89
Butcher Bird No 1	1912	1918	2.836	63.416
Coronation	1938	1938	0.217	2.832
Dolly Pot	1948	1948	0.015	0.327
Dolly Pot Hill	1935	1941	–	0.315
Dolly Pot Hill	1935	1941	0.532	0.065
Dolly Pot Hill	1935	1941	0.532	8.225
Flemington	1911	1911	–	0.136
General Jackson	1912	1912	0.037	0.817
Glen Esk	1937	1937	0.012	0.205
Golden Reef	1937	1940	0.252	4.685
Great Unknown	1911	1947	–	1.663
Great Unknown	1911	1947	2.562	139.84
Great Unknown North	1911	1913	–	0.952
Great Unknown North	1911	1913	0.026	1.105
Hazel Merle	1936	1936	0.113	1.159
Inglewood	1912	1912	0.014	0.279
Just In Time	1913	1954	11.85	0.062
Just In Time	1913	1954	11.85	62.224
Known Best	1912	1912	0.012	0.433
Lone Chance	1913	1913	0.01	0.211
Marda East	1911	1911	0.008	0.374
Miners Dream	1912	1937	0.484	7.672
Mount Jackson G Ms Ltd	1903	1907	19.873	71.702
Mount Jackson G Ms Ltd	1903	1907	19.873	407.564
Mount Jackson G Ms Ltd (1897)	–	1903	9.69	193.172
Mount Jackson Leases	1908	1909	0.254	3.718
Mount Jackson Wonder	1912	1912	0.122	1.377
Newmarket	1913	1913	0.009	0.948
Newmarket	1913	1913	–	1.327
North Yilgarn	1936	1938	0.628	8.374
Numeralla	1975	1979	0.481	1.639
Persian	1912	1912	0.016	0.994
Queen Of The Hills	1911	1911	0.008	0.649
Standard	1912	1935	0.29	27.471
Three Kings	1911	1940	0.116	0.694
Tiger Show	1940	1941	–	0.342
Tiger Show	1940	1941	0.172	4.471
Titanic	1912	1913	0.026	0.775
Unknown South	1915	1915	0.019	0.486
Victoria Reef	1912	1912	0.027	0.16
Well Known	1912	1912	0.006	0.216
West Wickham	1937	1937	0.096	0.962

NOTES: (a) Contained metal = tonnage × grade

REFERENCE: TOWNSEND, D. B., GAO MAI, and MORGAN, W. R., 2000, Mines and mineral deposits of Western Australia: digital extract from MINEDEX — an explanatory note: Western Australia Geological Survey, Record 2000/13, 28p.

Appendix 5

Mineral resources on JACKSON

Site	Resource category[a]	Resource type[b]	Tonnage (Mt)	Grade (g/t)	Contained metal (kg)[c]
Gold					
Dolly Pot	MES	MIN	0.255	2.28	581.4
Python	MES	MIN	0.308	2.38	733.04
Marda Group	DEM	I/S	1.003	0.72	722.16
Marda Group	IND	I/S	0.594	1.83	1 087.02
Marda Group	DEM	MIN	0.821	2.34	1 921.14
Marda Group	INF	I/S	0.346	1.72	595.12
Marda Group	MES	I/S	1.265	1.95	2 466.75
Goldstream	MES	I/S	0.103	1.47	151.41
Goldstream	INF	I/S	0.016	1.23	19.68
Goldstream	MES	MIN	0.065	2.63	170.95
Goldstream	MES	I/S	0.1	2.44	244
Dugite	MES	MIN	0.193	2.26	436.18
Cobra–Marda	INF	I/S	0.069	1.89	130.41
Taipan	IND	I/S	0.043	1.07	46.01
Taipan	INF	I/S	0.065	1.16	75.4
Greentree	IND	I/S	0.004	4.47	17.88
Greentree	INF	I/S	0.004	4.47	17.88
King Brown – Marda	INF	I/S	0.189	3.43	648.27
Pencil Tiger	IND	I/S	0.047	1.53	71.91
Golden Orb	INF	I/S	0.45	3	1 350
Iron					
Mount Jackson	IND	I/S	52	60.4%	31.408 Mt
Windarling Range	DEM	I/S	25.5	64.6%	16.473 Mt

NOTES: (a) Resource category is either measured (MES), indicated (IND), inferred (INF), or demonstrated (DEM)
(b) Resource type is either in situ (I/S) or mineable (MIN)
(c) Contained metal = tonnage × grade

REFERENCE: TOWNSEND, D. B., GAO MAI, and MORGAN, W. R., 2000, Mines and mineral deposits of Western Australia: digital extract from MINEDEX — an explanatory note: Western Australia Geological Survey, Record 2000/13, 28p.

The JACKSON 1:100 000 sheet covers the north-central portion of the JACKSON 1:250 000 sheet within the Southern Cross Granite–Greenstone Terrane, in the central part of the Archaean Yilgarn Craton. These Explanatory Notes complement the 1:100 000-scale map, and describe the Precambrian rock types, and the structural and metamorphic geology of the granites and greenstones. The greenstone stratigraphy and the constraints on the age of the various components of the greenstone succession, the deformation history, and its relationship to granitoid intrusion are discussed. JACKSON has been explored for gold and iron, and a number of supergene-enriched iron deposits have been identified.

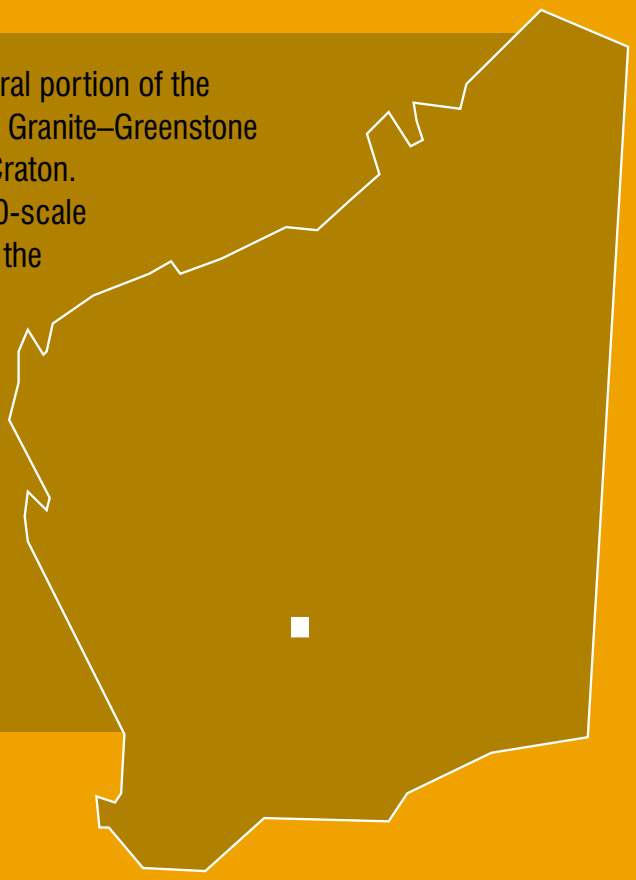

Further details of geological publications and maps produced by the Geological Survey of Western Australia can be obtained by contacting:

Information Centre
Department of Mineral and Petroleum Resources
100 Plain Street
East Perth WA 6004
Phone: (08) 9222 3459 Fax: (08) 9222 3444
www.mpr.wa.gov.au

JACKSON

GEOLOGICAL SURVEY OF WESTERN AUSTRALIA

DIAGRAMMATIC SECTIONS

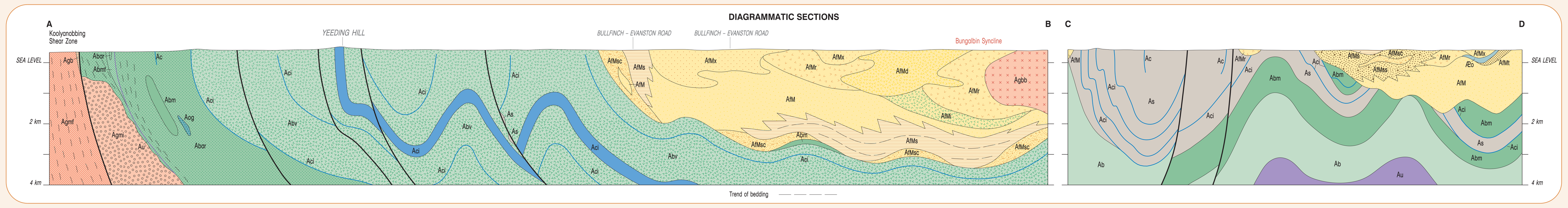

PHANEROZOIC — CAINOZOIC

Colluvial units
- *C* Mixed gravel from different rock types as proximal talus; includes sand and silt; locally ferruginous
- *Cf* Ferruginous gravel and reworked duricrust
- *Cgpg* Quartzofeldspathic sand and gravel
- *Clci* Talus from banded iron-formation and chert; locally cemented
- *Cq* Quartz-vein debris

Sheetwash units
- *W* Clay, silt, and sand; locally ferruginous
- *Wf* Sheetwash deposits with abundant ferruginous grit

Alluvial units
- *A* Clay, silt, sand, and gravel in channels and on floodplains
- *Ap* Clay and silt in claypans

Lacustrine units
- *Ll* Saline playa lake deposits
- *Ld* Stabilized dune deposits adjacent to playa lakes
- *Lm* Mixed dune, evaporite, and alluvial deposits adjacent to playa lakes

Sandplain units
- *S* Residual and eolian sand
- *Sl* Yellow sand with minor pisolitic laterite, silt, and clay

Relict units
- *Rd* Siliceous and ferruginous duricrust, undivided
- *Rf* Lateritic duricrust; includes iron-cemented reworked products
- *Rfc* Lateritic duricrust; ironstone over ridge-forming units
- *Rgpg* Quartzofeldspathic sand over granitoid rock; sparse granitoid outcrop
- *Rk* Calcrete
- *Rz* Silcrete

PROTEROZOIC

- q Quartz vein
- Ɇo Gabbro and dolerite

ARCHAEAN — YILGARN CRATON

- g Granitoid dyke

- Ag Granitoid rock, undivided; includes deeply weathered rock
- Agb Foliated granite; locally interleaved with amphibolite
- Agf Strongly foliated granitoid rock
- Agm Monzogranite; locally weakly foliated
- Agmf Strongly foliated monzogranite
- Agcw **CHATARIE WELL GRANITE:** granite; typically deeply weathered
- Agmi **MILLARS MONZOGRANITE:** quartz-rich monzogranite
- *c.* 2711 Ma — Ang Granitoid gneiss
- *c.* 2730 Ma — Agbb **BUTCHER BIRD MONZOGRANITE:** fine- to medium-grained monzogranite; typically granophyric

< 2729 Ma

DIEMALS FORMATION
- Aesh Metamorphosed shale, mudstone, and siltstone
  - Aeshd Andalusite-bearing metapelite

c. 2733 Ma

MARDA COMPLEX
- AfM Felsic volcanic and volcaniclastic rock, undivided; typically deeply weathered; metamorphosed
  - AfMd Dacite, rhyodacite, and minor andesite; commonly feldspar-phyric; metamorphosed
  - AfMf Strongly foliated felsic rock; commonly deeply weathered
  - AfMi Andesite and basaltic andesite; locally amygdaloidal; includes minor dacite; metamorphosed
    - AfMiy Andesite with quartz(–siderite)-filled amygdales; metamorphosed
  - AfMp Rhyolitic to dacitic feldspar porphyry; metamorphosed
  - AfMr Rhyolite; commonly porphyritic; metamorphosed
  - AfMt Felsic tuff and tuffaceous sedimentary rock; metamorphosed
  - AfMx Rhyolitic ignimbrite with minor rhyolite flows and volcaniclastic sedimentary rock; metamorphosed
  - AfMs Volcaniclastic and sedimentary rock, undivided; commonly weathered; metamorphosed
    - AfMsc Polymictic and rhyolitic oligomictic conglomerate with minor siltstone and sandstone; commonly poorly cemented; metamorphosed
    - AfMsh Volcaniclastic shale and siltstone; metamorphosed; locally ferruginous
    - AfMshd Foliated metapelite with andalusite(–staurolite)
    - AfMsq Quartzite and quartz arenite; metamorphosed
    - AfMss Sandstone and minor siltstone with a common volcaniclastic component; metamorphosed

- Altq Quartz-bearing talc schist

- As Metasedimentary rock, undivided; commonly weathered; metamorphosed
- Asc Polymictic conglomerate with minor siltstone and sandstone; includes deeply weathered and poorly cemented rocks; metamorphosed
- Ash Metashale
- Ashg Metamorphosed graphitic shale (subsurface only)
- Asi Ferruginous metasedimentary rock; includes shale, siltstone, and banded iron-formation; deeply weathered
- Asq Quartz-rich metasedimentary rock; mainly quartzite
- Ass Sandstone with minor siltstone; metamorphosed
- Ac Banded chert with minor banded iron-formation and quartzite; metamorphosed
- Aci Banded iron-formation and minor banded chert; local jaspilite; metamorphosed
- Acj Jaspilite with minor banded iron-formation; metamorphosed

- Af Fine-grained felsic rock, undivided; typically deeply weathered; metamorphosed
- Afp Quartz–feldspar porphyry; metamorphosed
- Afpm Sericitized feldspar porphyry; metamorphosed
- Afs Strongly foliated felsic rock; typically deeply weathered
- Afv Fine-grained felsic volcanic and volcaniclastic rock; metamorphosed

- Aog Metagabbro; medium- to coarse-grained mafic rock; includes minor microgabbro
- Aogf Strongly foliated metagabbro
- Aogx Pyroxene-phyric microgabbro

- Ab Metamorphosed mafic rock, undivided; mainly fine-grained; typically deeply weathered
- Abar Amphibolite; retrogressed to greenschist facies assemblages
- Abf Strongly foliated, metamorphosed basaltic rock; local amphibolite
- Abm Metamorphosed high-Mg basalt with relict pyroxene-spinifex and/or variolitic textures
- Abmf Strongly foliated high-Mg basalt; locally variolitic; metamorphosed
- Abs Chlorite(–talc–tremolite) schist
- Abt Mafic tuff; commonly banded; metamorphosed
- Abv Metabasalt; massive to weakly foliated; minor metamorphosed basaltic-andesite
- Abx Metamorphosed mafic-volcanic breccia

- Au Metamorphosed ultramafic rock, undivided; typically deeply weathered
- Auk Metakomatiite; with relict olivine spinifex texture
- Aukf Strongly foliated metakomatiite
- Aup Metamorphosed peridotite; typically serpentinized
- Aur Tremolite–chlorite(–talc) schist
- Aus Serpentinite (subsurface only)
- Aut Talc–tremolite(–chlorite) schist
- Aux Pyroxenite; metamorphosed

Symbols

Geological boundary
- exposed
- concealed
- concealed, interpreted from aeromagnetic data

Structural symbols are labelled according to the sequence of deformation events, where known
- D_2 and D_3
- D_2
- D_1

Fault or shear
- exposed
- concealed
- concealed, interpreted from aeromagnetic data
- strongly foliated rock

Fold, showing axial trace and generalized plunge direction
- syncline; exposed, concealed
- antiform; exposed, concealed
- synform; exposed, concealed

Small-scale fold axis, showing trend and plunge
- unspecified
- anticline
- syncline
- Z-vergence

Bedding, showing strike and dip
- inclined
- vertical

Igneous flow banding, showing strike and dip
- inclined
- vertical
- dip indeterminate

Way-up indicator
- pillow structure
- graded bedding
- cross-bedding
- fining upwards sequence

Foliation, showing strike and dip
- inclined
- vertical
- dip indeterminate

Gneissic banding, showing strike and dip
- inclined
- vertical

Stretching lineation, showing trend and plunge
- inclined
- vertical

Axis of crenulation, showing trend and plunge

Structural lineation, showing trend and plunge
- inclined

Fracture, joint, or extension vein, showing strike and dip
- inclined

Airphoto lineament

Aeromagnetic lineament

Isotopic age determination site with identification number — 168956

Formed road

Major track

Track

Fence, generally with track

Homestead — Mount Jackson

Building

Yard — Yard

Horizontal control; minor

Breakaway

Sand dune

Contour line, height in metres — 400

Watercourse

Gnamma hole — Gnamma hole

Rockhole — Rockhole

Soak, spring — Soak, Spring

Well — Well

Windpump

Dam, tank — Dam, Tank

Abandoned — (abd)

Position doubtful — (PD)

Mining centre — MOUNT JACKSON

Mining locality — BOONDING

Mine (gold, unless otherwise indicated) — Allens Find

Mine, abandoned (for commodities other than gold)

Opencut

Quarry or pit

Prospect — Mount Jackson

Battery or treatment plant, abandoned

Tailings or stockpile

Subsurface data from drillhole, costean, or shallow shaft — Ab

Mineral occurrence
- Copper — Cu
- Iron — Fe
- Road material — Rm

INTERPRETED BEDROCK GEOLOGY

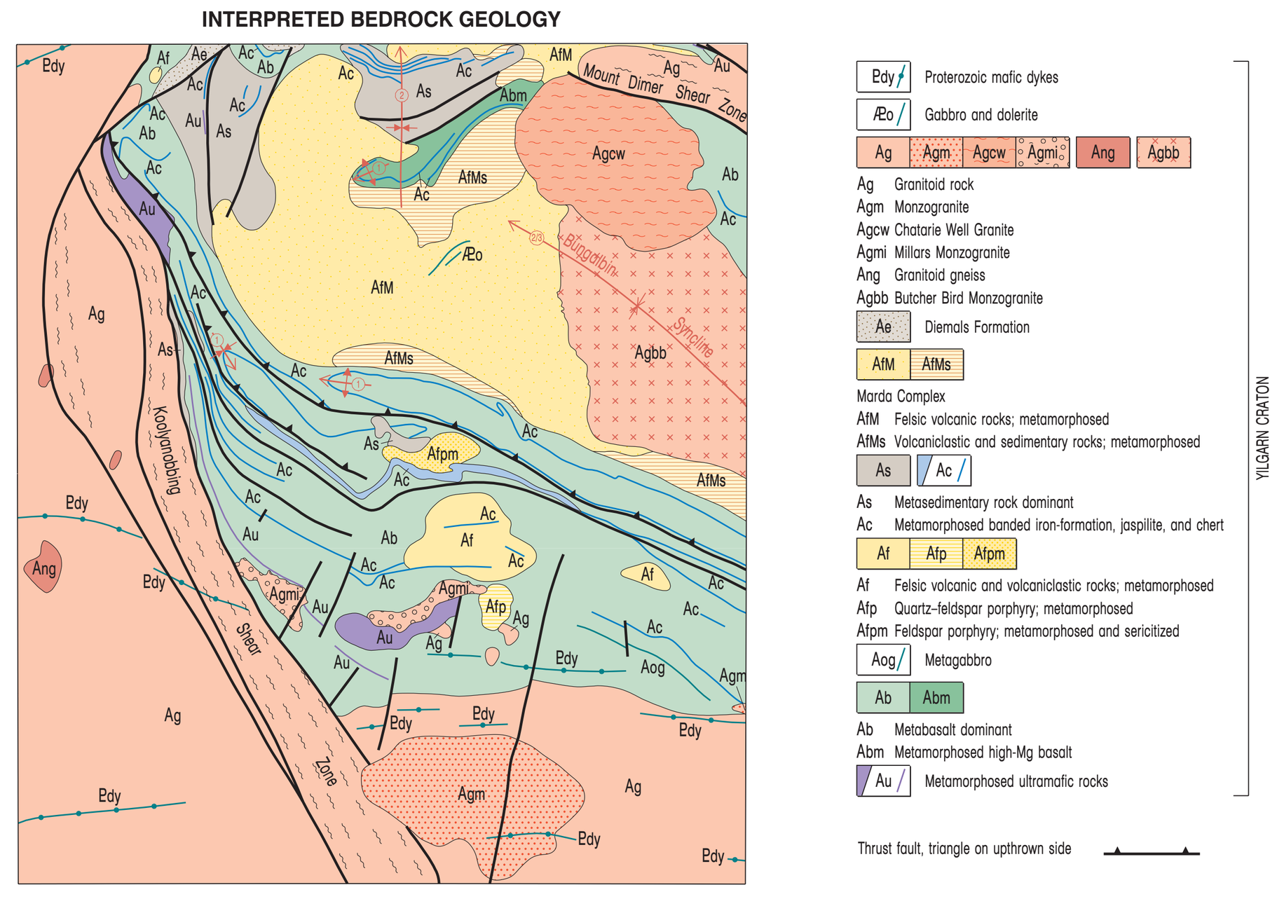

SHEET INDEX

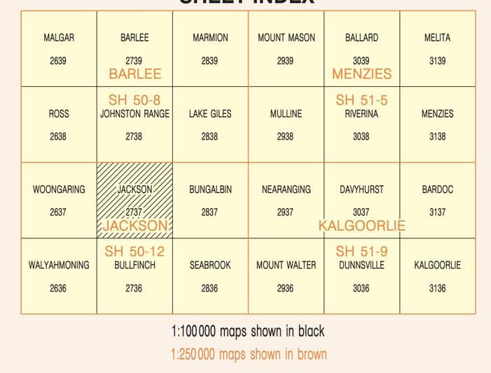

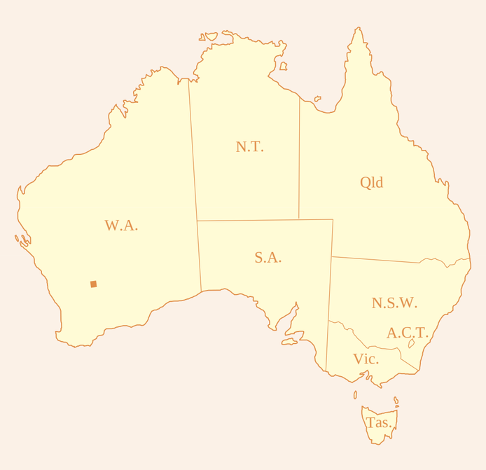

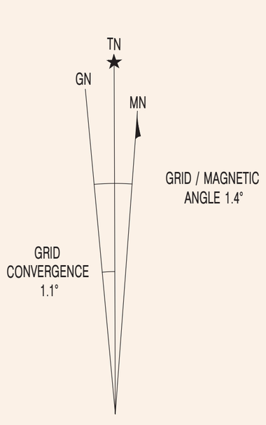

True north, grid north and magnetic north are shown diagrammatically for the centre of the map. Magnetic north is correct for 2000 and moves easterly by about 0.1° in 2 years.

Geology by A. Riganti and S. F. Chen 1998

Geochronology by D. R. Nelson

Edited by N. Tetlaw and G. Loan

Cartography by S. Coldicutt and K. Greenberg

Topography from the Department of Land Administration Sheet SH 50-12, 2737, with modifications from geological field survey

Published by the Geological Survey of Western Australia. Copies available from the Information Centre, Department of Minerals and Energy, 100 Plain Street, East Perth, WA, 6004. Phone (08) 9222 3459, Fax (08) 9222 3444

This map is also available in digital form

Printed by the Sands Print Group, Western Australia

The recommended reference for this map is:
RIGANTI, A., and CHEN, S. F., 2000, Jackson, W.A. Sheet 2737: Western Australia Geological Survey, 1:100 000 Geological Series

Department of Industry and Resources

CLIVE BROWN, M.L.A.
MINISTER FOR STATE DEVELOPMENT

JIM LIMERICK
DIRECTOR GENERAL

Geological Survey of Western Australia

TIM GRIFFIN
DIRECTOR

SCALE 1:100 000

1000 Metres 0 1 2 3 4 5 6 7 8 9 10 Kilometres

UNIVERSAL TRANSVERSE MERCATOR PROJECTION
HORIZONTAL DATUM: GEOCENTRIC DATUM OF AUSTRALIA 1994
VERTICAL DATUM: AUSTRALIAN HEIGHT DATUM

Grid lines indicate 1000 metre interval of the Map Grid Australia Zone 50

The Map Grid Australia (MGA) is based on the Geocentric Datum of Australia 1994 (GDA94)
GDA94 positions are compatible within one metre of the datum WGS84 positions

Reference points to align maps based on the previous datum, AGD84, have been placed near the map corners

JACKSON

SHEET 2737 FIRST EDITION 2000
Version 1.1 — August 2003